A Dissertation for the Degree of Doctor of Philosophy

AHNAK ablation promotes browning of white adipose tissue and counteracts obesity

AHNAK 유전자 결손에 의한 백색지방에서 갈색지방 발생과 항비만 효과 연구

Feburary 2016

By

Jae Hoon Shin, D.V.M.

Department of Veterinary medicine

Graduate School

Seoul National University

수의학박사 학위논문

AHNAK ablation promotes browning of white adipose tissue and counteracts obesity

AHNAK 유전자 결손에 의한 백색지방에서 갈색지방 발생과 항비만 효과 연구

Jae Hoon Shin

(Supervisor: Je Kyung Seong, D.V.M., Ph.D.)

Department of Veterinary Medicine

Graduate School

Seoul National University

AHNAK ablation promotes browning of white adipose tissue and counteracts obesity

지도교수 성 제 경
이 논문을 수의학박사 학위논문으로 제출함
2016 년 2 월

서울대학교 대학원
수의학과 수의해부학 전공
신 재 훈

신재훈의 수의학박사 학위논문을 인준함
2016 년 2 월

위 원 장 윤 여 성 (인)
부위원장 성 제 경 (인)
위 원 배 윤 수 (인)
위 원 구 승 회 (인)
위 원 이 윤 희 (인)

ABSTRACT

AHNAK, a large size-phosphoprotein, plays a crucial role in the cell adhesion, proliferation and calcium signaling. Recently emerging evidence has suggested that AHNAK expression is altered in obese condition. Nevertheless, the role of AHNAK during adipose tissue development remains unclear. The objective of this study was to determine the molecular mechanism of AHNAK in adipogenesis and glucose homeostasis. In this study, *AHNAK* KO mice displayed resistance to diet-induced obesity due to reduction of fat accumulation. We found that adipogenesis from adipose derived mesenchymal stem cells (ADSCs) was severely impaired in *AHNAK* KO mice, which could contribute to whole-body fat accumulation. We also observed that loss of AHANK led to a decreased BMP4/SMAD1 signaling, resulting in decreased expression of key regulators for adipocyte differentiation. AHNAK directly interacts with Smad1 on the PPARγ2 transcription activity. Concomitantly, *AHNAK* KO mice displayed a better degree of metabolic profiles, including improved glucose tolerance, enhanced insulin sensitivity, and higher energy expenditure without alteration in food intake and physical activity. Taken together, Ahnak plays a crucial role in body fat accumulation by regulation of adipose tissue development through interaction with Smad1 protein and can be involved in metabolic homeostasis.

Changes in brown adipose tissue (BAT) activity and energy expenditure through thermogenesis would be a promising therapeutic target against obesity. In adipose tissue, agonists of the β3-adrenergic receptor

(ADRB3) regulate lipolysis, lipid oxidation, and thermogenesis. AHNAK deficiency induced thermogenesis in white adipose tissue (WAT) of mice fed high-fat diet, suggesting that AHNAK may stimulate energy expenditure via the development of beige fat. Here, we report that AHNAK deficiency promoted browning and thermogenic gene expression in WAT but not in brown adipose tissue of mice stimulated with the ADRB3 agonist CL-316243. Consistent with increased thermogenesis, *AHNAK* KO mice exhibited an increase in energy expenditure, accompanied by elevated mitochondrial biogenesis in WAT depots in response to CL-316243. CL-316243 activated PKA signaling and enhanced lipolysis, as evidenced by increased phosphorylation of hormone sensitive lipase and release of free glycerol in *AHNAK* KO mice compared to the wild-type mice. AHNAK deficient WAT contains more eosinophil and type 2 cytokines (IL-4/IL-13) to promote browning of WAT and mitochondrial biogenesis in response to CL. This is associated with enhanced sympathetic tone in WAT via upregulation of adrb3 and tyrosine hydroxylase (TH) expression in *AHNAK* KO mice in response to β-adrenergic activation. Overall, these findings suggest an important role of AHNAK in the regulation of thermogenesis and lipolysis in WAT via β -adrenergic signaling.

.

Keywords: Ahnak, obesity, adipogenesis, BMP4/SMAD1, energy expenditure, browning, lipolysis, thermogenesis, β-adrenergic signaling

Student Number: 2009-21627

CONTENTS

List of Figures

List of Table

Chapter I

Obesity resistance and enhanced insulin sensitivity in Ahnak$^{-/-}$ mice fed a high fat diet are related to impaired adipogenesis and increased energy expenditure

(Publishied in 2010, PLoS One)

1.1. Introduction

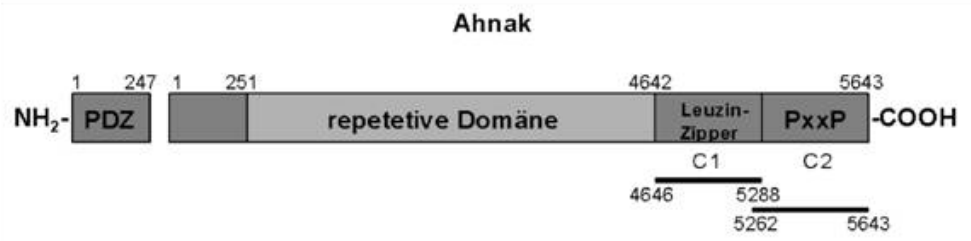

Figure 1-1. Structure of AHNAK protein.

(http://edoc.hu-berlin.de/dissertationen/petzhold-daria-2007-07-31/HTML/chapter1.html)

AHNAK, located on human chromosome 11q 12-13, is a giant protein of approximately 700kD in size initially identified in human neuroblastomas and skin epithelial cells (Hashimoto et al., 1995; Shtivelman and Bishop, 1993; Shtivelman et al., 1992). In epithelial cells, AHANK is mainly localized in the nucleus in low calcium concentrations, but an increase in intracellular calcium levels leads to translocation of the protein to the plasma membrane (Nie et al., 2000). AHNAK, as a scaffolding protein, plays an important role in the formation of cytoskeletal structure, calcium homeostasis, and muscle regeneration (Alvarez et al., 2004; Hohaus et al., 2002; Huang et al., 2007). The protein structure of AHNAK contains three main parts (Figure 1-1): N-terminal, central, and C-terminal domain.

PDZ-containing N-terminal domain has 251 amino acids and the carboxyl-terminal includes 1002 amino acid residues which are involved in skeletal muscle regeneration and calcium signaling (Davis et al., 2014; Hohaus et al., 2002). The central domain with 36 central repeated units (CRU) activates phospholipase C-γ1 (PLC γ 1) as well as protein kinase C-α (PKC-α) (Lee et al., 2008; Lee et al., 2004). Moreover, AHANK is involved in plasma membrane differentiation and repair by calcium-induced exocytosis called enlargosome, and functions in brain endothelial cells in maintenance of the integrity of the blood brain barrier (Borgonovo et al., 2002; Gentil et al., 2005).

It had been assumed that deficiency of AHNAK would lead to significant phenotypes since it is implicated in multiple organs. Nevertheless, AHNAK deficiency displayed no overt phenotypes in muscle cells and epidermis of null mutation mice (Komuro et al., 2004; Kouno et al., 2004) A previous study using AHNAK knockout mice has shown that AHANK is required for the activation and proliferation of T cells and calcium influx in $CD4^+$ T cells (Matza et al., 2008). Recent studies suggested that AHNAK plays a crucial role in not only the cell cycle to stimulate the activation of c-raf, MEK, and Erk signaling in mouse embryonic fibroblast cells (MEF), but also the activation of Erk and Rac in PDGF-dependent migration of mouse aortic smooth muscle cells (ASMC) (Lee et al., 2008; Lim et al., 2013). Furthermore, it has also been suggested that AHNAK is a tumor suppressor as an important component of TGFβ/Smad signaling pathway (Lee et al., 2014).

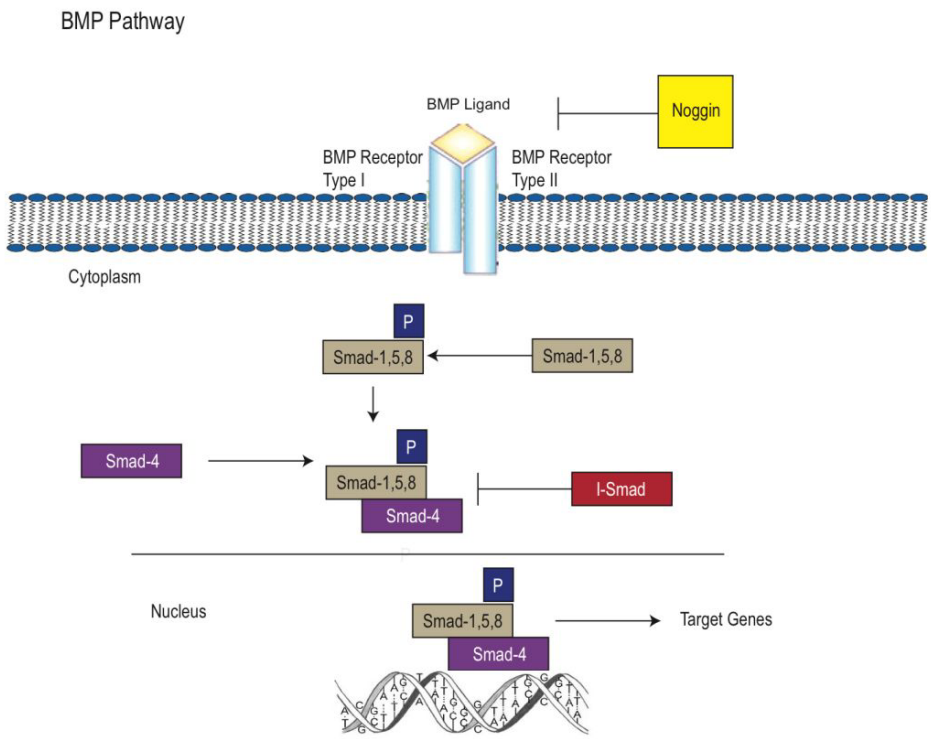

Figure 1-2. Bone Morphogenetic Protein Pathway. (Hyun et al. INTECH Open Access Publisher, 2011)

White adipose tissue (WAT) is important for maintaining energy balance, storing calories in the form of lipids, and supplying energy sources in response to hormonal stimulation(Rosen and Spiegelman, 2006). We first reported that AHNAK KO mice are protected from diet-induced obesity due to alteration of metabolomic profiles in urine and blood between high fat-fed wild-type and AHNAK KO mice (Kim et al., 2010). This finding was

reconfirmed by Ramdas *et al*. (Ramdas et al., 2015). In addition, Li *et al*. showed upregulation of AHNAK in the adipose tissue of diet-induced obesity rat models (Li et al., 2002). However, the molecular mechanism of AHNAK during adipogenesis remains unclear.

Bone morphogenetic proteins (BMPs) are important regulators of proliferation, apoptosis and differentiation during various developmental processes (Chen et al., 2004; Margoni et al., 2012). Several evidences have suggested that BMP signaling promote cell fate determination in the mammalian systems (Kang et al., 2008; Schulz and Tseng, 2009; Zhao, 2003). The effects of BMP2 and -4 in the mesenchymal stem cell line C3H10T1/2 induce commitment to preadipocyte and promote adipogenic differentiation (Huang et al., 2009; Tang et al., 2004; Wang et al., 1993). BMP signal trasnduction stimulates phophorylation of Smad1/5/8. The heterodimeric complex Smad1/5/8 and Smad4 translocates the nucleus and modulate the transcriptional activity of C/EBP family and PPARγ (Figure 1-2) (Huang et al., 2009; Rosen and MacDougald, 2006; Zamani and Brown, 2011).

It was proposed that AHNAK regulates cell growth by mediating TGFβ/Smad signaling (Lee et al., 2014). Studies have shown that bone morphogenetic proteins (BMPs), members of the transforming growth factor β (TGFβ) are involved in adipocyte differentiation and Smad family plays important roles in BMP/TGFβ signaling (Huang et al., 2009; Rosen and MacDougald, 2006; Zamani and Brown, 2011). The present study aimed to elucidate the molecular mechanism leading to impaired adipogenesis in Ahnak KO which have been subjected to enhanced metabolic features.

Furthermore, we demonstrate the critical role of Ahnak in adipogenesis via regulation of the BMP4/Smad1 pathway.

1.2. Materials and Methods

Animals

Ahnak knockout mice were generated by disruption of exon 5 in the Ahnak gene, as previously described (Lee et al., 2008). AHNAK-KO (*Ahnak*$^{-/-}$) mice were obtained by crossing heterozygous breeders. 6-week-old male KO and wild-type mice were fed either a regular chow (RC) diet or a high fat diet (HFD; 20% carbohydrate, 60% fat, 20% protein; D12492; Research Diets Inc., New Brunswick, NJ, USA). Mice were maintained under a 12-h light-dark cycle and had free access to water in a specific pathogen-free barrier facility. Mice were randomly assigned. These procedures were approved by the Institutional Animal Care and Use Committee of Seoul National University (Permit Number: SNU-201004-14) in accordance with the Principles of Laboratory Animal Care (NIH publication no. 85–23, revised 1985).

Cell culture, reagents, and plasmids

Murine 3T3-L1 and C3H10T1/2 cells were kindly provided as a gift by Dr. Jae Woo Kim (Yonsei University, Seoul, South Korea)(Bowers et al., 2006; Lee et al., 2012a). Cells were differentiated into mature adipocytes as described (Bowers et al., 2006), with modifications. Flag-*Ahnak* (N-terminal, amino-acid residues 1-150) and HA-*Smad1*(Liu et al., 1996) expression vectors were purchased from GeneCopoeia (Rockville, MD, USA) and Addgene, respectively. C3H10T1/2 cells were transfected directly with total

of 4μg plasmid DNA using Lipofectamine LTX with Plus reagent (Invitrogen, Carlsbad, CA, USA) according to the manufacturer's protocol. FlexiTube small interfering RNA (siRNA) directed against murine *Ahnak* mRNA (accession no. NM_001039959) was from Qiagen. siRNA transfections were performed with Lipofectamine RNAiMAX (Invitrogen), according to the manufacturer's protocol. AllStars Negative Control siRNA was obtained from Qiagen (Hilden, Germany).

Isolation and expansion of adipose-derived stem cells (ADSCs)

The establishment of wild-type (WT) and AHNAK-KO ADSCs isolated from epididymal and inguinal WATs of 8–10-week-old mice was described previously (Rajkumar et al., 1999; Yamamoto et al., 2007). Briefly, adipose tissue was minced and digested with 0.75 mg/ml collagenase (Wako Pure Chemical Industries, Ltd., Osaka, Japan) for 2 h at 37°C. Cells were added to RBC lysis buffer (eBioscience, San Diego, CA) and filtered through a 100-μm cell strainer (BD Falcon, Franklin Lakes, NJ, USA) to generate single-cell suspensions. Cells were diluted to 1×10^5 cells/cm^2 in DMEM/F12 medium (Gibco, pH 7.4) containing 10% FBS and maintained in 5% CO_2 at 37°C.

Immunostaining

ADSCs were grown on chamber slides and exposed to BMP4 for 1 hour. Cells were fixed and then permeabilized in 0.25% Triton-X 100 at room temperature for 10 min. After washing with PBS, the cells were blocked with 10% normal goat serum. For nuclear staining, the samples were coverslipped in mounting medium with DAPI (Immunobioscience). Images

were captured using a confocal microscope system (LSM 710, Carl Zeiss).

In situ proximity ligation assays

The interactions between AHANK and SMAD1 were determined by performing Duolink™ in situ proximity ligation assays (PLAs; Sigma), according to the manufacturer's instructions. HEK293 and C3H10T1/2 cells were stimulated with BMP4 (25 ng/ml) or not stimulated and then fixed, permeabilized, and incubated with a mouse anti-AHNAK monoclonal antibody in combination with a polyclonal rabbit anti-SMAD1 antibody, followed by incubation with secondary antibodies conjugated to PLA probes.

Cellular viability assay

The cell viability was examined by using an EZ-Cytox Cell viability assay kit (Daeil Lab Service, Seoul, Korea). The relative cell viability was determined by measuring the absorbance at 450 nm using a Tecan microplate reader.

Immunoblotting and immunoprecipitation experiments

For immunoblot analysis, cells were lysed in PRO-PREP buffer (iNtRON Biotechnology Inc., Seoul, Korea) containing a phosphatase-inhibitor cocktail (GenDEPOT, Barker, TX, USA). Protein extracts were separated by sodium dodecyl sulfate-polyacrylamide gel electrophoresis, transferred to a polyvinylidene fluoride membrane (Millipore, Billerica, Massachusetts, USA), and subjected to immunoblot analysis. Cytosolic and nuclear fractions used in immunoblot analysis were prepared using the NE-PER Nuclear and Cytoplasmic Extraction Kit (Thermo Scientific, Rockford, IL, USA), according to the manufacturer's instructions. For

immunoprecipitation experiments, lysates were immunoprecipitated with an anti-HA antibody at 4ºC overnight. Immunocomplexes were washed three times with lysis buffer (1% Triton X-100, 20 mM HEPES at pH 7.5, 150 mM NaCl, 12.5 mM, 10% glycerol, 5 mM EDTA, proteinase inhibitor cocktail (GenDEPOT), and a phosphatase inhibitor), mixed with 2X sample buffer, and separated from the protein A/G agarose beads (Santa Cruz) by boiling. Immunoblot analysis was performed using the indicated antibodies. Proteins were visualized by ECL chemiluminescence (AbClon, Seoul, Korea). GAPDH was detected as a loading control. Immunoreactive signals were detected through their enhanced chemiluminescence and recorded using the MicroChemi 4.2 system (DNR Bio-Imaging Systems, Jerusalem, Israel).

Antibodies

The primary antibodies used for western blot analysis were specific for: pSMAD1/5, SMAD1, SMAD4, PPARγ, LAMIN B1, GAPDH (Cell Signaling Technologies), C/EBPβ, AHNAK (Abcam, Cambridge, UK), and GAPDH (all from Cell Signaling Technology, Beverly, MA, USA). The antibodies used for immunoprecipitation experiments were AHNAK (Abcam) and SMAD1 (Cell Signaling). A peroxidase-conjugated secondary antibody (Abclon) was also used. Anti-SMAD1/5 (Abcam) and anti-pSmad1/5 (Millipore) antibodies were used for immunostaining. Following secondary antibodies were used: Alexa Fluor 488- or 594-conjugated antibody. DAPI (ImmunoBioScience Co., Washington, USA) was used for nuclear staining.

Metabolic assays

For glucose-tolerance tests (GTTs), mice were fasted for 16 h and injected intraperitoneally with 1.5 mg of glucose/g of body weight. For insulin-tolerance tests (ITTs), mice were fasted for 6 h and injected intraperitoneally with insulin (Humulin R; Eli Lilly, Indianapolis, IN) at 1 unit/kg of body weight.

Basal study

A comprehensive animal metabolic monitoring system (CLAMS; Columbus Instruments, Columbus, OH) was used to evaluate activity, food consumption, and energy expenditure before and after HFD feeding. Energy expenditure and food intake data were normalized with respect to lean body weight. Energy expenditure and RQ were calculated from the gas exchange data.

Body composition

Fat and lean body masses were assessed by ^{1}H magnetic resonance spectroscopy (Bruker BioSpin, Billerica, MA) before and after mice were subjected to an HFD.

Quantitative PCR (qPCR) analysis

Total RNA was extracted using a total RNA purification system (Invitrogen) following to the manufacturer's protocol. Extracted mRNA was reverse-transcribed using AccuPower® CycleScript RT PreMix (Bioneer). Quantitative PCR was performed with SYBR Green dye using the ABI Step One Real Time PCR instrument (Applied Biosystems, Cheshire, U.K.). For relative quantification of gene expression, we used the comparative Ct method (ΔΔCt). Results were normalized to the control gene (36B4). The

specific primers sequences used for PCR are listed in Supplementary Table 1.

Biochemical assay

Serum epinephrine was determined using a commercially available ELISA kit according to the manufacturer's instructions (Abnova, Taipei, Taiwan). Serum triglyceride, total cholesterol, HDL-cholesterol and LDL-cholesterol concentrations were analyzed by Cobas c111 (Roche). Adipokines, including adiponectin, leptin, IL-6, MCP1, PAI-1, and TNF-α were measured using MILLIPLEX™ MAP kits (Merck Millipore, Germany) according to the manufacturer's instructions.

Oil red O staining

Oil red O staining was performed on day 8 following adipogenesis induction. Cells were washed and fixed with 4% paraformaldehyde. The cells were then washed with 60% isopropanol, dried completely, and stained with oil red O (6 parts of 0.5% oil red O powder in isopropanol and 4 parts water) for 10 min and washed with phosphate-buffered saline.

GEO search for AHNAK expression

We used the GEO (Gene Expression Omnibus) database to assess AHNAK expression differences in obesity. In this study, we used only GEO dataset (GDS)- samples that were already curated. Those datasets contained normalized expression values for each gene from each sample. Total 30 GDS samples were searched in GEO. The differential expression of the Ahnak gene was identified by t-test method and a P value < 0.05.

Statistics

All values were expressed as the mean± SEM. Statistical analysis was performed using the Student's t-test between two groups. $P<0.05$ was considered significantly.

1.3. Results

1.3.1. Requirement of AHNAK for adipocyte differentiation in vitro

To study the potential correlation between AHNAK expression and obesity in humans, we analyzed existing GEO data. AHNAK expression was significantly increased in both subcutaneous mature adipocytes (GDS 1495, $P<0.01$) and omental adipose tissues (GDS 3688, $P<0.05$) from obese subjects (Figure 1-3A). The *AHNAK* mRNA levels in normal (B6) and obese (Ob/Ob) mice markedly increased in the SVF of WAT, which contains multipotent mesenchymal stem cells (Figure 1-3B). AHNAK expression was also decreased during adipocyte differentiation in 3T3-L1 cells (Figure 1-3C), where fully differentiated cells contained mainly adipocytes. C3H10T1/2 cells transfected with *AHNAK*-specific siRNA, were stained with oil red O to examine lipid accumulation (Figure 1-4A,B). We found that the expression of *C/ebp* family members *Pparγ*2, aP2, and adiponectin significantly decreased during adipogenesis following *AHNAK* silencing, relative to that observed in control-siRNA transfectants (Figure 1-4C). Consistently, ADSCs from KO mice showed significantly inhibited formation of lipid-containing adipocytes (Figure 1-4D). The adipogenic markers were significantly suppressed in AHNAK deficient ADSCs (Figure 1-4E). Formation of lipid-laden droplets was apparently reduced in fully differentiated 3T3-L1 cells by transfection with *AHANK*-specific siRNA (Figure 1-4F). Thus, AHNAK expression in the SVF in WAT may explain

the low efficiency of mature adipocyte differentiation observed in AHNAK-deficient mesenchymal stem cells and the reduced adiposity of *AHNAK* KO mice.

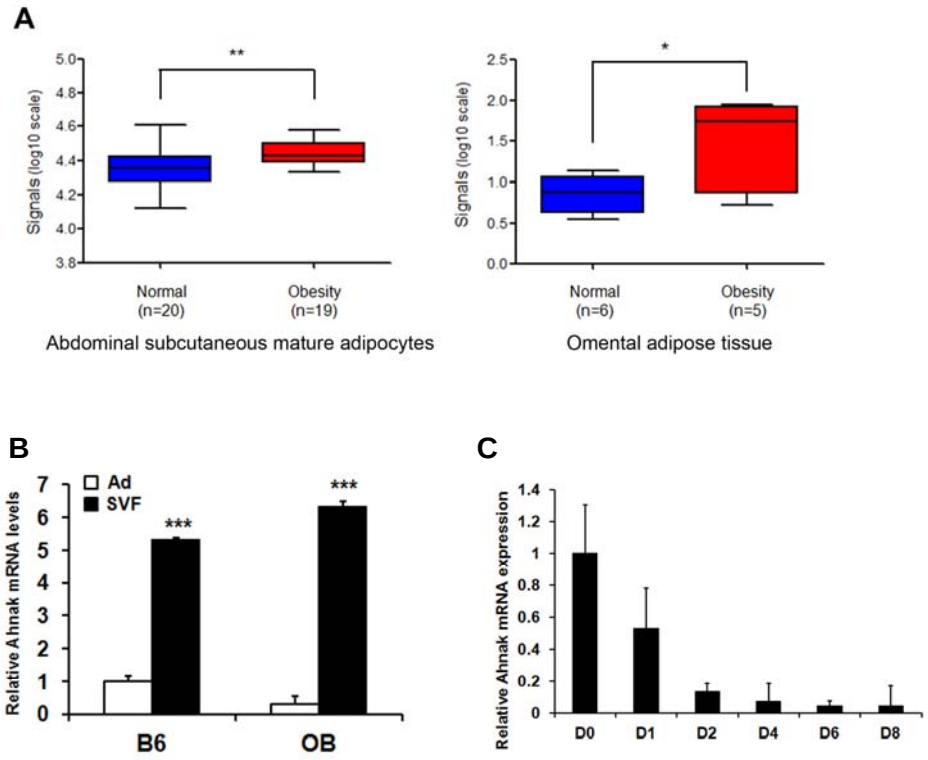

Figure 1-3. AHANK expression in adipose tissue.

(A) AHNAK expression of obese human subjects. (B) mRNA expression of *AHNAK* in the adipocyte fraction (Ad) and stromal vascular fraction (SVF) of eWATs (n=4). (C) mRNA expression of *AHANK* during adipogenesis in 3T3-L1 cells. The data shown are means±SEM, **P*<0.05, ***P*<0.01, ****P*<0.001 between WT and KO mice.

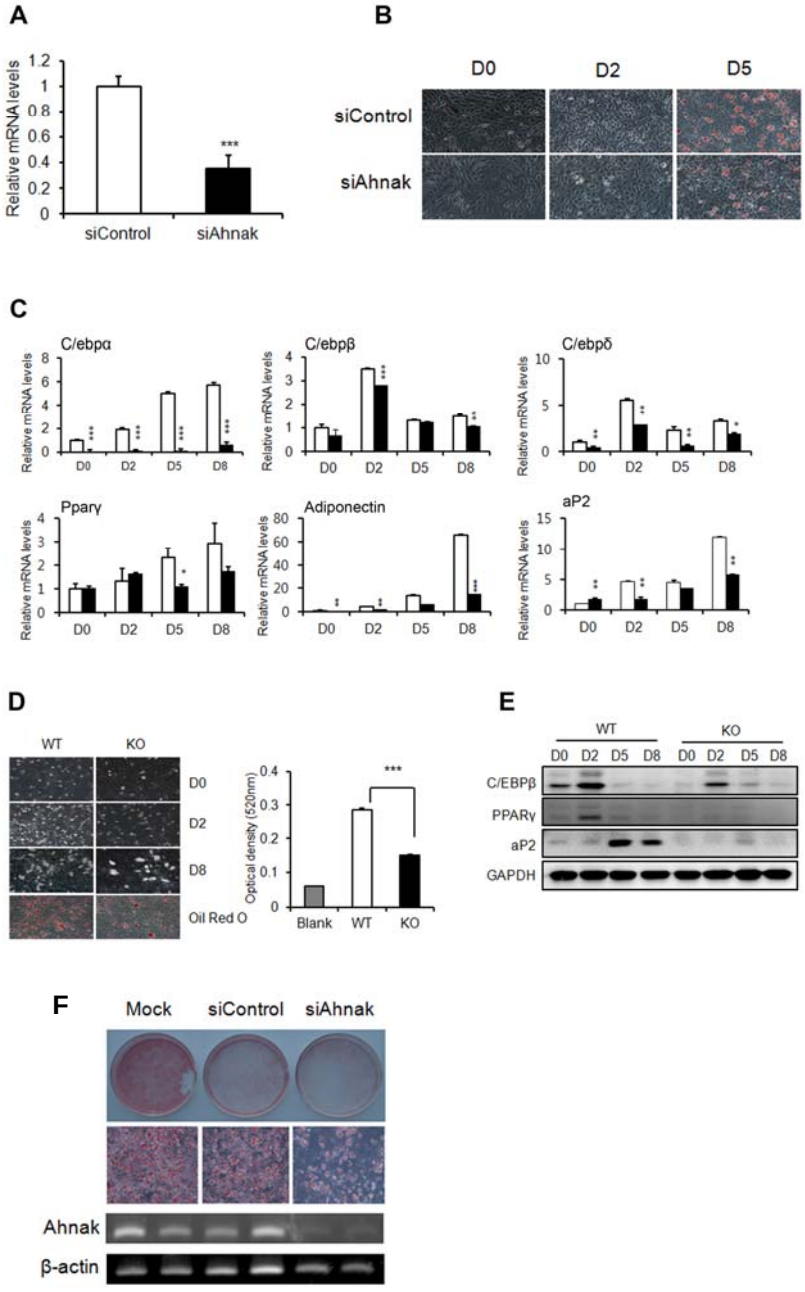
A
Relative mRNA levels
1.2
1
0.8
0.6
0.4
0.2
0
***
siControl
siAhnak
B
D0
D2
D5
siControl
siAhnak
C
C/ebpα
C/ebpβ
C/ebpδ
Pparγ
Adiponectin
aP2
Relative mRNA levels
D0
D2
D5
D8
D
WT
KO
D0
D2
D8
Oil Red O
Optical density (520nm)
0.4
0.3
0.2
0.1
0
***
Blank
WT
KO
E
WT
KO
D0 D2 D5 D8 D0 D2 D5 D8
C/EBPβ
PPARγ
aP2
GAPDH
F
Mock
siControl
siAhnak
Ahnak
β-actin

Figure 1-4. AHNAK plays a role in adipogenesis in vitro.

(A) C3H10T1/2 cells were transfected with control siRNA and *AHANK* siRNA. (B) C3H10T1/2 cells underwent adipocyte differentiation, as determined by oil red O staining. (C) Expression levels of adipogenic genes were measured by qPCR. All genes were normalized to *36B4*. (D) Representative pictures showing differentiated ADSCs stained with oil red O at day 8 after the induction of differentiation. (E) Immunoblot analysis of adipogenic proteins from differentiated cells. GAPDH was used as a loading control. (F) 3T3-L1 cells were transfected with siRNA before differentiation induction and subsequently stained with oil red O.

1.3.2. AHNAK is required for SMAD1/5 activation, which is essential for BMP4-dependent adipogenic differentiation

BMP signaling induces the commitment of mesenchymal stem cells into preadipocytes (Huang et al., 2009; Tang et al., 2004). SMAD1/5/8 phosphorylation is critical for BMP4-mediated transcriptional regulation and subsequent commitment to adipocyte differentiation. Thus, we examined whether AHNAK is required for BMP4 signaling. Control C3H10T1/2 cells and ADSCs treated with recombinant BMP4 showed increased SMAD1/5 phosphorylation in a time-dependent manner (Figure 1-5A,B). However, in AHNAK-deficient C3H10T1/2 cells and ADSCs, BMP4-induced SMAD1/5 phosphorylation was repressed (Figure 1-5A,B). Importantly, nuclear pSMAD1/5 translocation occurred following BMP4 treatment in WT ADSCs, but not in KO ADSCs (Figure 1-5C,D). AHNAK protein is also translocated into nucleus following BMP4 stimulation (Figure 1-5E). In addition, the expression of SMAD4, a co-SMAD that binds to R-SMADs such as SMAD1/5/8 to form an active SMAD complex, was suppressed in AHNAK-KO ADSCs after BMP4 treatment, compared to that in WT ADSCs. The early adipogenic transcription factor C/EBPβ showed a similar trend in terms of expression (Figure 1-5C). Our data suggested that the AHNAK protein potentiates BMP4 signaling by interacting with SMAD1. To study this potential interaction, Flag-*Ahnak* and HA-*Smad1* expression vectors were co-transfected into C3H10T1/2 cells and subjected to co-immunoprecipitation with an anti-HA antibody. The transfection of Flag-*Ahnak* expressed vector had no effect on cell viability (Figure 1-6A). These results indicated that AHNAK interacted with SMAD1

in a BMP4-independent manner (Figure 1-6B). Moreover, a proximity ligation assay (PLA) using AHNAK and SMAD1 probes showed that AHNAK-SMAD1 complexes were detected as fluorescent spots, both in BMP4-treated and vehicle-control cells (Figure 1-6C). BMP2/4-SMAD signaling induced adipogenic commitment, which regulates PPARγ expression (Hata et al., 2003; Huang et al., 2009). We thus evaluated the effects of AHNAK on SMAD1-dependent *Pparγ2* transcriptional regulation using a chromatin immunoprecipitation (ChIP) assay. The ChIP complex detected with an anti-SMAD1 antibody revealed significantly increased association with the Smad-binding element (SBE) in the *Pparγ2* promoter following BMP4 treatment in control siRNA-transfectants. However, *Ahnak*-downregulated cells did not exhibit a SMAD1-bound *Pparγ2* promoter DNA fragment (Figure 1-6D). These results indicate that AHNAK is required for SMAD1 activation and SMAD1 binding to the *Pparγ2* promoter.

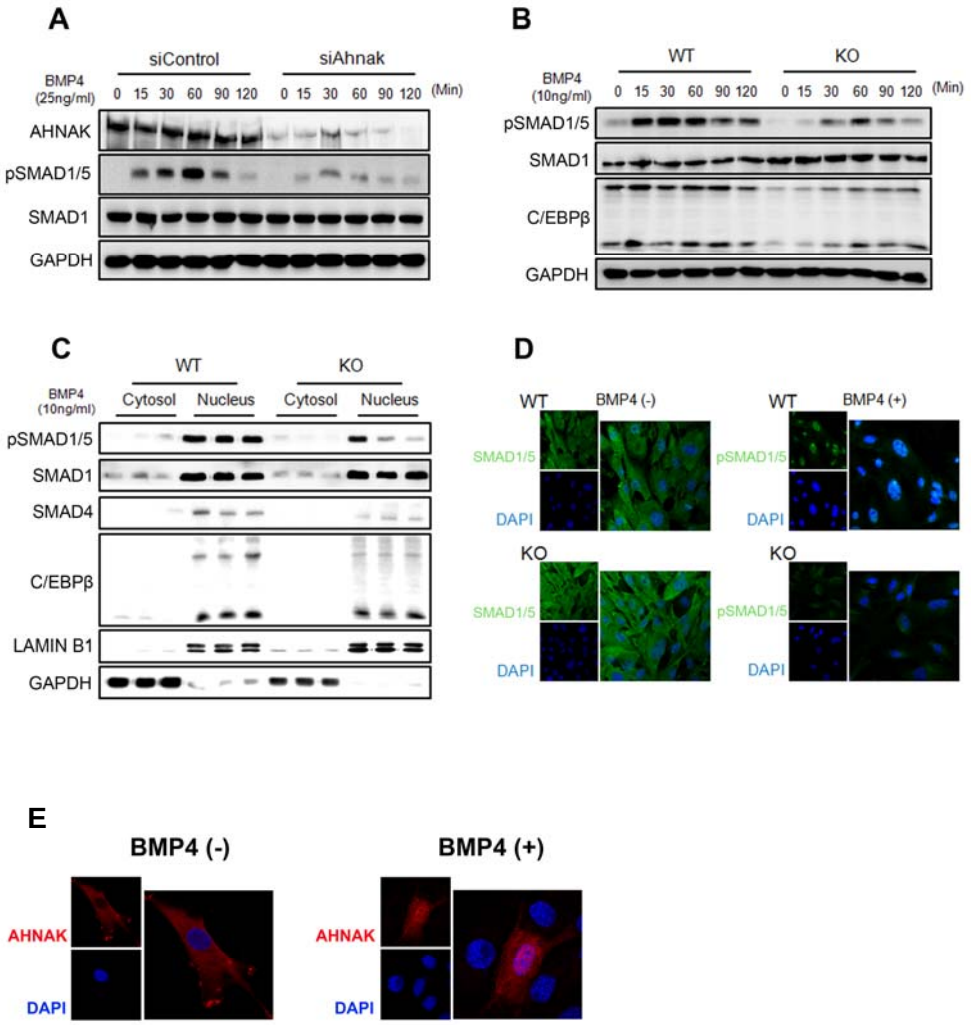

Figure 1-5. AHNAK is required for SMAD1/5 activation, which is essential for adipogenic effects caused by BMP4 signaling. (A, B) Following BMP4 stimulation of C3H10T1/2 cells (A) and ADSCs (B) for the indicated times, the levels of indicated proteins were measured by immunoblotting. (C) Following BMP4 treatment for 1h, cell lysates from ADSCs were subjected to nuclear and cytoplasmic fractionation. Proteins from each fraction were studied by immunoblot

analysis. LAMIN B1 and GAPDH were used as nuclear and cytoplasmic markers, respectively. (D) Immunofluorescence staining showing the subcellular localizations of SMAD1/5 in ADSCs. DAPI was used for nuclear staining. (E) The subcellular localizations of Ahnak in C3H10T cells. DAPI indicates nuclear staining.

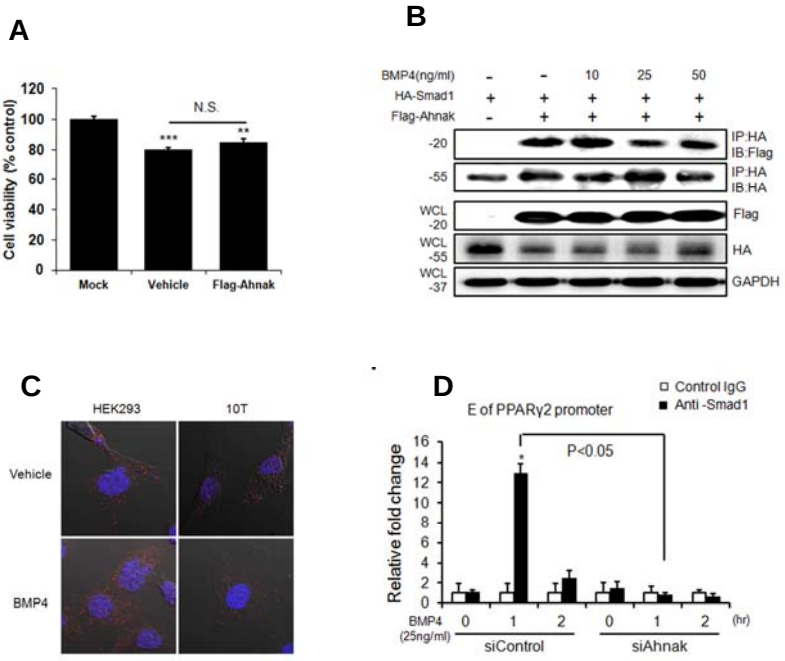

Figure 1-6. Effects of AHNAK on SMAD1-dependent *Pparγ2* transcriptional regulation.

(A) Cell viability following transfection of Flag AHANK expressed vector in C3H10T cells. **P*<0.05, ***P*<0.01, ****P*<0.001 vs Mock.(B) C3H10T1/2 cells were transfected with plasmids expressing Flag-*AHNAK* and HA-*SMAD1*, after which the cells were incubated without or with BMP4 for 60 min. (C) Interaction between AHANK and SMAD1. The AHNAK-SMAD1 complexes were detected as spots in situ Duolink PLA. (D) DNA-protein complexes from C3H10T1/2 cells were immunoprecipitated with an anti-SMAD1 antibody or a control IgG. Enrichment of the DNA fragment containing SMAD-binding sites on the *Pparγ2* promoter was evaluated by qPCR. The data shown are the mean values ± SEM, **P*<0.05, ***P*<0.01, ****P*<0.001 vs Mock.

1.3.3. AHNAK ablation attenuates adiposity in mice

The tissue distribution of Ahnak was examined in C57BL/6 mice by qPCR analysis. AHNAK mRNA was abundantly expressed in white adipose tissue (WAT), brown adipose tissue (BAT), heart, and lung tissue (Figure 1-7A). To determine the expression of AHNAK in different fat depots, multiple adipose tissues were classified as visceral (vis), subcutaneous (subQ) and brown fat (BAT). Notably, AHNAK was significantly increased in two visceral fat (epididymal, and mesenteric) compared to subQ and BAT (inguinal and axillary) (Figure 1-7B). AHNAK gene expression was significantly elevated in BAT, epididymal (eWAT) and inguinal (iWAT) fat depot in a high fat diet (HFD) fed mice compared to mice fed a regular chow (RC) diet (Figure 1-7C). To elucidate the physiological role of AHNAK in vivo, we maintained $Ahnak^{-/-}$ (KO), $Ahnak^{+/-}$ (hetero) mice, and WT littermates. No differences in body weights were observed between WT and hetero mice (Figure 1-7D). However, at 18 weeks of age, Ahnak KO mice had gained markedly less weight, compared to theWT controls fed either RC or an HFD (Figure 1-7E). Furthermore, *AHNAK* KO mice had significantly reduced body fat contents and major fat pads of KO mice were significantly smaller than those of WT mice (Figure 1-8A, B). Adipocytes in KO mice contained a higher frequency of small adipocytes and a lower frequency of mid- and large-sized adipocytes than their WT counterparts (Figure 1-8C). In agreement, the expression of adipogenic-related genes such as Pparγ2, a key regulator of adipogenesis; aP2, a late adipocyte differentiation marker; and adiponectin, were reduced in eWAT from HFD-

fed KO mice compared to WT mice. Furthermore, the expression of genes related to lipid metabolism, including Dgat2, Plin2, CD36, Lpl, and Hsl was significantly decreased in eWATs from HFD-fed KO mice (Fig. 1-8D).

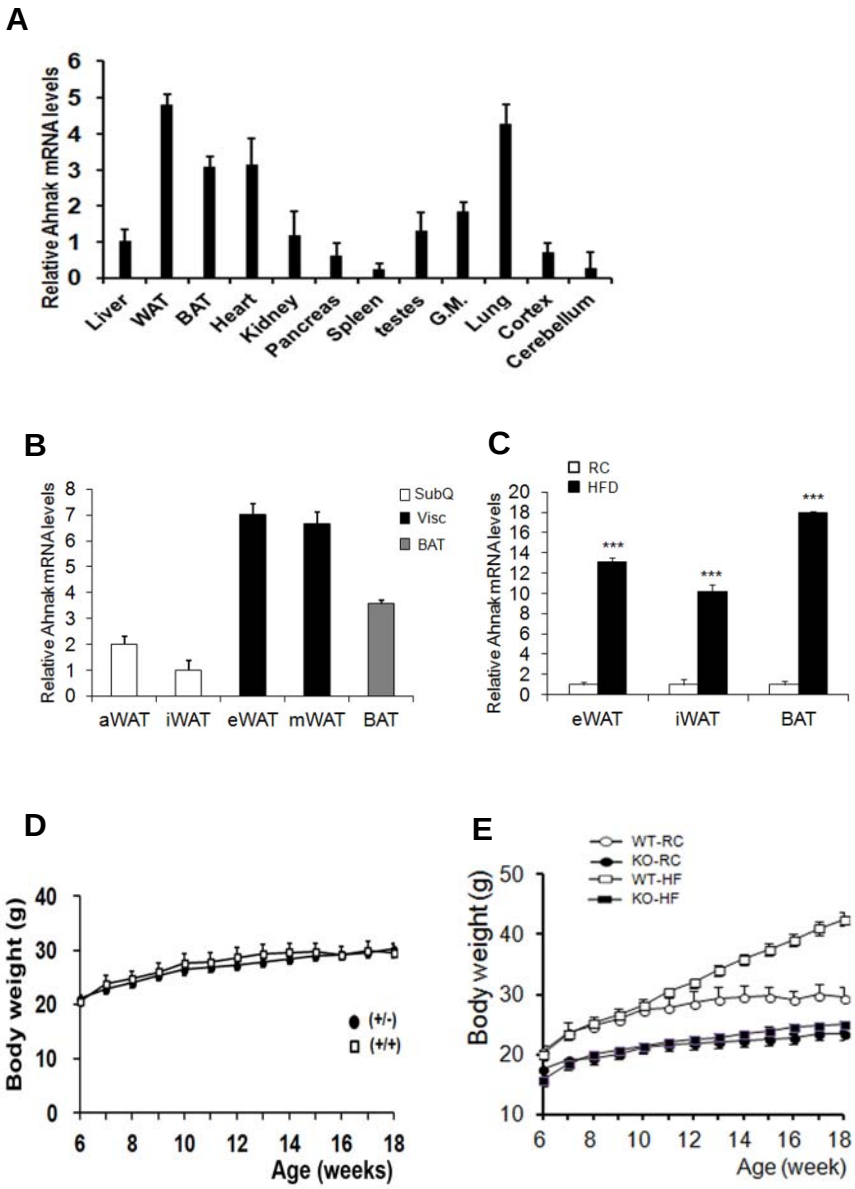

Figure 1-7. Role of AHNAK in obesity. (A) AHNAK expression in various tissues from 6-week-old C57BL6 mice (n=4–6). Values were normalized to Gapdh. (B) *AHNAK* mRNA expression by qPCR analysis from multiple adipose tissues

from 10-to12-week old male wild-type mice(n= 4) and normalized to 36B4. (C) *AHNAK* mRNA in epididymal WAT, inquinal WAT and BAT from wild-type mice fed RC or HFD (n=5-7 per group). (D) Comparison of body weights from wild type ($Ahnak^{+/+}$) and hetero($Ahnak^{+/-}$) mice (n=3). (E) Changes in body weights during 12 weeks of feeding on RC or an HFD; n = 3 for WT and KO mice on regular chow diet (RC), n = 4 for WT and KO mice on HFD.

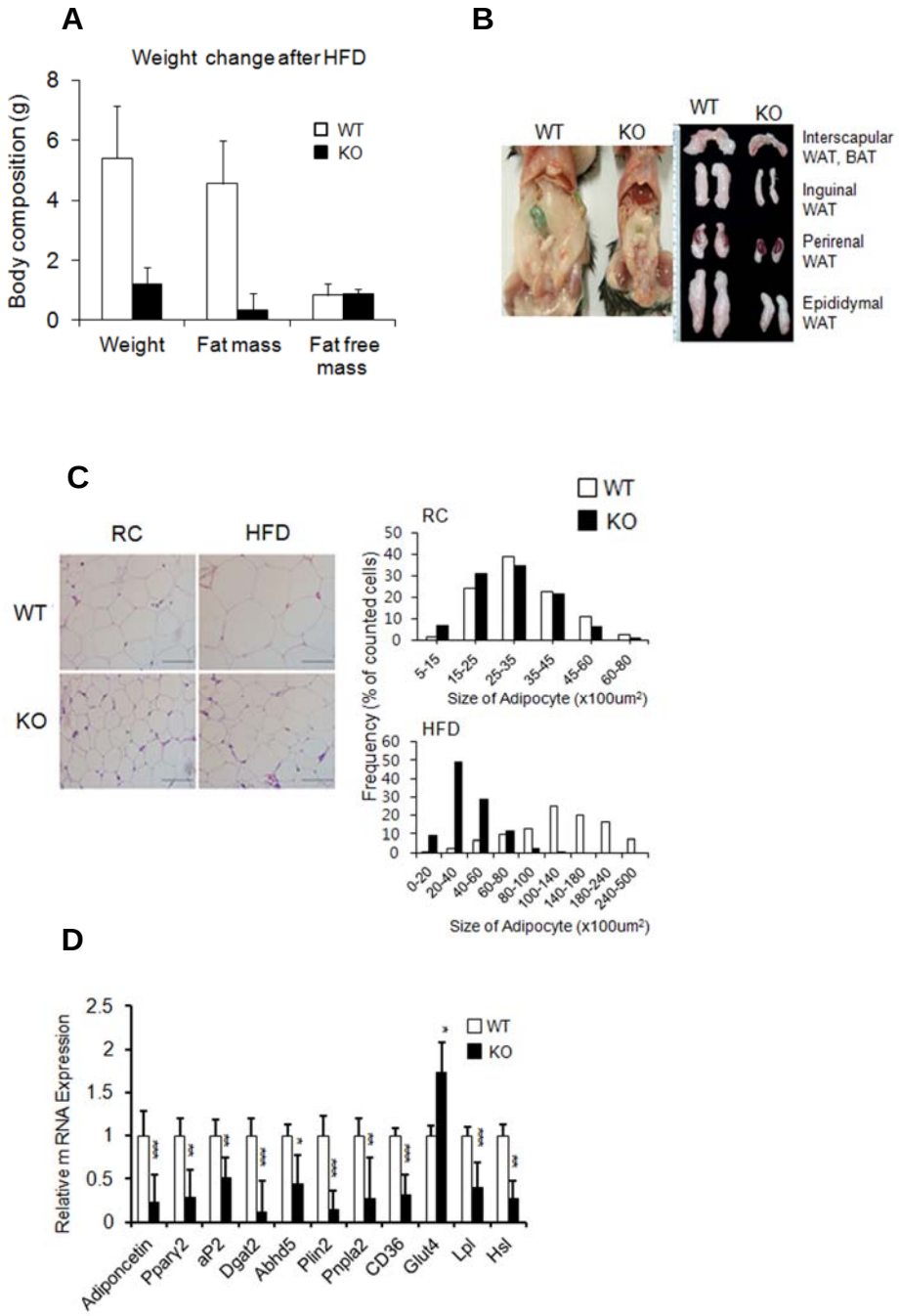

Figure 1-8. Effect of AHNAK ablation in fat tissue.

(A) Changes of body composition of WT and KO mice fed HFD analyzed by MRS (n=7-9). (B) Representative pictures of fat pads from mice fed an HFD. (C) H&E staining (left) of eWAT and distribution of adipocyte sizes (right); *n*=3 Scale bar, 200μm. (D) Relative mRNA levels of the indicated genes in WATs were measured by qPCR. Values were normalized to *36B4*. WT: *n*=5, KO: *n*=8 The data shown are the mean±SEM. **P*<0.05, ***P*<0.01, ****P*<0.001 between WT and KO mice. eWAT, epididymal white adipose tissue.

1.3.4. AHNAK KO mice are resistant to detrimental effect of obesity

Gene profiling of eWAT from HFD fed *AHNAK* KO mice showed downregulation of inflammation mediated genes. On the other hands, insulin signaling, glucose metabolism, and thermogenic related genes are increased in *AHNAK* KO mice (Figure 1-9A). Consistent with gene profile analysis, macrophage infiltration in adipose tissue was evaluated by immunohistochemical staining using *Mac-2* antibody. *AHNAK* KO mice showed less abundant macrophage infiltration (Figure 1-9B). To determine the source of this signal, we investigated inflammation related gene expression. Expression levels of inflammatory genes, such as CD68, F4/80, monocyte chemoattractant protein-1 (MCP1), IL6, and TNF-α were significantly down-regulated in eWAT of HFD-fed *AHNAK* KO mice with activation of M2 macrophage specific transcripts, including macrophage galactose N-acetyl-galactosamine specific lectin 2 (Mgl2), mannose receptor, C type 2 (Mrc2) and *IL10* (Lumeng et al., 2007; Yadav et al., 2011)(Figure 1-9C). AHANK ablation was also accompanied by a significant reduction of proinflammatory mediators such as IL-6, MCP-1, and PAI-1 in serum, as observed for adipose tissues (Figure 1-9D).

To assess the systemic effect of reduced adiposity in *AHNAK* KO mice, we measured lipid metabolism parameters in serum. The triglyceride levels were reduced in KO mice, although the FFA levels remained unchanged (Figure 1-10A,B). The levels of total and LDL-cholesterol were substantially decreased in HFD-fed KO mice (Figure 1-10C,D). Next, we

performed intraperitoneal GTT to determine the ability to clear glucose, with blood samples from RC- and HFD-fed mice. Glucose tolerance and insulin sensitivity were not significantly different in RC-fed mice (Figure 1-11A,B). However, KO mice fed an HFD displayed lower blood glucose levels under fasting conditions and after glucose administration (Figure 1-11C) than did WT mice. ITTs revealed that the blood-glucose lowering effect of insulin was slightly better in KO mice (Figure 1-11D). Key mediators of insulin signaling were examined to clarify the mechanisms of improved glucose metabolism in KO mice fed a HFD. The phospho-AKT levels in WAT, BAT, and gastrocnemius muscle, and phospho-IRb levels in liver increased in HFD-fed KO mice after insulin stimulation (Figure 1-12A-D). Taken together, these results indicated that AHNAK-deficiency caused reduced adiposity and increased glucose tolerance and insulin sensitivity.

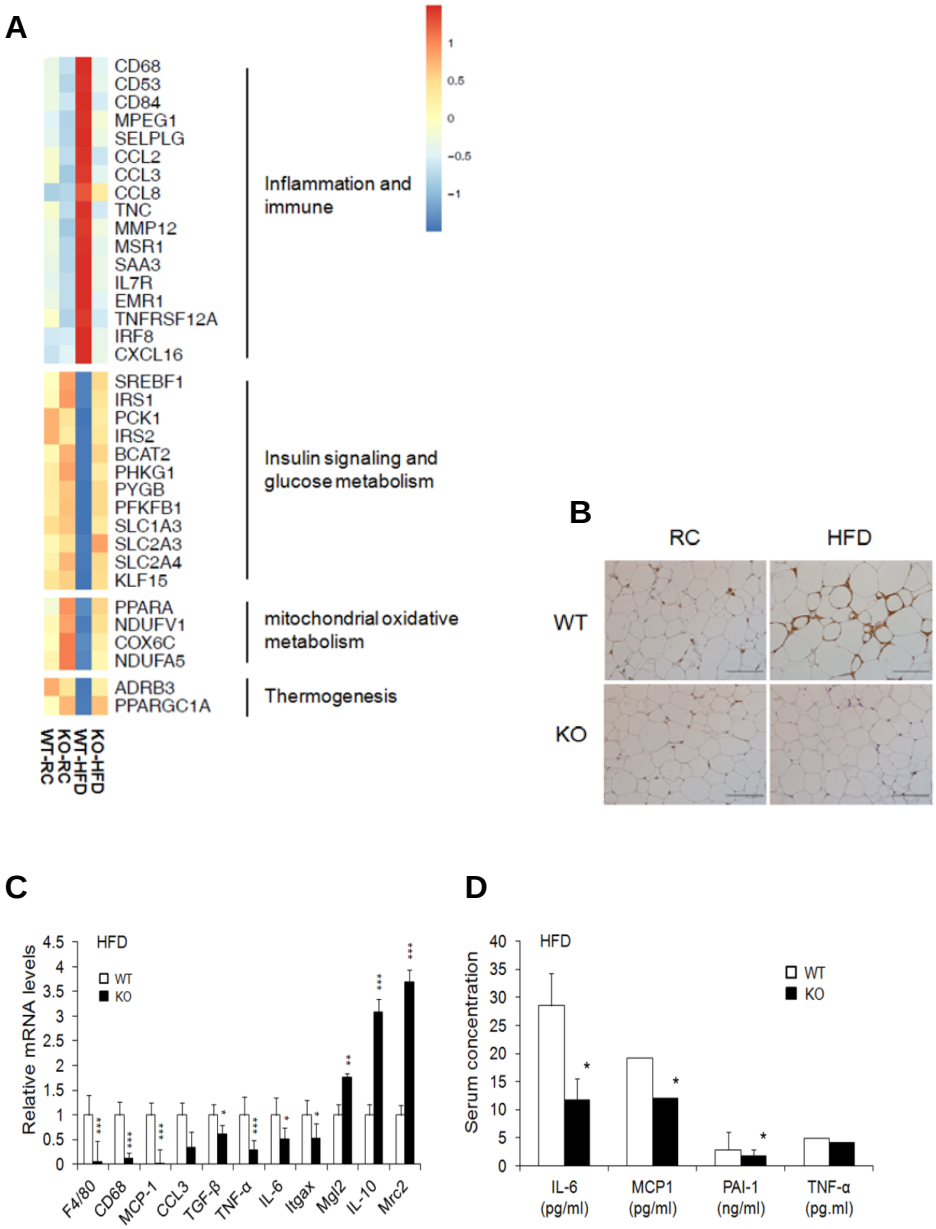

Figure 1-9. Resistance to detrimental effect of obesity in *AHNAK* KO mice.

(A) Representative gene expression profiles displaying differentially expressed

gene in eWAT from RC-or HFD-fed WT and KO mice (full dataset available online as NCBI GEO data set GSE37218). (B) Representative pictures of immunostaining of eWAT with antibody to Mac-2 (C) mRNA expression of inflammatory-related genes in mice fed HFD (n = 6-9). (D) Serum biochemistry of inflammatory profiles in overnight fasted mice fed HFD (n=5-9).

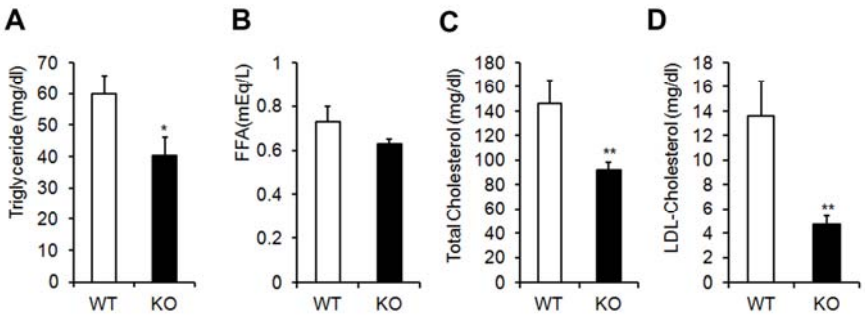

Figure 1-10. Serum lipid profiles from AHNAK KO mice.

(**A**) Serum triglyceride. (**B**) FFA. (**C**) Total cholesterol. (**D**) LDL-cholesterol in WT and KO mice on an HFD. Serum levels were measured after a 16-h fasting period; *n* = 9/group (a-d). The data shown are the mean±SEM. **P*<0.05, ***P*<0.01, ****P*<0.001 between WT and KO mice.

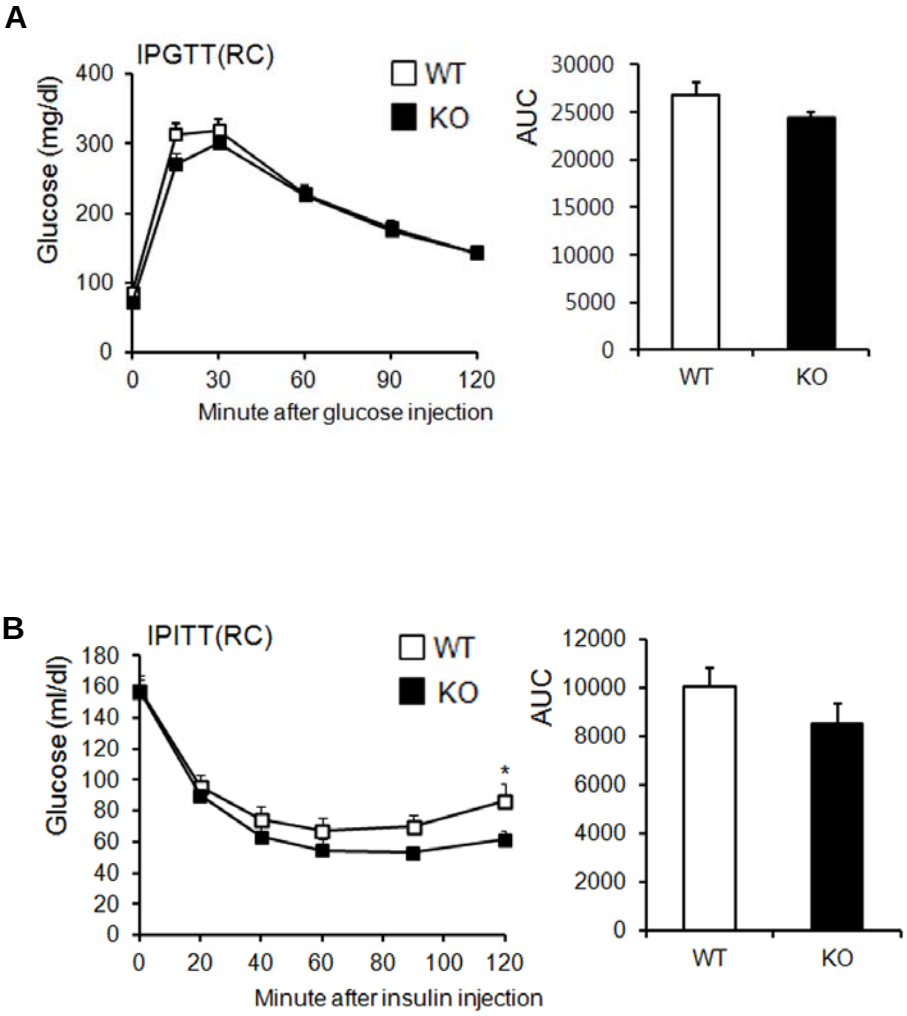
A
IPGTT(RC)
WT
KO
Glucose (mg/dl)
400
300
200
100
0
0
30
60
90
120
Minute after glucose injection
AUC
30000
25000
20000
15000
10000
5000
0
WT
KO
B
IPITT(RC)
WT
KO
Glucose (ml/dl)
180
160
140
120
100
80
60
40
20
0
0
20
40
60
80
100
120
Minute after insulin injection
*
AUC
12000
10000
8000
6000
4000
2000
0
WT
KO

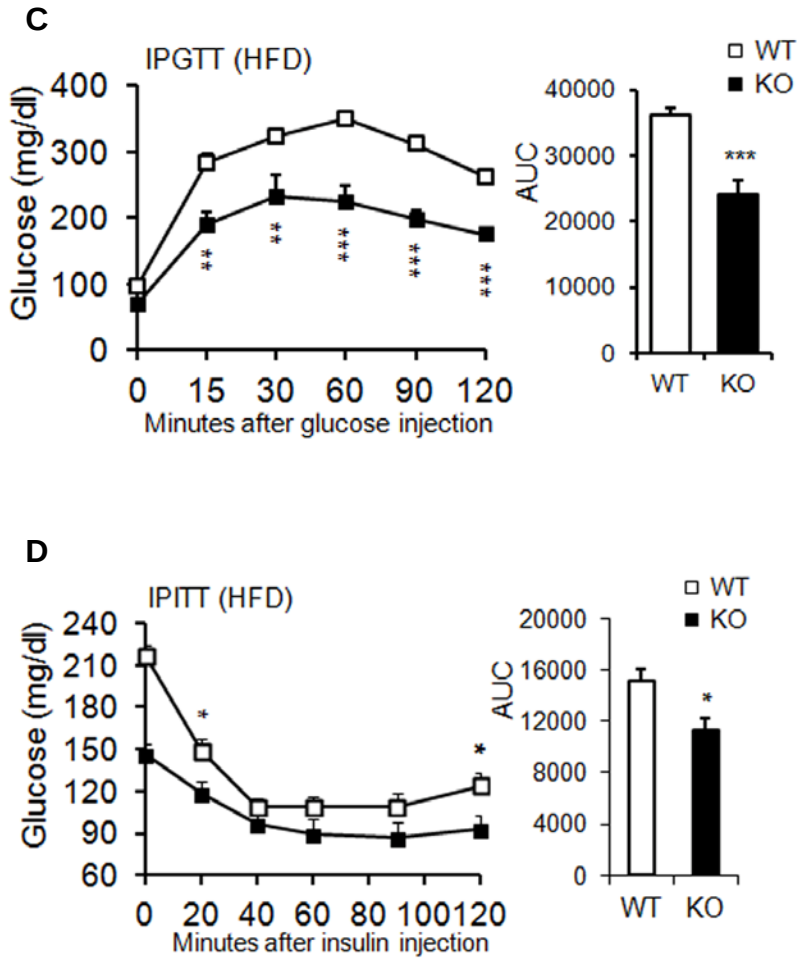

Figure 1-11. *AHNAK* KO mice exhibit enhanced glucose tolerance and insulin sensitivity.

(A) Glucose tolerance after feeding on RC; WT: *n*=6, KO: *n*=4. (B) Insulin tolerance after of feeding on RC; WT: *n*=4, KO: *n*=6. (C) Glucose tolerance after an 8-week HFD; *n* = 9 for WT and n = 6 for KO mice. (D) Insulin tolerance after an 8-week HFD; *n* = 6 for WT and n = 6 for KO mice. The data shown are the mean values ± SEM, **P*<0.05, ***P*<0.01, ****P*<0.001 between WT and KO mice.

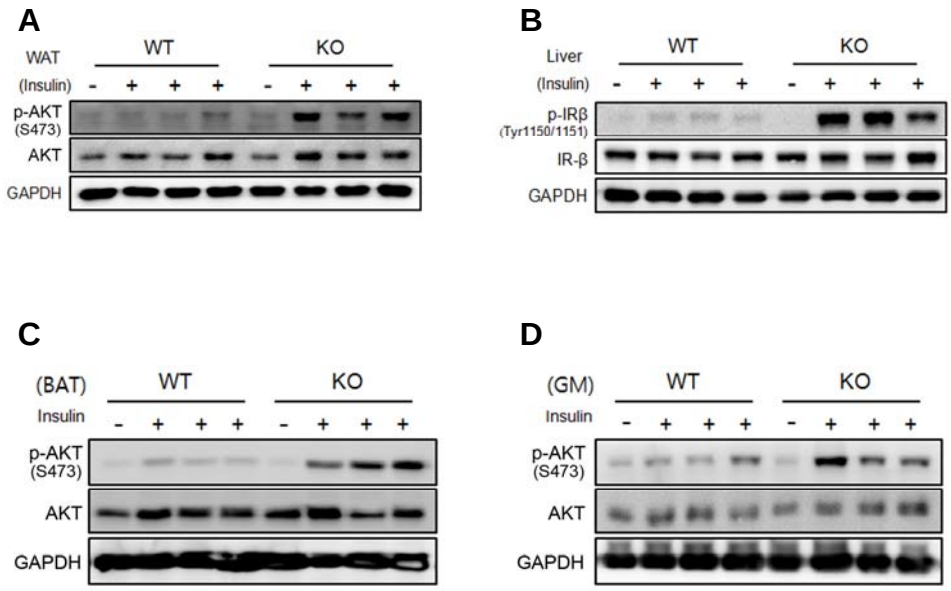

Figure 1-12. Insulin signaling pathway in *AHNAK* KO mice.

HFD fed *AHNAK* KO mice and WT littermates were fasted overnight and then administered insulin (1.5U/Kg fo body weight) intraperitoneally. (A) eWAT, (B) liver, (C) BAT, and (D) gastrocnemius muscle (GM) were removed 10min after insulin injection.

1.3.5. *AHNAK* KO mice show increased energy expenditure

Changes in body weights often correlate with energy-balance alterations. The amount of calorie uptake/h in both RC- and HFD-fed mice was unaltered when normalized to body weight (Figure 1-13A). Serum leptin levels decreased in HFD-fed KO mice, despite their similar food intake (Figure 1-13B). These data suggested that leptin sensitivity was enhanced in KO mice and that the reduction in leptin levels in KO mice resulted from a reduction in fat mass, as leptin levels are associated with fat mass (Maffei et al., 1995). Despite similar food intake levels between the two groups, KO mice showed greater leanness and resistance to HFD-induced obesity. We thus hypothesized that KO mice have an increased metabolic rate or physical-activity rate. KO mice showed a slightly decreased level of activity (Figure 1-13C). Oxygen consumption and heat generation in KO mice were significantly increased compared to those of WT controls (Figure 1-13D,E). The RER remained unchanged in both groups (Figure 1-13F).

To confirm the effect of AHNAK ablation in WAT and BAT, we analyzed thermogenic gene expression profiles by qPCR. Thermogenic related genes, including Ucp1, Pgc-1α, Cidea, Cpt2, and Adrb3, were significantly increased in eWAT and iWAT of HFD-fed *AHNAK* KO mice (Figure 1-14A,B). Notably, ablation of AHANK leads to upregulation of Adrb3 expression, which is essential for the regulation of adaptive thermogenesis and oxidative metabolism (Lowell and Bachman, 2003). Furthermore, histologic evaluation of BAT displayed slightly reduced lipid-droplet accumulation in KO mice, compared to that in WT mice fed either

RC or an HFD (Figure 1-15A). However, the BAT weights between the two groups were comparable (Figure 1-15B). The expression of thermogenic genes was unaffected in BAT of KO mice fed a HFD, compared with that of WT mice (Figure 1-15C). These findings suggest that AHNAK ablation in WAT protects mice from obesity and its related complication accompanied by elevating energy expenditure.

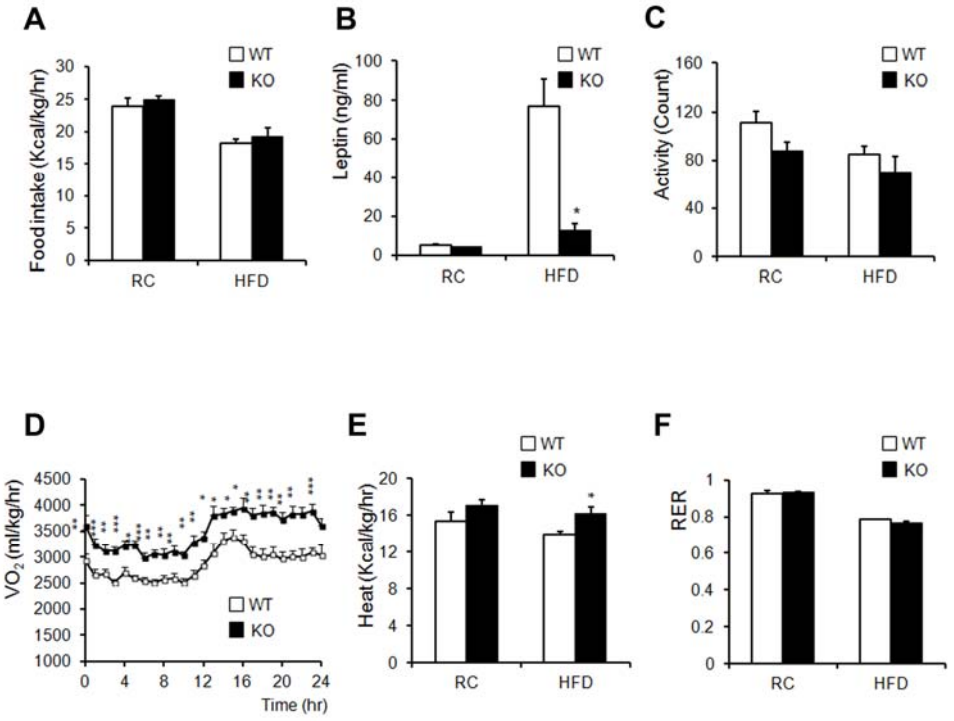

Figure 1-13. *AHNAK* KO mice display increased energy expenditure.

(A) Food intake (WT: n = 6, KO: n = 5). (B) Serum leptin concentrations (n=4). (C) Measurement of locomotor activity (WT: n=6, KO: n=5). (D) Whole-body oxygen consumption (VO_2) over the course of 24 h (WT: n=6, KO: n=5). (E) Average value of heat generation (WT: n=6, KO: n=5). (F) The respiratory exchange rate was calculated as CO_2 production/O_2 consumption (WT: n=6, KO: n=5). (G) Relative mRNA expression of genes involved in energy dissipation and in brown adipose-specific genes in WAT, as measured by qPCR (n=6). Values were normalized to *36B4* expression. The data shown are the mean±SEM; *P<0.05, **P<0.01, ***P<0.001.

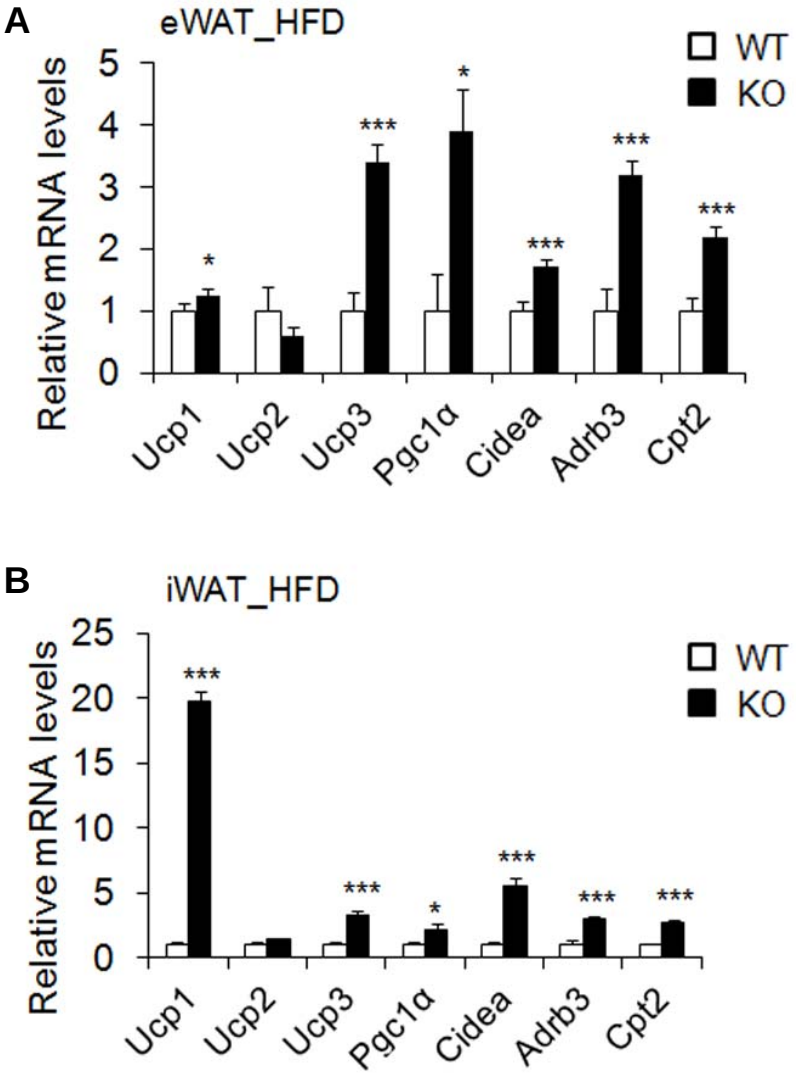

Figure 1-14. mRNA expression of thermogenic genes in eWAT (A) and iWAT (B) from HFD fed WT and KO mice (n=5). The data are presented as the means ± SEM. *P < 0.05, **P < 0.01, ***P < 0.001, wild-type (WT) versus *Ahnak*$^{-/-}$ (KO) mice.

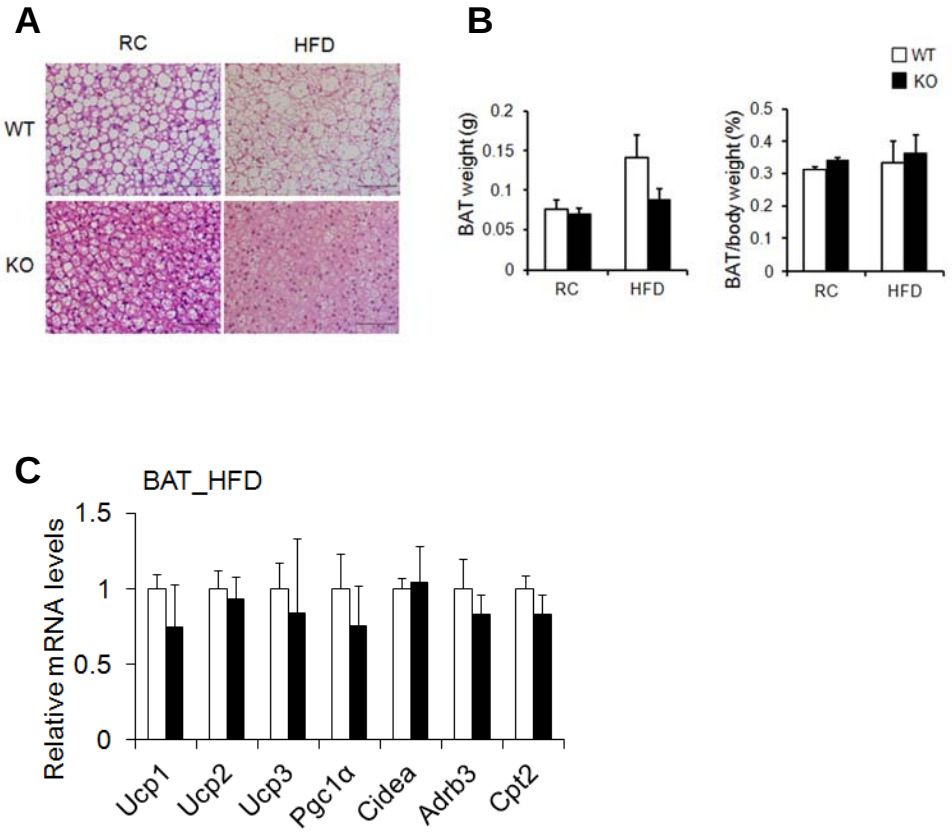

Figure 1-15. Phenotypic characteristics of BAT in *AHNAK* KO mice.

(A) H&E staining of BAT. Scale bar, 200 μm; (B) Quantification of BAT mass (left) and BAT mass normalized by body mass (right); WT: *n*=5, KO: n=4. (C) Relative mRNA expression involved in energy dissipation and brown adipose specific genes in BAT measured by qPCR from mice fed an HFD for 12 weeks (n=5). Values were normalized to *36B4* expression. The data shown are means±SEM; **P*<0.05, ***P*<0.01, ****P*<0.001

1.4. Discussion

The physiological functions of AHNAK in adipose tissues have been unclear, although AHNAK is highly expressed in WAT. Here, we provide evidence that AHNAK acts as a critical regulator of adipogenesis *in vitro* and *in vivo*. Studies on the role of Ahnak in adipose tissue have reported conflicting results. Alli and coworkers claimed that decreased AHNAK1 expression observed during adipocyte differentiation in 3T3-L1 cells indicated that AHNAK negatively regulates adipogenesis (Alli and Gower, 2009). In contrast, *AHNAK* gene expression was increased 6-fold in adipose tissue during early-phase obesity in rats (Li et al., 2002). Previous findings have demonstrated elevated AHNAK levels in WAT from mice with genetically or environmentally induced obesity (Li et al., 2002; Ramdas et al., 2015). Consistent with previous murine-model studies, AHNAK expression significantly increased in the fat tissues of obese human subjects.

Loss of AHNAK resulted in lowered fat-cell formation due to suppressed SMAD1/5 phosphorylation and nuclear translocation. Our results indicated that AHNAK regulates adipocyte differentiation by modulating BMP-induced canonical SMAD signaling. SMAD1 inactivation in AHNAK-deficient ADSCs led to impaired *Pparγ2* transcription. Our data indicate that AHNAK is required for adipocyte differentiation via SMAD11 binding to the *Pparγ2* promoter following BMP4 stimulation. Similar to AHNAK, SCHNURRI-2 interacts with SMAD1 and controls adipogenesis

through *Pparγ2* transcriptional activation (Jin et al., 2006). Although additional studies are required to elucidate the function of AHNAK-dependent SMAD1 signaling in adipose hypertrophy *in vivo*, previous evidence has shown that BMP/SMAD signaling promotes adiposity by Tob2 expression in mice (Takahashi et al., 2012).

Adipose tissue is composed of adipocytes and the stromal vascular fraction, which contains preadipocytes, mesenchymal stem cells, endothelial cells, and macrophages (Riordan et al., 2009). Adipocyte precursor cells in the stromal vascular fraction are capable of differentiation into mature adipocytes (Rodeheffer et al., 2008). BMPs have crucial roles in cell fate-determinations of multipotent mesenchymal stem cells (Gesta et al., 2007). BMPs regulate gene expression of *Runx2*, *Pparγ2*, *Sox9*, and *MyoD*, which are master regulators of lineage determination that control embryogenesis and organogenesis (Blitz and Cho, 2009; Pan et al., 2008; Phimphilai et al., 2006; Reshef et al., 1998; Zehentner et al., 1999; Zhao, 2003). Together, these findings imply that AHNAK present in the stromal vascular fraction of adipose tissue may explain the decreased AHNAK levels observed during adipogenesis, as well as the restricted adipogenic commitment and differentiation in AHNAK-KO mice. However, it remains unclear how AHNAK controls BMP4/SMAD1 signaling during mesenchymal differentiation into other cell types, such as the osteogenic, chondrogenic, and myogenic lineages. Furthermore, it would be interesting to determine whether AHNAK regulates BMP4 signal transduction via other inhibitory mechanisms such as BMP receptors, I-SMAD (SMAD6/SMAD7), or ubiquitination.

Previous studies reported that AHNAK activates PLC-γ1-PKCa and contributes to mitogenic signaling in response to growth factors (Lee et al., 2008; Lee et al., 2004). The AHNAK protein controls cell cycle progression through c-MYC, which is highly expressed in AHNAK deficient MEF cells (Lee et al., 2014). Cell proliferation, arrest, cell-cycle re-entry, and differentiation by hormonal stimulation are crucial processes during adipogenesis (Fajas, 2003). Consistently, increased levels of c-MYC lead to the inhibition of adipocyte differentiation by blocking cell cycle arrest in 3T3-L1 cells (Reichert and Eick, 1999). Therefore, it would be interesting to uncover the link between AHNAK and c-MYC in 3T3-L1 cells, which are committed to an adipogenic lineage.

While we focused on the role of AHNAK in adipogenesis, our data also implicate AHNAK in energy and glucose homeostasis. Recent evidence showed that AHNAK expression inversely correlates with oxygen consumption (Parikh et al., 2008b). Whole-body oxygen consumption and energy expenditure were significantly elevated in HFD-fed KO mice accompanied by increased levels of thermogenesis-related genes (*Ucp1*, *Dio2*, and *Adrb3*) and oxidation-related genes (*Pparα* and *Pparβ/δ*) in WAT, but no difference was found in BAT, which mainly controls heat generation. Adiposity influences systemic insulin resistance (Griffith et al., 2010). Here, we demonstrated that AHNAK KO mice are protected against HFD-induced insulin resistance, with reduced fat accumulation. A recent study showed that mice lacking AHNAK were glucose intolerant (Ramdas et al., 2014), and we also found that HFD-fed AHNAK-KO mice displayed markedly lower fasting insulin levels (Fig. 5G). This reduction suggests that the

increased glucose tolerance in AHNAK-KO mice was attributable to insulin sensitivity. Furthermore, our hyperinsulinemic/euglycemic clamp experiments revealed that HFD-fed AHNAK-KO mice displayed increased insulin-mediated suppression of hepatic glucose output, with higher glucose uptake in the peripheral tissues (Shin et al., 2015). In this regard, AHNAK deficiency also resulted in significantly improved glucose-disposal rates with a robust increase in insulin signaling in target tissues. These results may have been due to a difference in the fat contents of the diets. The authors performed their experiments with a lower fat-containing diet than was employed in the current study. Another possibility is that the mice had a different genetic background, which can influence metabolism in mice (Vaillant et al., 2014). While our mutant mice were derived from a C57BL/6 background, their mice originated from BDF1, a cross between female C57BL/6 and male DBA/2. Our mutant mice could display better glucose tolerance and greater responsiveness to insulin, because BDF1 mice are prone to develop obesity-induced diabetes more than B6 mice (Karasawa et al., 2011).

Results from this study demonstrated that AHNAK downregulation protects mice from obesity, hepatosteatosis, and insulin resistance. Furthermore, although AHNAK is implicated in the regulation of energy metabolism and glucose homeostasis, further studies are needed to determine the molecular mechanism whereby AHNAK regulates energy metabolism. We cannot exclude the possibility that AHNAK may influence other tissues or mouse development because we used mice carrying the null mutation. In particular, studying tissue-specific AHNAK inactivation will

likely be useful in that indirect effects may be involved in the overall regulation of adiposity and energy metabolism. Moreover, it should be determined whether AHNAK overexpression contributes to aggravated obesity and metabolic homeostasis.

Chapter II

Increased levels of eosinophils and type II cytokines in WAT mediates the browning and thermogenensis in *AHNAK* KO mice

2.1. Introduction

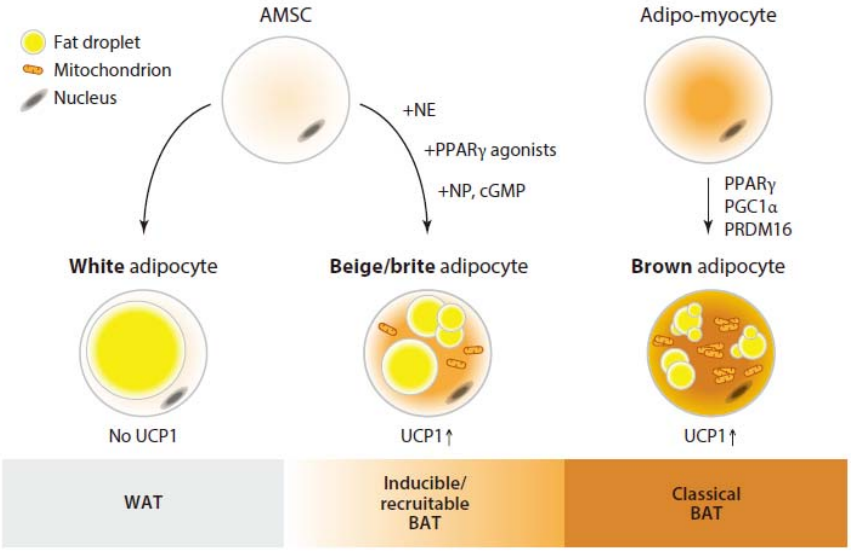

Figure 2-1. Types of adipose tissue. (Pfeifer *et al*. Annu. Rev. Pharmacol. 2015)

Obesity is associated with several metabolic disorders including type 2 diabetes, cardiovascular disease (Despres and Lemieux, 2006; Eckel et al., 2005; Grundy, 2006). Mammalian adipose tissue has been traditionally divided into two distinct types. WAT stores excessive energy in unilocular adipocytes. On the other hands, brown adipose tissue (BAT) dissipates energy through nonshievering thermogenesis in multilocular adipocytes (Cinti, 2001; Harms and Seale, 2013; Rosen and Spiegelman, 2014). Brown adipocytes generate heat and conteract obesity due to

containing abundant mitochondria and UCP1. Recently, alternative type of fat cell termed “beige adipocyte” or “browning” is emerging from several studies (Figure 2-1) (Bartelt and Heeren, 2014; Ishibashi and Seale, 2010; Wu et al., 2012). These beige fat cells exist within white adipose depots and share common morphological and functional features with classical brown adipocytes. Thus, there has been emerging interest in beige fat as an anti-obesity therapeutic potential (Harms and Seale, 2013; Pfeifer and Hoffmann, 2015; Yoneshiro et al., 2013).

Several secreted factors, such as Irisin, BMP8b, T4, natriuretic peptides and noradrenalin that induce browning in WAT have been reported (Figure 2-2) (Bordicchia et al., 2012; Bostrom et al., 2012; de Jesus et al., 2001; Harms and Seale, 2013; Hondares et al., 2011; Nguyen et al., 2011a; Whittle et al., 2012). Previous studies suggest that b-adrenergic signals including noradrenalin and b-adrenergic agonist enhance lipolysis and adaptive thermogenesis (Atgié et al., 1998; Bachman et al., 2002; Granneman et al., 2005; Himms-Hagen et al., 1994). Three adrenergic receptors mediate thermogenesis via sympathetic nerve activation. Of these receptors, especially, β_3 specific adrenergic receptors (Adrb3) alleviated obesity and diabetes (Arch and Wilson, 1996; Kim et al., 2006). Adrb3 are abundant in rodent adipose tissue (Lowell and Bachman, 2003; Nahmias et al., 1991). CL316243, β3 adrenergic receptor agonist has been utilized to mimic the effect of browning (Himms-Hagen et al., 2000; Schulz et al., 2013). CL-316243 in adipocytes stimulates cyclic AMP (cAMP) production, which binds to the protein kinase A (PKA). Activation of PKA has been considered as a mediator for UCP1 and PGC1α expression for

thermogenesis (Cao et al., 2001; Collins et al., 2010).

We recently reported that AHANK KO mice exhibit enhanced insulin sensitivity and higher energy expenditure under high fat diet (Shin et al., 2015). This was accompanied by reduction of whole body fat accumulation. The levels of Ucp1 mRNA were increased in eWAT from HFD fed *AHNAK* KO mice, compared with that of wild-type control mice. Although AHNAK is highly expressed in adipose tissue and increased obese murine models (Li et al., 2002; Ramdas et al., 2014), thermogenic function of AHNAK in adipose tissue has not been determined.

In the present study, we demonstrated that AHNAK ablation results in activation of eosinophils and type 2 cytokines which contribute to browning of WAT depot and promotes energy expenditure by ADRB3 agonist (CL-316243) treatment.

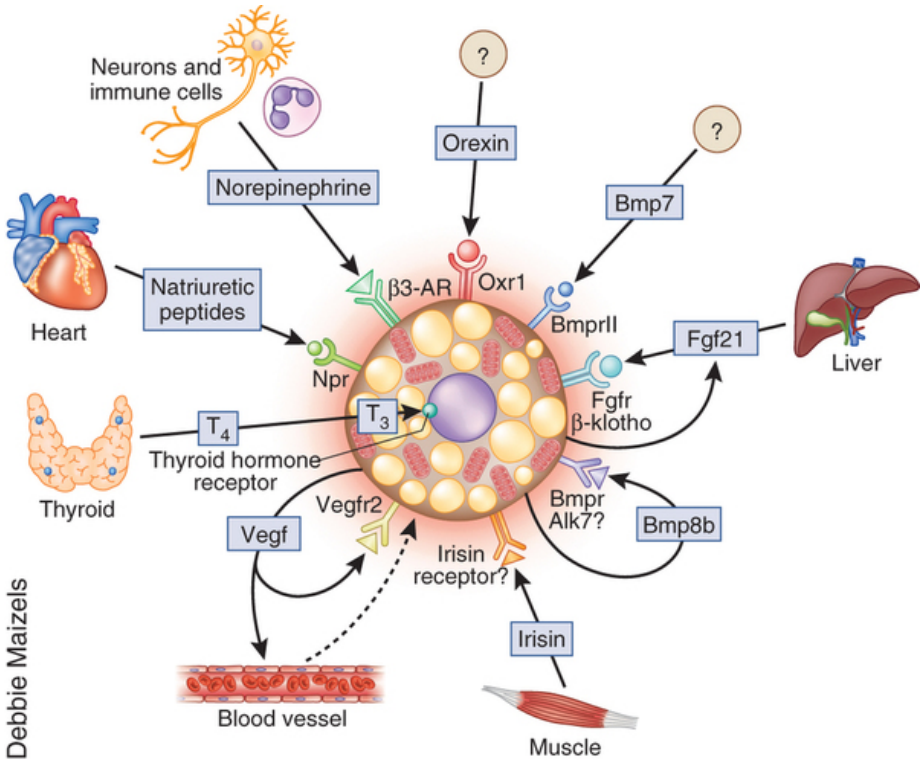

Figure 2-2. Secreted factors that recruit beige adipocytes. (Harms *et al*. Nat Med. 2013)

2.2. Materials and Methods

Animals

AHNAK-KO (*Ahnak*$^{-/-}$) mice were maintained under a 12-h light-dark cycle and had free access to water in a specific pathogen-free barrier facility. Mice were randomly assigned. To stimulate the browning of white adipose depots, 2-3 month-old mice were treated with daily intraperitoneal injections of 1mg/kg bodyweight CL-316,243 (Sigma-Aldrich) dissolved in PBS. The experiments were performed according to the "Guide for Animal Experiments" (Edited by Korean Academy of Medical Sciences) and approved by the Institutional Animal Care and Use Committee (IACUC) of the Seoul National University (Permit Number: SNU-130903-1).

Core body temperature measurement

Body temperature was measured with telemetry transmitters (TSE Systems). A transmitter was implanted into peritoneal cavity under anesthetics.

Indirect calorimetry study

Oxygen consumption (VO2), carbon dioxide production (VCO2), respiratory exchange ratios (RER) and heat production were measured using an indirect calorimetry system (TSE) installed. Mice in each chamber were maintained under 12h light/dark cycle with a constant environmental temperature (22 °C) and free access to food and water.

Immunostaining

Adipose tissue samples were fixed in 4% paraformaldehyde and embedded in paraffin, sectioned and stained. Primary antibodies were incubated overnight at 4℃. Images were captured using a confocal microscope system (LSM 710, Carl Zeiss).

Immunoblotting

For immunoblot analysis, cells were lysed in PRO-PREP buffer (iNtRON Biotechnology Inc., Seoul, Korea) containing a phosphatase-inhibitor cocktail (GenDEPOT, Barker, TX, USA). Protein extracts were separated by sodium dodecyl sulfate-polyacrylamide gel electrophoresis, transferred to a polyvinylidene fluoride membrane (Millipore, Billerica, Massachusetts, USA), and subjected to immunoblot analysis. Immunoblot analysis was performed using the indicated antibodies. Proteins were visualized by ECL chemiluminescence (AbClon, Seoul, Korea). GAPDH was detected as a loading control. Immunoreactive signals were detected through their enhanced chemiluminescence and recorded using the MicroChemi 4.2 system (DNR Bio-Imaging Systems, Jerusalem, Israel).

Antibodies

The primary antibodies used for western blot analysis were specific for: UCP1, PGC1α, CPT2, PPARα, AHNAK, and OXPHOS (oxidative phosphorylation) complexes (all from Abcam); GAPDH (Cell Signaling Technology, Beverly, MA, USA); PDGFRa (R&D Systems, UK); and Tyrosine hydroxylase (Millipore).

DAPI (ImmunoBioScience Co., Washington, USA) was used for nuclear staining.

Cell preparations and flow cytometric analysis

Epididymal white adipose tissues were chopped with scissors for 4 minutes. These are added 2mL Collagenase II (SIGMA C6885, 400U/mL) and incubated at 37℃ for 8 minutes. After digestion, single-cell suspensions were treated with 20μL of 0.5M EDTA and filtered using 70 μm meshes. The cells were centrifuged 385g for 10 minutes at 4℃ to remove floated adipocytes, and red blood cells were lysed by 1X RBC lysis buffer (eBioscience 00-4300-54) for 2 minutes on ice. After blocking Fc receptors using TruStain FcX^{TM} (Biolegend 101320), the cells were stained with the indicated fluorochrome conjugated antibodies. We used an LSRFortessa™ (BD) or FACSCanto™ II (BD), and analyzed flow cytometric data with FlowJo (Tree Star Inc). The antibody used in flow cytometry were PE conjugated PDGFRα (eBioscience 12-1401-81), PE conjugated IgG2a,κ (Biolegend, 400507), PerCP conjugated CD45 (Biolegend, 103130), PE/cy7 conjugated CD11c (Biolegend, 117318), APC conjugated CD11b (Biolegend, CD11b), APC conjugated CD44 (Biolegend, 103012), and BV421 conjugated siglecF (BD Horizon^{TM}, 562681).

Statistics

All values were expressed as the mean± SEM. Statistical analysis was performed using the Student's t-test between two groups. The Kruskal-Wallis Test was used for Flow cytometric analysis. $P<0.05$ was considered significantly.

2-3. Results

2.3.1 AHNAK ablation promotes thermogenic gene program and browning in WAT but not in BAT via β-adrenergic stimulation

To evaluate cold-induced adaptive thermogenesis in *AHNAK* KO mice, they were exposed to an ambient temperature of 4°C for 3 days and compared to the animals kept at thermoneutral conditions (30°C). *AHNAK* expressioin was selectively downregulated in eWAT and iWAT ($p<0.07$) (Figure 2-3A). Similary, the decrease of *AHNAK* mRNA was observed in fully differentiated 3T3-L1 after 6h exposure to 30°C compared with cells kept at 37°C (Figure 2-3B). At 30°C, *AHNAK* KO mice had few UCP1-positive adipocytes and their morphology was similar to that of the wild-type mice. However, after cold exposure, *AHNAK* KO mice demonstrated an increase in multilocular UCP1-expressing adipocytes in eWAT and inguinal iWAT (Figure 2-4). Both eWAT and iWAT but not BAT from AHNAK-deficient cold-exposed mice tended to have higher mRNA levels of thermogenic genes (*Pgc1α*, *Cidea*, *Dio2*, *Cpt1*); in addition, eWAT in these mice was enriched in beige adipocyte markers (*CD137*, *Tmem26*) compared to the wild-type mice after cold exposure (Figure 2-5A–C). These results suggest that *AHNAK* genetic ablation promotes adaptive browning of WAT under environmental stimulation.

The sympathetic nervous system (SNS) plays a critical role in BAT activation and adaptive thermogenesis mediated by β-adrenergic receptors (Lowell and Bachman, 2003; Robidoux et al., 2004). To examine whether β-adrenergic signaling influenced thermogenesis in *AHNAK* KO mice, they were administered CL-316243 (CL), an ADRB3 agonist. We found significantly lower expression of *AHNAK* in the eWAT and iWAT under CL treatment, but not BAT (Figure 2-6A). Histological analysis revealed that CL induced WAT of *AHNAK* KO mice resulted in morphological transformation of unilocular adipocytes to multilocular UCP1-expressing adipocytes, compared with that of wild-type controls. (Figure 2-6B,C). At the mRNA level, the expression of both brown adipocyte related genes (Ucp1, Cidea, Dio2 and Pgc1α) and mitochondrial genes (Cpt1, Cpt2 and Cox8b) was higher in the CL-stimulated eWAT and iWAT of *AHNAK* KO mice than WT mice (Figure 2-7A,B). Immunoblot analysis showed that UCP1, PGC1α and CPT2 were significantly elevated both in eWAT and iWAT from CL-stimulated *AHNAK* KO mice compared to that from WT mice (Figure 2-8A,B). However, there were no obvious changes in the histological morphology and activity of BAT between WT and *AHNAK* KO mice (Figure 2-6A, 2-7C, 2-8C). Furthermore, *AHNAK* KO mice exhibited higher core body temperature than wild-type mice after CL injection (Figure 2-9). Consistent with a previous report (Parikh et al., 2008a), oxygen consumption (VO_2) and energy expenditure were significantly elevated in *AHNAK* KO mice compared to WT mice after CL stimulation (Figure 2-10A,B). These results suggest that β3-adrenergic stimulation mediates the formation of multilocular adipocytes and enhances adaptive thermogenesis

through upregulation of thermogenic genes in the AHNAK deficient WAT depots, leading to increased energy expenditure.

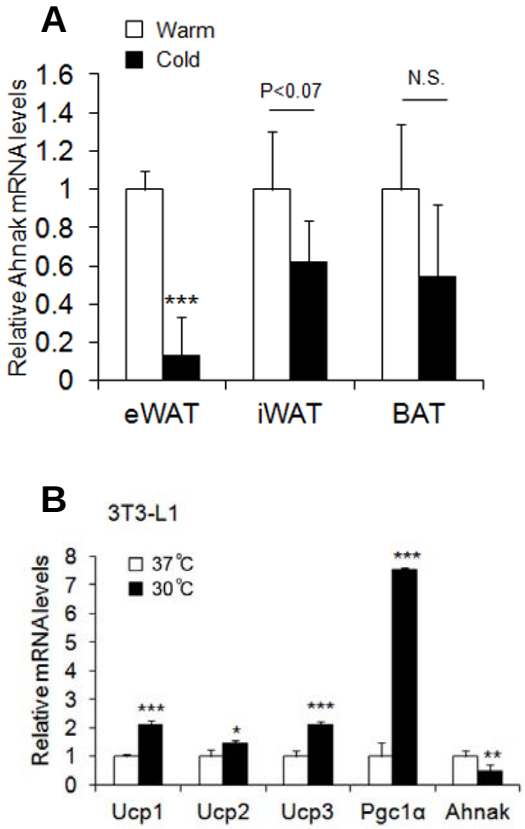

Figure 2-3. *AHNAK* mRNA expression by qPCR during cold chanllege.

(A) Expression levels of *AHANK* gene in fat depots (n=5). (B) 3T3-L1 cells were differentiated and maintained in for 10d (day 0–10) qPCR analysis of differentiated 3T3-L1 cells following maintaining in 37 °C or 30 °C for 6h (n=4). Values were normalized to 36B4. Data are means ± SEM; *P<0.05, **P<0.01, ***P<0.001.

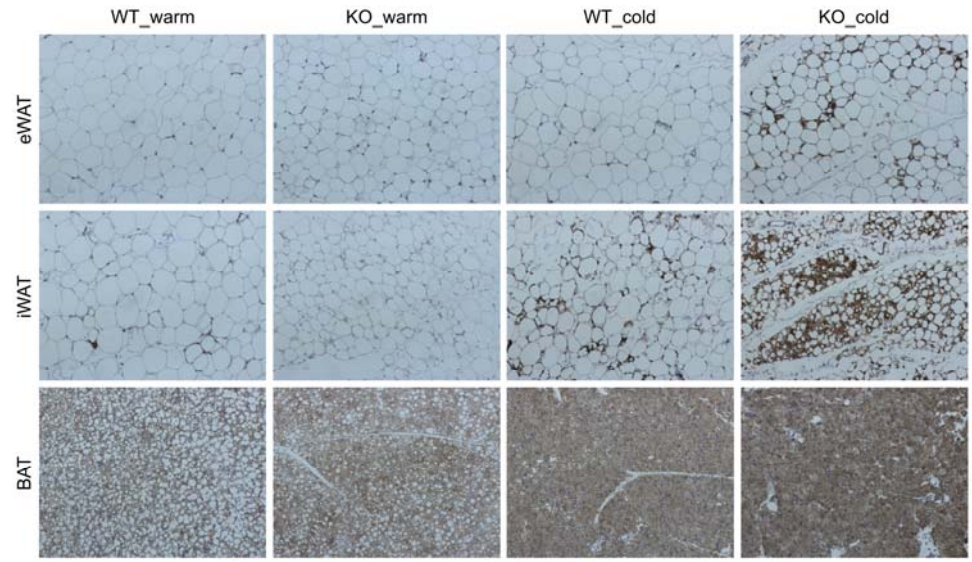

Figure 2-4. Browning phenotype of WAT in *AHNAK* KO mice under cold exposure. Representative pictures of UCP1 immunostaing in adipose tissues from mice maintained at 30°C (warm) or 4°C (cold) for 3 days. by cold exposure for 3days at 4°C.

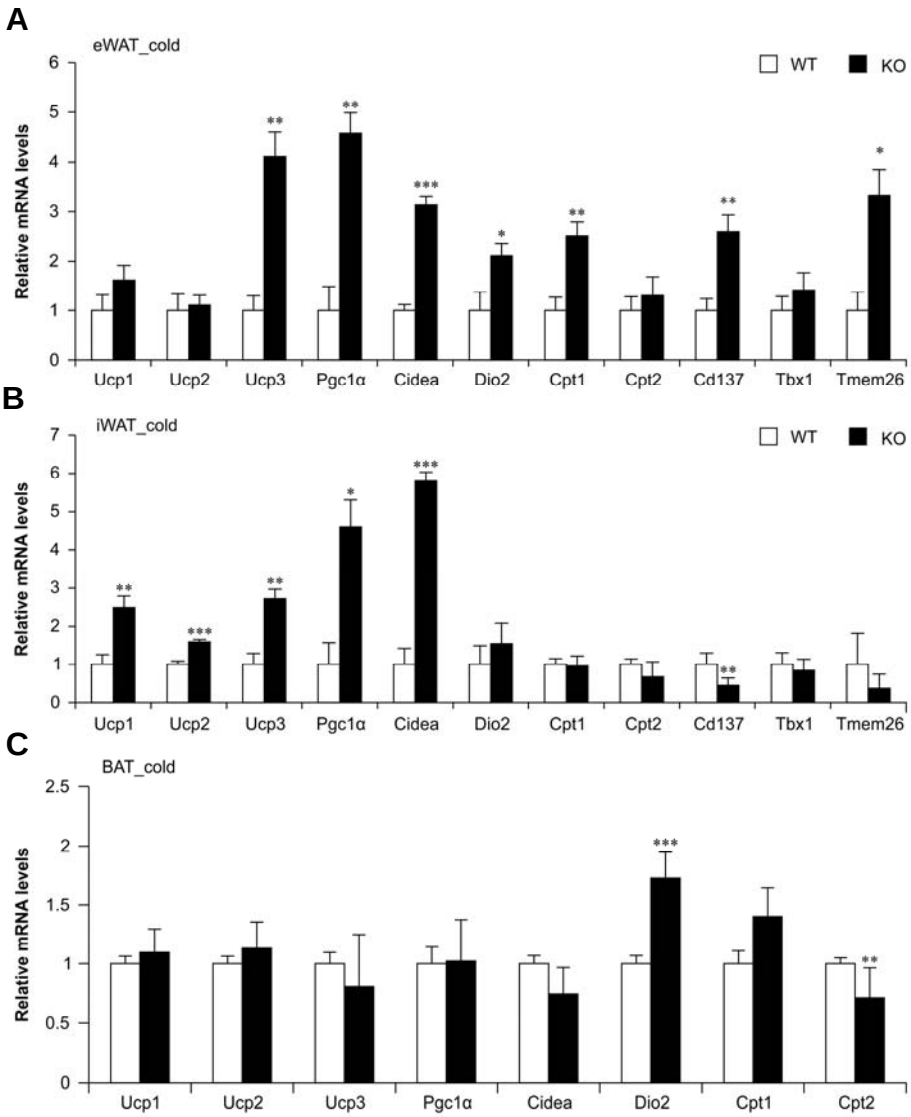

Figure 2-5. Expression of thermogenic related genes in *AHNAK* KO mice under cold exposure.

qPCR analysis in eWAT (A), iWAT (B) and BAT(C) from mice (n=5-6). Values were normalized to 36B4. Data are means ± SEM; *P<0.05, **P<0.01, ***P<0.001 between WT and KO mice.

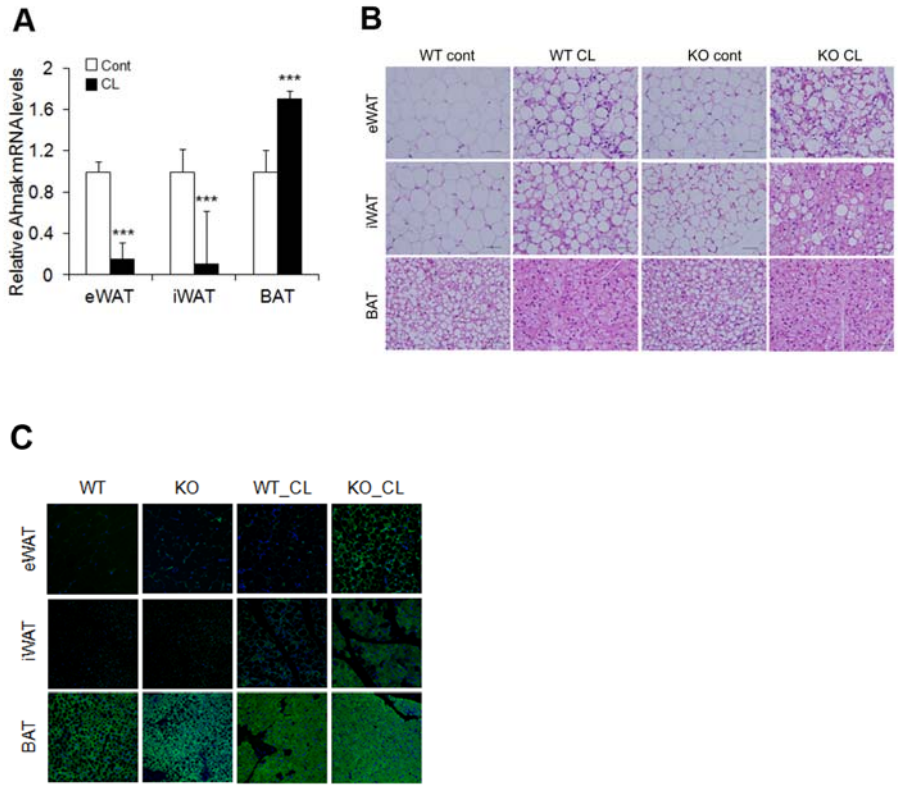

Figure 2-6. Ablation of AHANK induces white to brown fat transition.

(A) AHNAK mRNA expression of fat depot in control or CL treated mice (n=4-9 per group) and normalized to 36B4. (B) Representative hematoxylin and eosin staining of adipose tissues from mice treated with CL316243 (CL) for 3 days. (C) Immunofluorescence staining of UCP1 in adipose tissues of mice treated or not with CL CL-316243.

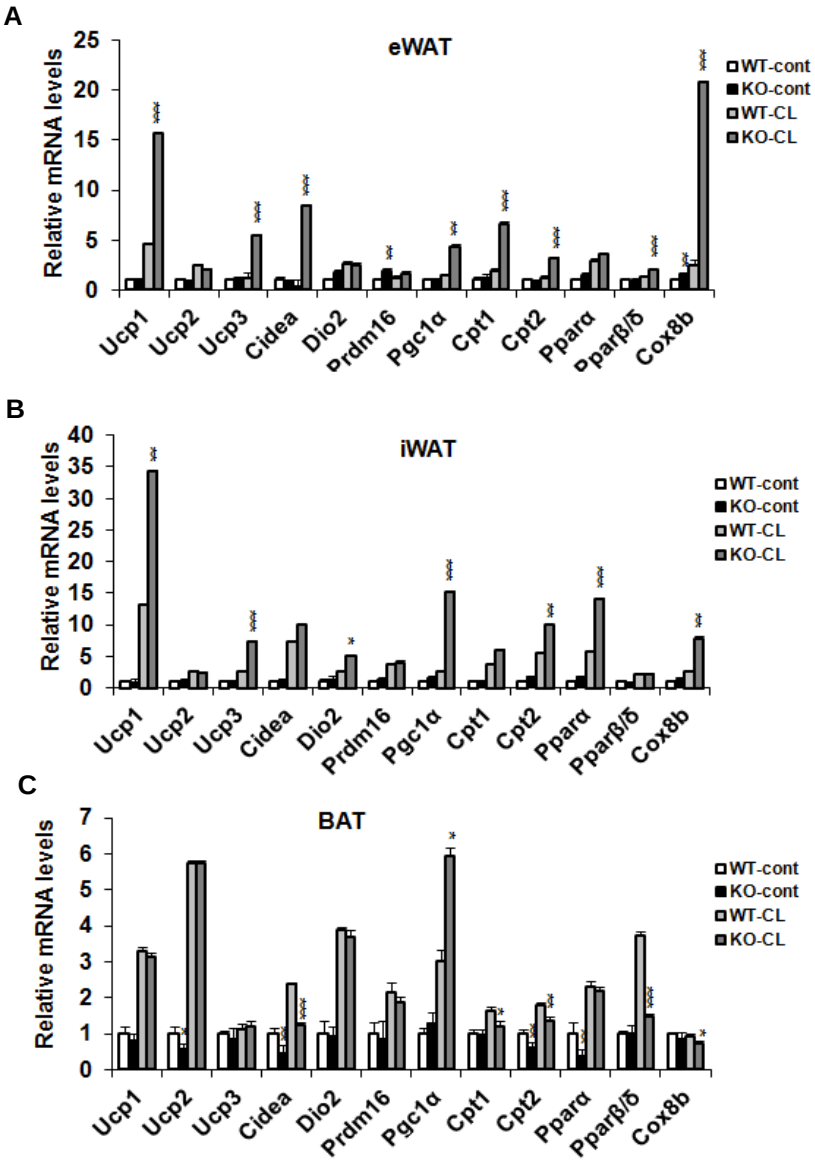

Figure 2-7. Expression of thermogenic related genes in *AHNAK* KO mice under CL-challenges.

(A-C) qPCR analysis of thermogenic related genes in eWAT (A), iWAT (B), and BAT (C) of mice (n=5). The data are presented as the means ± SEM. *P < 0.05,

**P < 0.01, ***P < 0.001, wild-type (WT) versus *Ahnak*⁻/⁻ (KO) mice.

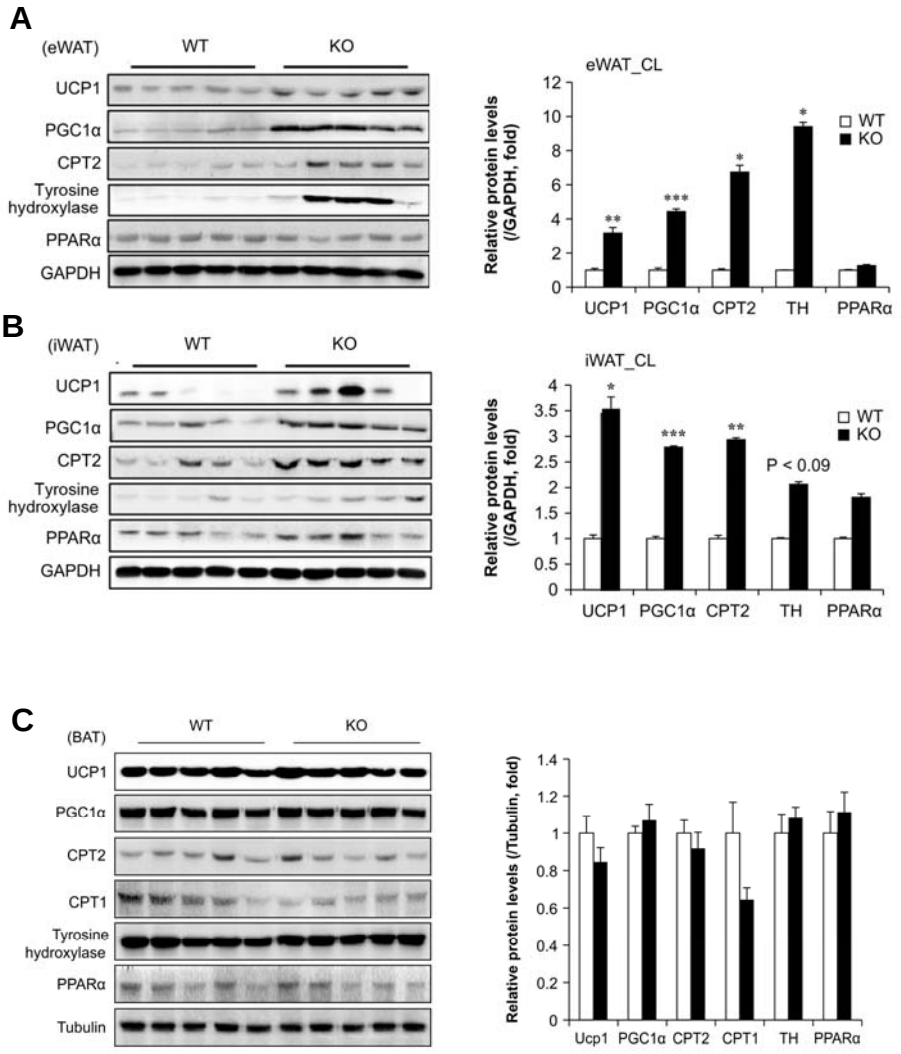

Figure 2-8. Thermogenic gene expression in *AHNAK* KO mice.

(A-C) Immunoblot analysis of eWAT (A), iWAT (B), and BAT (C) from mice treated with 3-day CL316243. The data are presented as the means ± SEM. *P < 0.05, **P < 0.01, ***P < 0.001, wild-type (WT) versus *Ahnak*$^{-/-}$ (KO) mice.

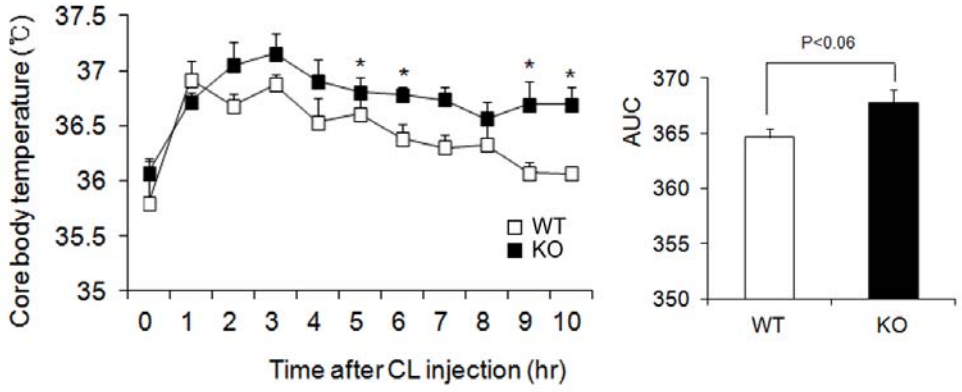

Figure 2-9. Measurement of body temperature in *AHNAK* KO mice after CL challege.

Core body temperature measured for WT and KO mice after CL injection at room temperature (n=12). The data are presented as the means ± SEM. *P < 0.05, **P < 0.01, ***P < 0.001, wild-type (WT) versus *Ahnak*$^{-/-}$ (KO) mice.

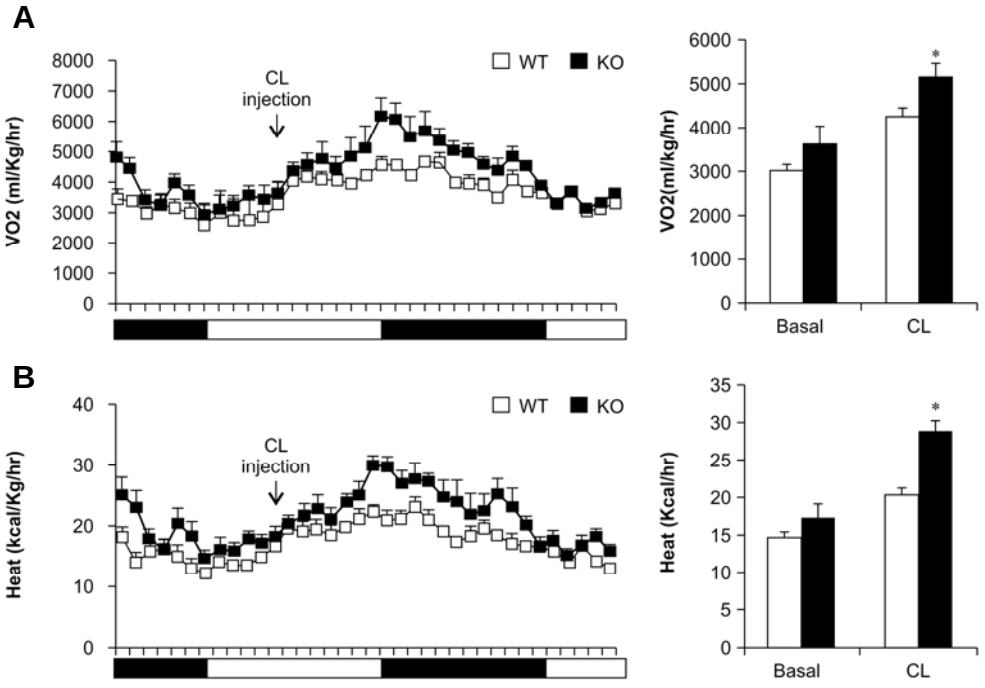

Figure 2-10. Enhanced thermogenesis in *AHNAK* KO mice after CL challenge.

(A) Oxygen consumption (VO_2) and (B) heat generation before and after CL-316243 injection (n = 7 per group). The data are presented as the means ± SEM. *P < 0.05, **P < 0.01, ***P < 0.001, wild-type (WT) versus *Ahnak*$^{-/-}$ (KO) mice.

In addition, ADRB3 stimulation has been associated with the reduction of fat mass and induction of mitochondrial biogenesis (Mottillo et al., 2007). To examine whether in AHNAK-deficient WAT the increase in energy expenditure and UCP1 expression was associated with mitochondrial activation, we investigated the changes in mitochondrial biogenesis in adipose tissues. The levels of the OXPHOS genes in the mitochondrial respiratory complexes I–V were remarkably increased in WAT of CL-treated *AHNAK* KO mice compared to the wild-type animals (Figure 2-11A,B); however, in BAT no significant effect was observed (Figure 2-12). Thus, increased mitochondrial function represented by the upregulation of the OXPHOS genes may underlie induced higher energy expenditure, and metabolic activity in AHNAK-deficient WAT.

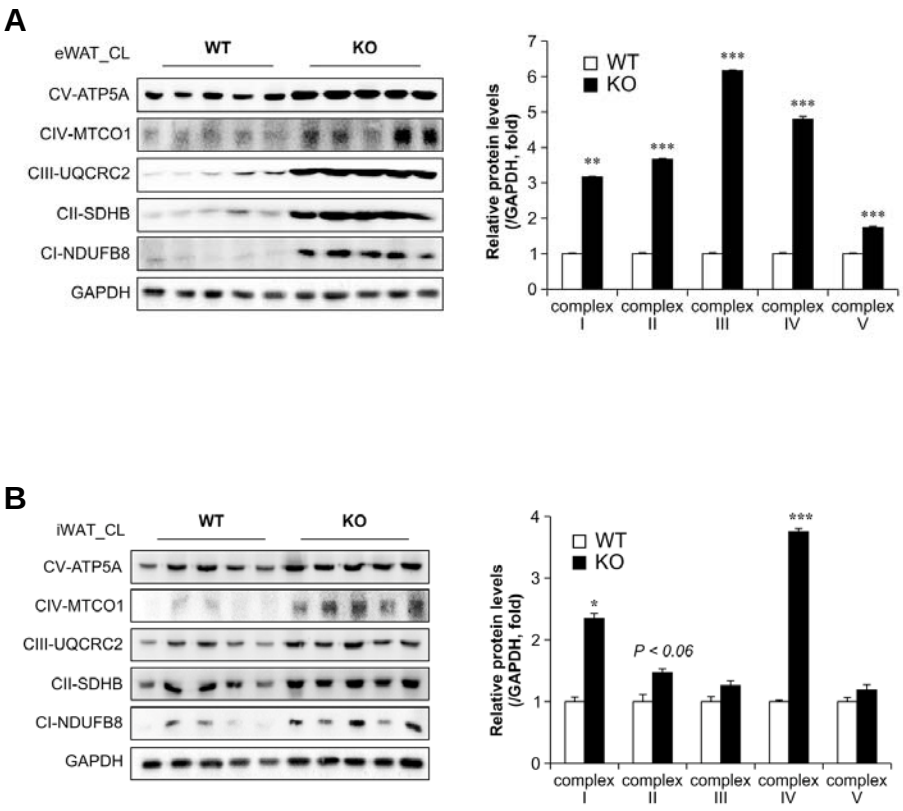

Figure 2-11. Mitochondrial biogensis of WAT in *AHNAK* KO mice

Immunoblotting analysis of mitochondrial respiratory chain complexes in eWAT (A) and iWAT (B); GAPDH was used as a loading control. The data are presented as the means ± SEM. *P < 0.05, **P < 0.01, ***P < 0.001, wild-type (WT) versus *Ahnak*$^{-/-}$ (KO) mice.

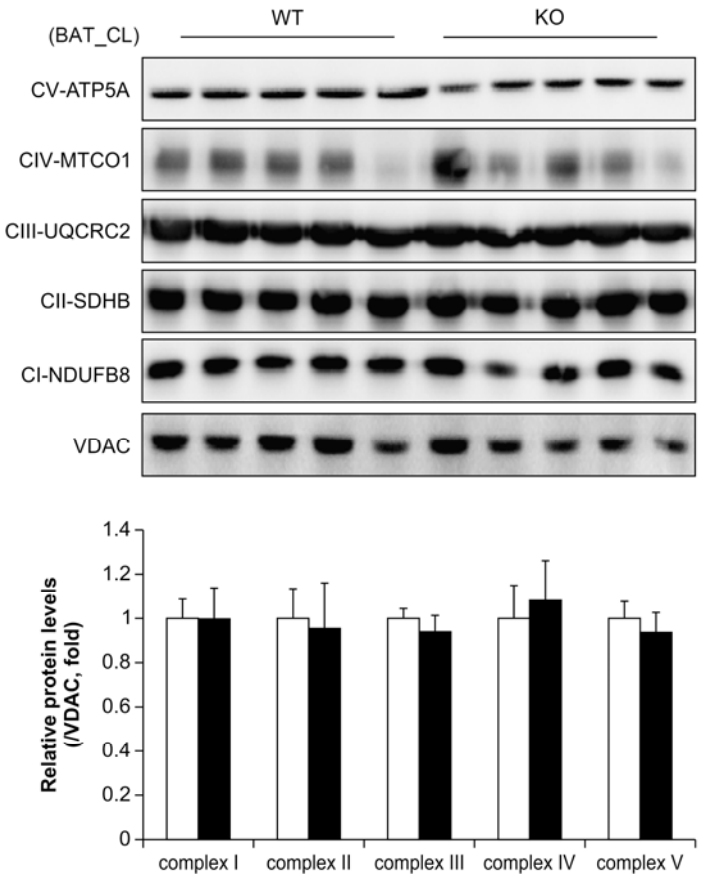

Figure 2-12. Mitochondrial biogensis of BAT in *AHNAK* KO mice

Immunoblot analysis of mitochondrial respiratory chain complexes in BAT of CL-treated mice (n=5). GAPDH was used as a loading control. Data are mean values ± SEM, *P<0.05, **P<0.01, ***P<0.001 between WT and KO mice.

2.3.2. Increased levels of eosinophils and type 2 cytokines in AHNAK deficient WAT

We observed phenotypic change into a brown-like adipocyte in CL-stimulated AHNAK deficient WAT although we used mice with a null mutation. We therefore hypothesize that this enhanced thermogenesis by β-adrenergic signaling can be induced by non-adipose progenitor cell types. Recent studies have focused on the eosinophil mediated regulation of beige fat development (Brestoff et al., 2014; Lee et al., 2015b; Qiu et al., 2014). To investigate whether eosinophils mediate WAT browning induced by β-adrenergic stimulation, we isolated eWAT and identified cell lineages that express sialic acid-binding immunoglobulin receptor (Siglec-F) and CD11b as molecular markers for eosinophils (Figure 2-13A). CL exposure increased the frequency and number of Siglec-F^+/$CD11b^+$ cells representing eosinophils in AHNAK-deficient eWAT (Figure 2-13B,C). Consistently, mRNA levels of eosinophil (Siglec-F and Ccr3), type 2 cytockines (IL-4, IL-4ra, and IL-13) and alternatively activated M2 specific gene (IL-10) were also significantly increased in eWAT and iWAT of CL-treated *AHNAK* KO mice(Figure 2-13D,E), but not in BAT (Figure 2-13F). Eosinophils and type 2 cytokines are implicated in regulating the biogenesis of thermogenic beige fat (Nguyen et al., 2011b; Qiu et al., 2014). This increase was accompanied by significant increase of $PDGFRa^+$/$CD44^+$ progenitor cells in Ahnak KO mice (Figure 2-14A,B). $PDGFRa^+$ cells were identified as a bipotential progenitor differentiating white or beige adipocytes (Lee et al., 2012b). Together, these results indicate that genetic ablation of *AHNAK* augments

eosinophil content and type 2 cytokine signals in CL-treated WAT, which could promote WAT browning upon β3-adrenergic stimulation.

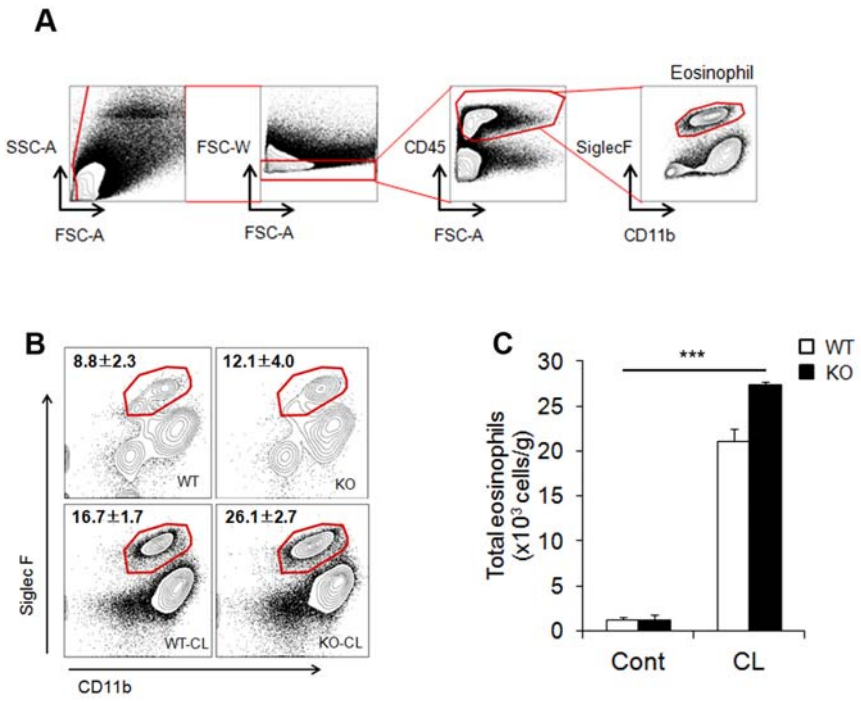

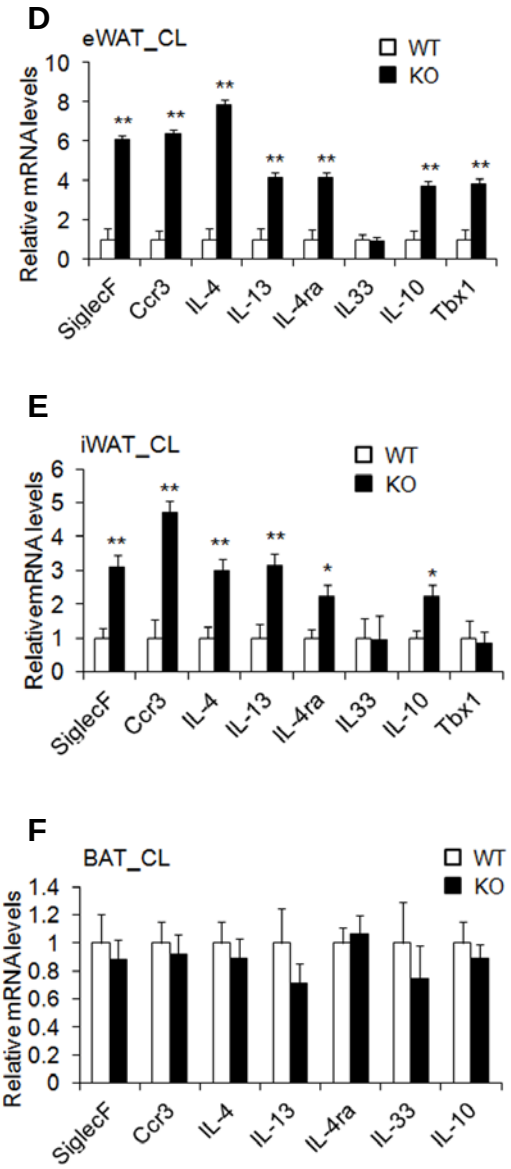

Figure 2-13. Increased levels of eosinophils and type 2 cytokines in *AHANK* deficient WAT.

(A) Gating strategy for identification of eosinophil lineage defined as $CD45^+$ $CD11b^+$ Siglec F^+. (B,C) Representative plots and frequencies (B) and number (C) of eosinophils in eWAT of mice treated with CL-316243 (n=4 per group pooled

from 7-10 mice). Statistical analysis was performed using the Kruskal-Wallis Test (***P<0.001)

(D-F) qPCR analysis of eosinophil and type 2 cytokine related gene in eWAT (D), iWAT (E) and BAT (F) of mice treated with CL-316243 (n= 5-7) and normalized to 36B4. Data are means ± SEM; *P<0.05, **P<0.01, ***P<0.001

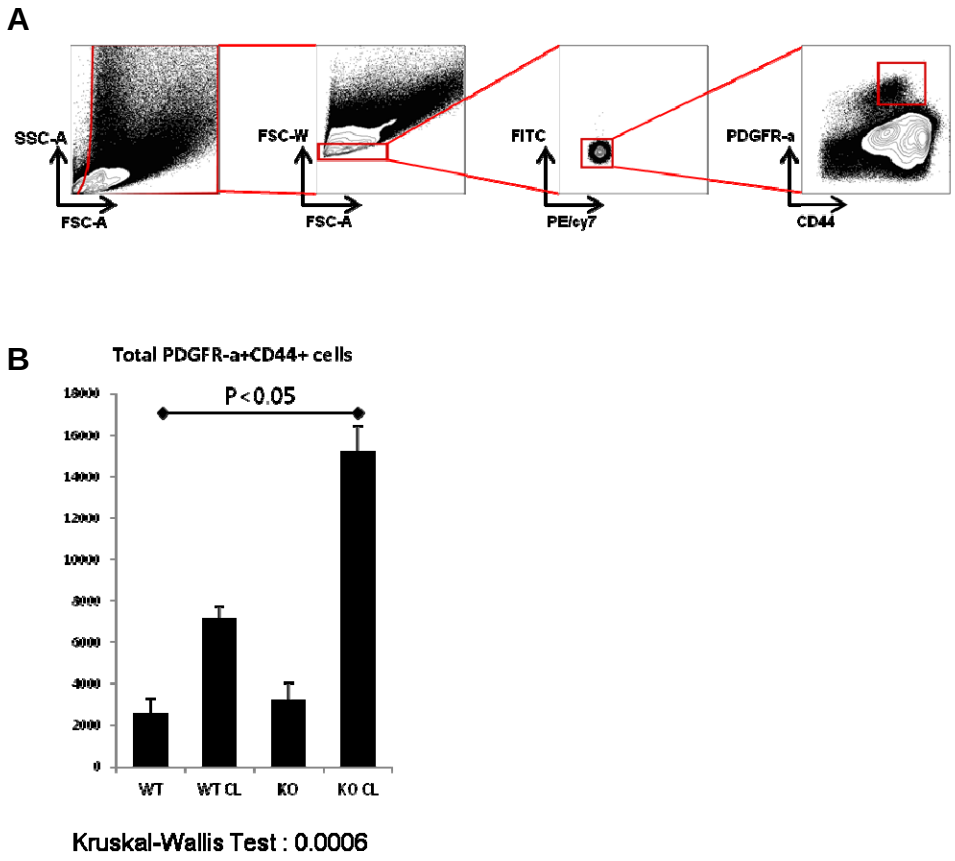

Figure 2-14. PDGFRa^{+} CD44^{+} progenitor cells in AHNAK deficient eWAT of Cells.

(A, B) Representative plots (A) and frequencies (B) of progenitor cells in eWAT of mice treated with CL-316243.

2.4. DISCUSSION

Understanding of signaling pathways that regulate thermogenesis and enhance energy expenditure, and identification of their potential targets is important for the development of measures to control obesity. It has been suggested that the activation of brown adipocytes and increase of BAT mass may constitute effective strategies to counteract obesity (Pfeifer and Hoffmann, 2015; Yoneshiro et al., 2013). Recent studies have reported catecholamine resistance in adipose tissue could be associated with obesity (Guo et al., 2014; Jocken et al., 2008). AHNAK-deficient mice displayed increased energy expenditure during high fat diet challenge, indicating resistance to obesity (Shin et al., 2015). Here, we revealed a critical role of AHNAK in regulating browning of WAT in response to β-adrenergic stimulation. AHNAK deficiency promotes the increase of functional brown-like adipocytes in WAT depots, which results in higher energy expenditure following β3-adrenergic stimulation.

ADRB3 agonists have been recognized as critical mediators of lipolysis and thermogenesis. ADRB3-activated PKA stimulates a transcriptional coactivator PGC1α leading to increased UCP1 expression and thermogenesis (Collins et al., 2010; Fredriksson et al., 2001). Efforts have been made to develop therapeutic approaches targeting ADRB3 to fight obesity and metabolic disorders, and CL-316243 has been used for generating brown-like adipocytes in WAT (Granneman et al., 2005; Lee et al., 2012b). However, the development of such drugs has been challenging because of insufficient oral bioavailability and cross-reactivity with ADRB1

(Arch, 2002, 2011). Nevertheless, new ADRB3 agonists have been investigated in clinical trials and shown improved bioavailability and binding affinity (Cypess et al., 2009; Cypess et al., 2015; Larsen et al., 2002; Redman et al., 2007). Several factors have been reported to be involved in fat browning and thermogenesis. PGC1 α has been recognized as a key regulator of energy metabolism and mitochondrial biogenesis. PGC1α activation regulated by mitogen-activated protein kinase p38 enhances the expression of thermogenic genes in adipose tissues in response to β-adrenergic signaling (Cao et al., 2004). It has been shown that *Pgc1α*$^{-/-}$ mice exhibited abnormal thermogenic phenotype, suggesting that PKA activation which regulates PGC1 α expression mediates thermogenesis (Leone et al., 2005). CPT2 is a crucial regulator of long chain fatty acid transport and is involved in initiation of β-oxidation in mitochondria. Mice overexpressing vitamin D receptor had reduced energy metabolism, which correlated with the downregulation of fatty acid oxidation and lipolysis, and suppression of CPT2 in WAT (Wong et al., 2011). Mice with adipose tissue-specific CPT2 ablation are defective in cold- or CL-induced thermogenesis because of deregulation of fatty acid oxidation, suggesting that CPT2 increase underlies enhanced lipolysis and thermogenesis in *AHNAK* KO mice (Lee et al., 2015a).

Local thermogenic circuit involving eosinophils and type 2 cytokines activates WAT browning and induces thermogenesis (Brestoff et al., 2014; Qiu et al., 2014), while the inhibition of tyrosine hydroxylase, a rate-limiting enzyme of catecholamine biosynthesis, or IL-4/13 signaling causes disruption of browning-related responses IL-4/13 signaling or

tyrosine hydroxylase (TH), a rate-limiting enzyme of catecholamine biosynthesis, causes the disruption of browning response (Qiu et al., 2014; Rao et al., 2014). Here, we investigated the process of generating functional beige cells in AHNAK-deficient WAT. AHNAK ablation led to robust recruitment of eosinophils into WAT and induced the secretion of eosinophil-derived cytokines after β-adrenergic stimulation, resulting in the production of epinephrine accompanied by increased expression of IL-10 and tyrosine hydroxylase, which promotes WAT browning and enhances mitochondrial biogenesis. It is still unclear whether eosinophils are regulated in an AHNAK-dependent manner because these parameters are also increased in unstimulated AHNAK-deficient eWAT. These results suggest that the increase in eosinophils and cytokine (IL-4/IL-13) secretion by adipocyte precursors could lead to catecholamine-induced WAT browning in *AHNAK* KO mice.

Chapter III

Effect of enhanced β-adrenergic and NPs signaling on lipolytic activity in AHNAK KO mice

3.1. Introduction

Lipolysis in adipocytes is important reactions in the management for energy reserves. Nonesterified fatty acids (NEFAs) are released by lipolysis of adipose tissue triacylglycerols (TAG) stored in the adipocytes. They serve as a source of energy during fasting and conditions of stress. After TAG hydrolysis, NEFAs and glycerol are transported by the bloodstream to other tissues. However, some NEFAs generated during lipolysis are re-esterified in a futile cycle back into the adipocytes as intracellular TAG (Lafontan et al., 2005). The glycerol formed during lipolysis is mainly used as an important substrate for glucose synthesis by the liver. Lipolytic reactions are controlled by catecholamines and insulin. Natriuretic peptides (NPs) which are involved in regulation of salt and water balance and blood pressure homeostasis, has been reported to have potent lipolytic effects (Figure 3-1) (Lafontan et al., 2005). In adipocytes, catecholamines stimulate lipolysis mainly through increase in cAMP and PKA activation, which phosphorylates HSL and perilipin, a protein coating the lipid droplet (Figure 5) (Deiuliis et al., 2010; Holm, 2003).

There are three members of the cardiac natriuretic peptides (NPs) family; atrial NP (ANP) was identified and synthesized in heart atria, brain NP (BNP) was isolated from porcine brain and mainly secreted from the heart ventricles, and C-type NP (CNP) is not only expressed in the central nervous, but also endothelial cells and chondrocytes (Lafontan et al., 2005). Their actions are mediated by binding to 3 subtypes of NP receptors (NPR) which

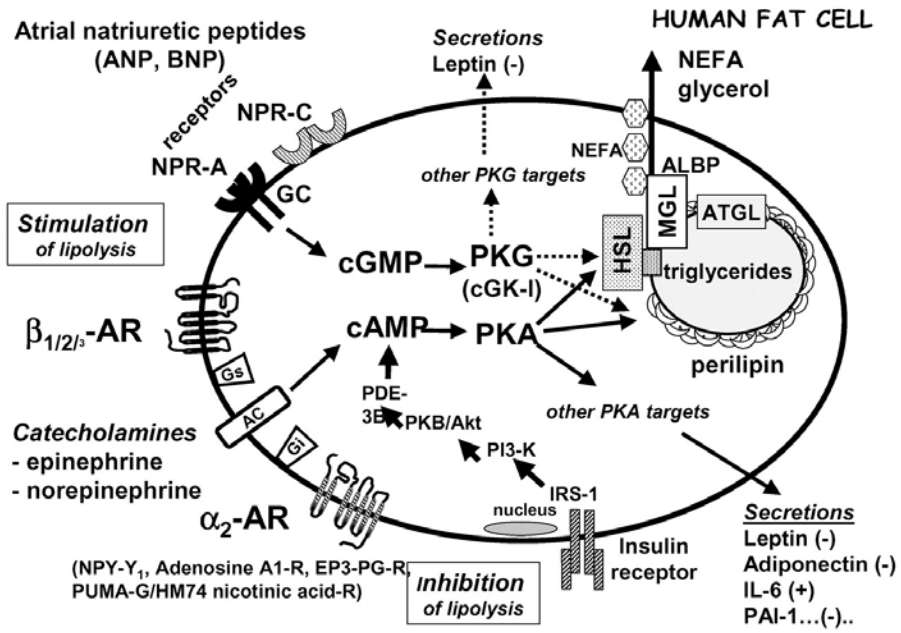

Figure 3-1. Major pathways involved in the control of human fat cell lipolysis.
(Lanfontan *et al*., Arterioscler Thromb Vasc Biol, 2005)

either possesse guanylyl cyclase (GC) activity (NPR-A and NPR-B) to generate the second messenger cGMP or do not (NPRC, which is referred to as the clearance receptor) (Bordicchia et al., 2012; Chinkers et al., 1989). Previous studies reported that NPs showed potent lipolytic effects similar to those induced by the β-AR agonist (Sengenès et al., 2002; SENGENÈS et al., 2000). Notably, the levels of NPRC in adipose tissue were decreased in the fasting condition in rats (Sarzani et al., 1995). A physiological role for NPs in exercise-induced lipolysis in humans suggest that heart has a central role in regulating the supply of fatty acids for both cardiac and skeletal muscle under aerobic conditions (Moro et al., 2004; Moro et al., 2006).

Several studies reported that NPs have also been associated with obesity (Chen-Tournoux et al., 2010; Sugisawa et al., 2010). NPs are implicated in brown fat thermogenesis in adipocytes via cGMP and PKG, as effectively as catecholamines through cAMP and PKA (Bordicchia et al., 2012).

In this study, the effects of elevated sympathetic tones and NPs signaling on lipolysis in AHNAK KO mice were investigated.

3.2. Materials and Methods

Animals

AHNAK-KO (*Ahnak*$^{-/-}$) mice were maintained under a 12-h light-dark cycle and had free access to water in a specific pathogen-free barrier facility. Mice were randomly assigned. To stimulate the liplysis of white adipose depots, 2-3 month-old mice were treated with daily intraperitoneal injections of 1mg/kg bodyweight CL-316,243 (Sigma-Aldrich) dissolved in PBS. The experiments were performed according to the "Guide for Animal Experiments" (Edited by Korean Academy of Medical Sciences) and approved by the Institutional Animal Care and Use Committee (IACUC) of the Seoul National University (Permit Number: SNU-130903-1).

Lipolysis assay

To assess in vivo lipolysis, serum free fatty acids (FFAs) were measured in cardiac blood obtained from non-fasted mice before and 20 min after i.p. injection of CL316243 (1 mg/kg). Ex vivo and in vitro lipolysis was measured as described previously (Guo et al., 2013; Guo et al., 2014) with some modifications. Briefly, for ex vivo analysis, adipose tissues were surgically removed from male and female mice, weighed, and washed with cold PBS; fat depots were incubated with CL316243 (1 μM) or vehicle in Krebs-Ringer Bicarbonate Buffer (KRBH, Sigma) containing 1% fatty acid-free BSA (GenDEPOT) and glucose (2.5 mM) for 2 h at 37°C with mild shaking. After incubation, FFA and glycerol were measured using a glycerol-free reagent (Sigma) and the FFA quantification kit (BioVision, Mountain View, CA, USA) and normalized to the weight of adipose tissue samples. For in vitro lipolysis, differentiated 3T3-L1 adipocytes were

transfected with *Ahnak*-specific siRNA (Bioneer) and negative control siRNA and incubated with CL316243 (1 μM) or vehicle in KRBH for 3 h at 37°C. FFA and glycerol release to the medium was measured as described above.

Antibodies

The primary antibodies used for western blot analysis were specific for: pHSL, HSL, pPKA substrates, and GAPDH (all from Cell Signaling Technology, Beverly, MA, USA)

Statistics

All values were expressed as the mean± SEM. Statistical analysis was performed using the Student's t-test between two groups. $P<0.05$ was considered significantly.

3.3. Results

3.3.1. Enhanced β-adrenergic signaling lipolysis in WAT of *AHNAK* KO mice treated with CL-316243

Stimulation of β3-adrenergic receptor agonist induces activation of protein kinase A (PKA), which then leads to lipolysis mediated by phosphorylation of hormone sensitive lipase (HSL) (Deiuliis et al., 2010). Therefore, we investigated catecholamine signaling in adipose tissue of CL-treated *AHNAK* KO mice. There was no difference in serum concentration of free glycerol between *AHANK* KO and wild type mice after CL injection probably because of a decrease in body fat in *AHNAK* KO mice (Figure 3-2A). However, the exposure to CL316243 resulted in a higher fold increase in glycerol release in *AHNAK* KO mice than wild type mice (Figure 3-2B). Importantly, AHNAK deficient WAT also displayed increased expression of tyrosine hydroxylase, the rate-limiting enzyme in the synthesis of catecholamines (Figure 2-8A,B). Moreover, circulating levels of epinephrine were also increased in KO mice (Figure 3-2C), suggesting that white fat browning may be attributed to enhanced sympathetic input to WAT in AHNAK-deficient mice. Moreover, Adrb3 mRNA expression was significantly increased after CL stimulation in WAT but not in BAT of *AHNAK* KO mice (Figure 3-3A). However, the levels of other adrenergic receptor subtypes, Adrb1 and Adrb2 were not altered (Figure 3-3B,C).

Previously decribed (Nunn et al., 2010), the levels of Rgs2, a negative regulator of adrenergic signaling, also displayed no differences between the two groups (Figure 3-3D). These results suggest that robust sympathetic tone and enhanced catecholamine sensitivity may alter β-adrenergic responsiveness in AHNAK-deficient WAT. In agreement with this notion, PKA activity in WAT was substantially elevated in *AHNAK* KO mice as evidenced by the increase in the level of phosphorylated PKA substrates and hormone sensitive lipase (HSL) in both eWAT and iWAT of AHNAK-deficient mice after CL injection (Figure 3-4A,B); however, no changes were observed in BAT (Figure 3-5). Further, *AHNAK* KO mice exhibited higher CL-stimulated lipolytic response after HFD feeding (Figure 3-6A,B). Thus, AHNAK may regulate catecholamine sensitivity in WAT.

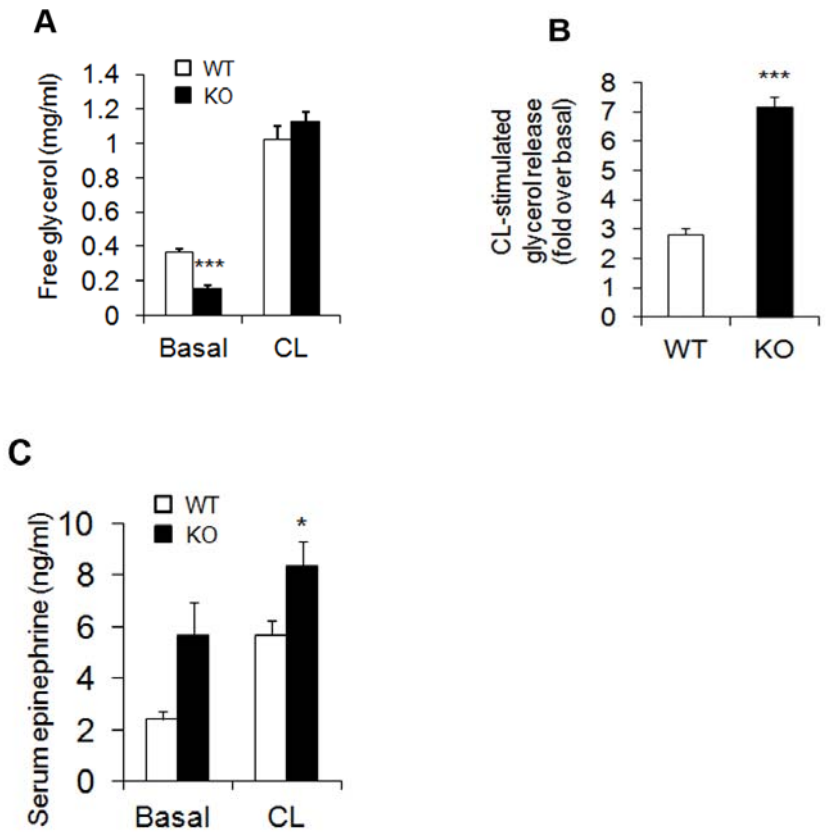

Figure 3-2. Enhanced β-adrenergic signaling in WAT of *AHNAK* KO mice.

(A) CL-316243 stimulated glycerol levels in serum from RC fed mice (20 min after CL injection) (n=5). (B) Fold changes of glycerol levels over basal after CL316243 stimulation s in serum (n=5). (C) Serum epinephrine (n = 7–9 for basal, n = 17–20 for CL). The data are presented as the means ± SEM; *P < 0.05, **P < 0.01, ***P < 0.001, wild-type (WT) versus *Ahnak*$^{-/-}$ (KO) mice.

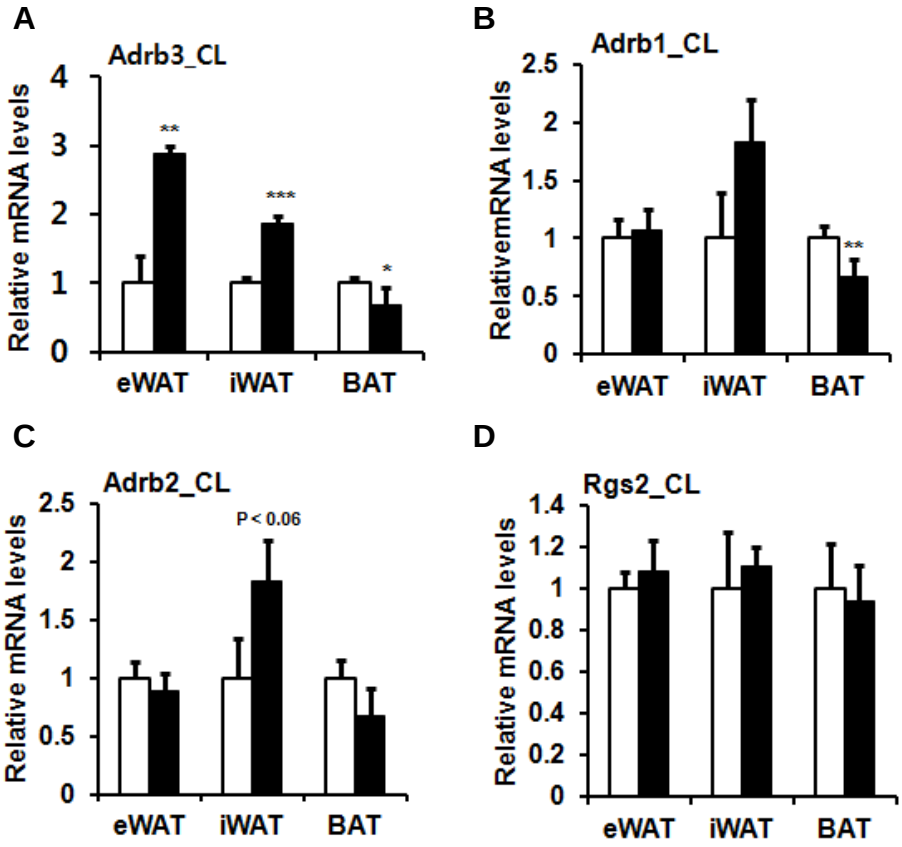

Figure 3-3. Expression of β-adrenergic receptors in adipose tissue of *AHNAK* KO mice.

Relative mRNA levels of the Adrb3 (A), Adrb1(B), Adrb2 (C), and Rgs2 (D), assessed by qRT-PCR in CL treated adipose tissue (n = 5); the expression was normalized to 36B4. Values were normalized to 36B4. The data are presented as the means ± SEM; *P < 0.05, **P < 0.01, ***P < 0.001, wild-type (WT) versus *Ahnak*$^{-/-}$ (KO) mice.

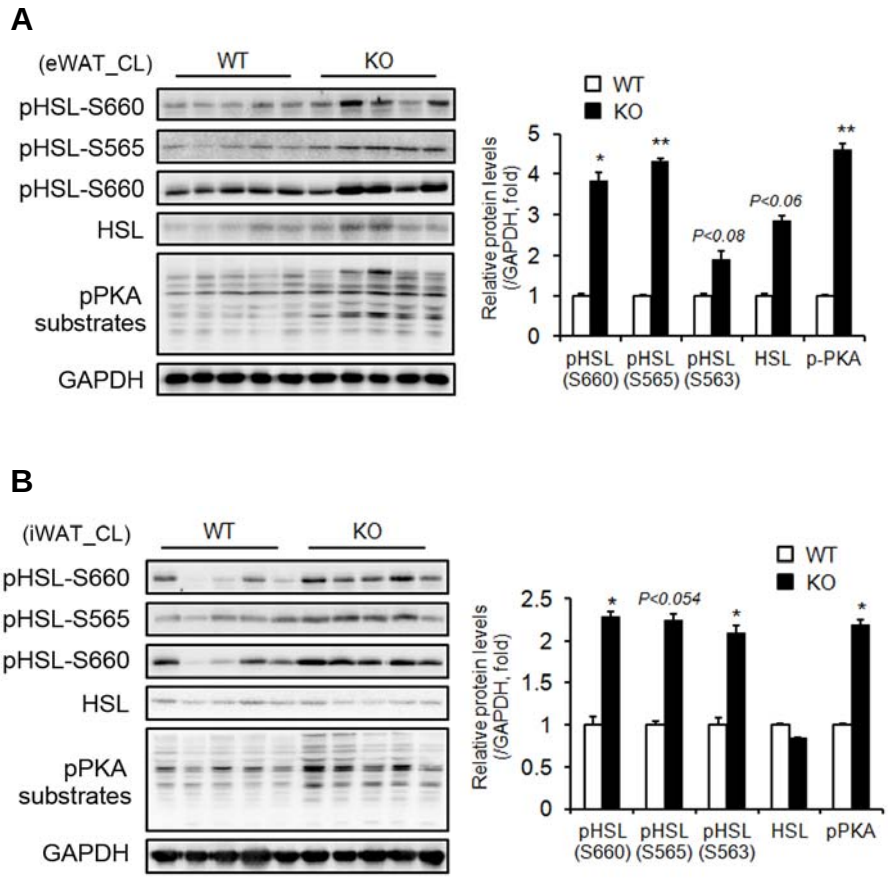

Figure 3-4. Lipolysis signaling pathway in WAT of *AHNAK* KO mice by β-adrenergic signals.

Levels of phosphorylated HSL and PKA substrates assessed by immunoblotting in eWAT (A) and iWAT (B); GAPDH was used as a loading control. The data are presented as the means ± SEM; *P < 0.05, **P < 0.01, ***P < 0.001, wild-type (WT) versus *Ahnak*$^{-/-}$ (KO) mice.

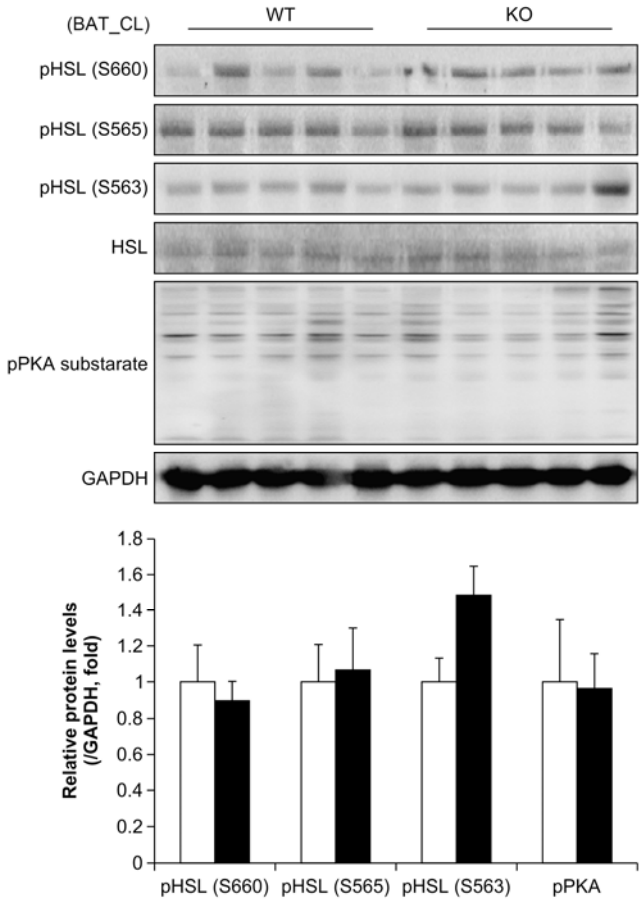

Figure 3-5. Lipolysis signaling pathway in BAT of *AHNAK* KO mice by β-adrenergic signals

Levels of phosphorylated HSL and PKA substrates assessed by immunoblotting in BAT; GAPDH was used as a loading control. The data are presented as the means ± SEM; *P < 0.05, **P < 0.01, ***P < 0.001, wild-type (WT) versus *Ahnak*$^{-/-}$ (KO) mice.

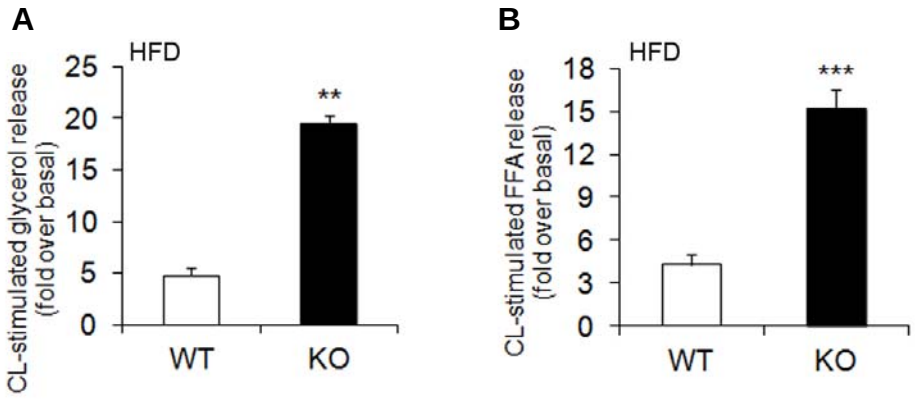

Figure 3-6. Enhanced β-adrenergic signaling in WAT of *AHNAK* KO mice fed a HFD.

CL-316243 stimulated glycerol (A) and FFA (B) levels in serum from HFD fed mice (20 min after CL injection)(n=4-5). The data are presented as the means ± SEM; *P < 0.05, **P < 0.01, ***P < 0.001, wild-type (WT) versus *Ahnak*$^{-/-}$ (KO) mice.

3.3.2. AHNAK negatively regulated β-adrenergic signaling in adipocytes

Mice lacking AHNAK exhibited enhanced β-adrenergic signaling in WAT; therefore, we examined the effect of AHNAK on acute adrenergic signaling in murine adipose tissue and adipocytes. For this, isolated adipose tissues were incubated with CL for 2h at 37°C and the release of FFA and glycerol to media was determined and normalized to fat tissue weight. In both eWAT and iWAT of AHNAK-deficient mice under either RC or HFD feeding, CL treatment led to significantly increased lipolysis, as indicated by FFA and free glycerol release. (Figure 3-7A-D). Taken together, these results suggest that fat increased lipolysis in AHNAK ablation is mediated by β3-adrenergic signaling through induction of Adrb3.

Next, we employed 3T3-L1 cell to evaluate the role of Ahnak in adrenergic signaling *in vitro*. The amount of released FFA and free glycerol were remarkably elevated in Ahnak knock-down cells (Figure 3-8A-C). In consistent with increased lipolysis on adrenergic signaling, the levels of phosphorylated HSL and PKA substrates were increased in Ahnak knock-down cell after CL treatment (Figure 3-8D). Taken together, these results suggest that Ahnak is implicated in regulation of β-adrenergic signaling in adipocytes.

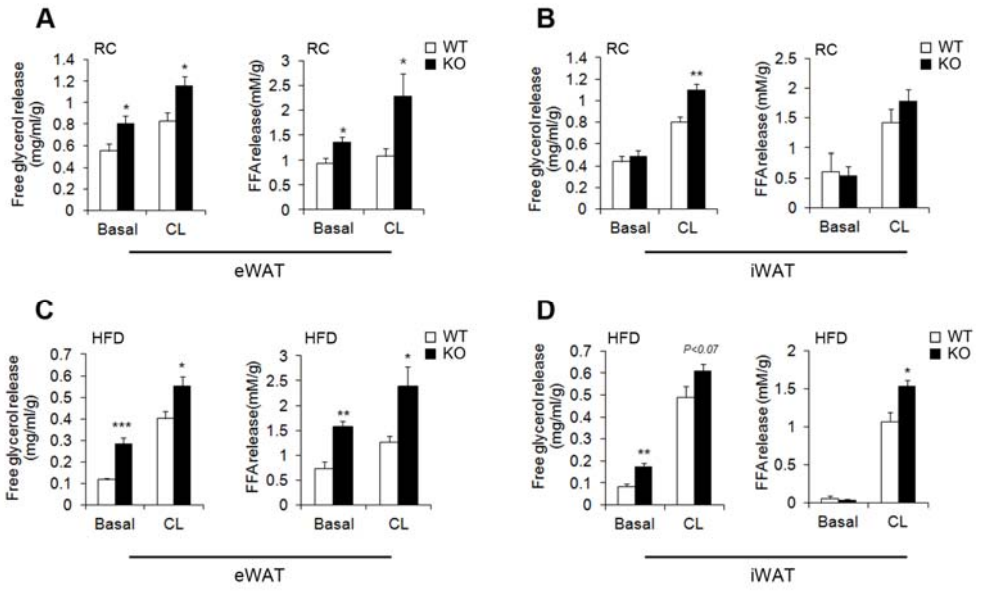

Figure 3-7. *Ex vivo* lipolysis in response to β-adrenergic stimulation from *AHNAK* KO mice.

(A–D) Explants from RC-fed eWAT (A), iWAT (B), HFD fed eWAT (C) and HFD-fed iWAT (D) were treated or not with CL-316243 for 2 h at 37°C and analyzed for the release of glycerol and FFA (n=4-6 per group). The values were normalized to the wet weight of the explants. The data are presented as the means ± SEM; *P < 0.05, **P < 0.01, ***P < 0.001, wild-type (WT) versus *Ahnak*$^{-/-}$ (KO) mice.

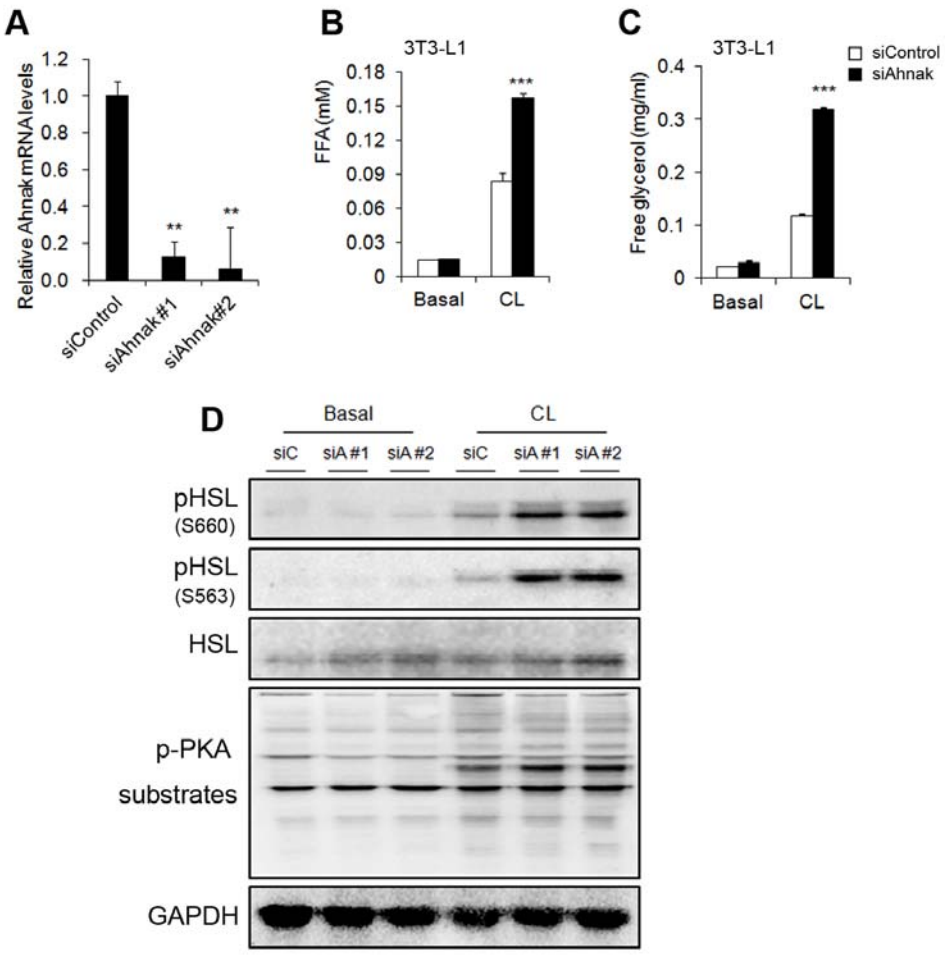

Figure 3-8. AHNAK deficiency enhanced lipolysis in adipocytes *in vitro* in response to β-adrenergic stimulation .

(A) 3T3-L1 adipocytes were transfected with *Ahnak*-specific or control siRNA, stimulated with CL-316243 for 3 h, and analyzed for FFA (B) and glycerol (C) release, and *Ahnak* mRNA levels by qPCR. (D) The expression of phosphorylated HSL and PKA substrates analyzed by immunoblotting. siC, siControl; siA, siAHNAK. The data are presented as the ± SEM, *P < 0.05, **P < 0.01, ***P < 0.001, wild-type (WT) versus *Ahnak*$^{-/-}$ (KO) mice.

3.3.3. Lipolytic action via NPs in *AHNAK* KO mice

Increases in sympathetic activity by β3 adrenergic stimulation led to activation of lipolytic mechanisms of AHNAK deficient WAT. Given the parallel nature of β-AR and NP signaling and responses, we next investigated whether changes in the NP system were stimulated by CL exposure. As shown in Figure 38, *AHNAK* KO mice injected by CL had significantly increased levels of ANP, BNP, and CNP in eWAT (Figure 3-9A). Concomitantly, in eWAT, the ratio of gene expression of NPR-A to NPR-C was also increased in CL treated *AHNAK* KO mice, because elevation of *NPRA* mRNA levels was accompanied by a decrease in *NPR-C* levels in AHNAK deficient eWAT (Figure 3-9B). However, there were no differences in BAT between WT and KO mice (Figure 3-10). Furthermore, expression levels of NPs were elevated with a contemporaneous decrease in NPR-C levels in the fasting state in *AHNAK* KO mice (Figure 3-11). Interestingly, cardiac expression of NPs was not altered in the fasting condition between WT and KO mice (Figure 3-12). Therefore, these changes in eWAT suggest that the NP system may function together with the activation of β3-AR and enhance fat lipolysis in *AHNAK* KO mice

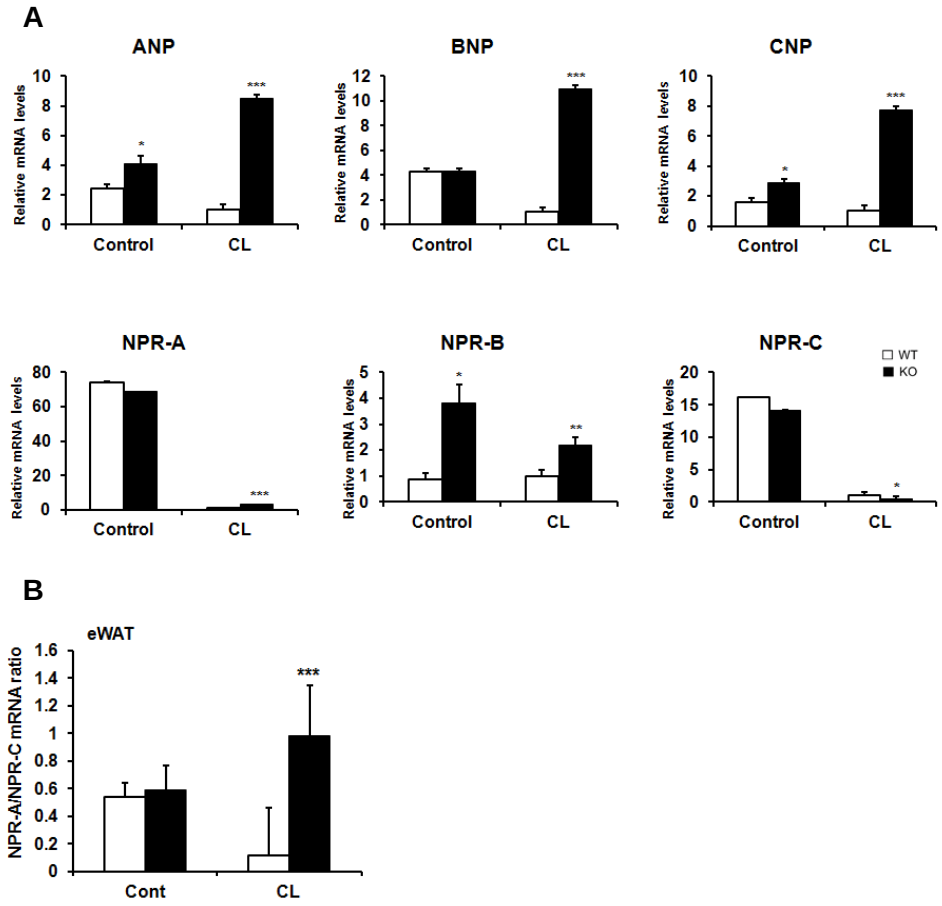

Figure 3-9. AHNAK deficiency enhanced NPs expression in eWAT in response to β-adrenergic stimulation.

(A) mRNA levels of NPs and NP receptors in eWAT (n=5-7). (B) Ratio of NPR-A to NPR-C in eWAT. The data are presented as the ± SEM, *P < 0.05, **P < 0.01, ***P < 0.001, wild-type (WT) versus *Ahnak*$^{-/-}$ (KO) mice.

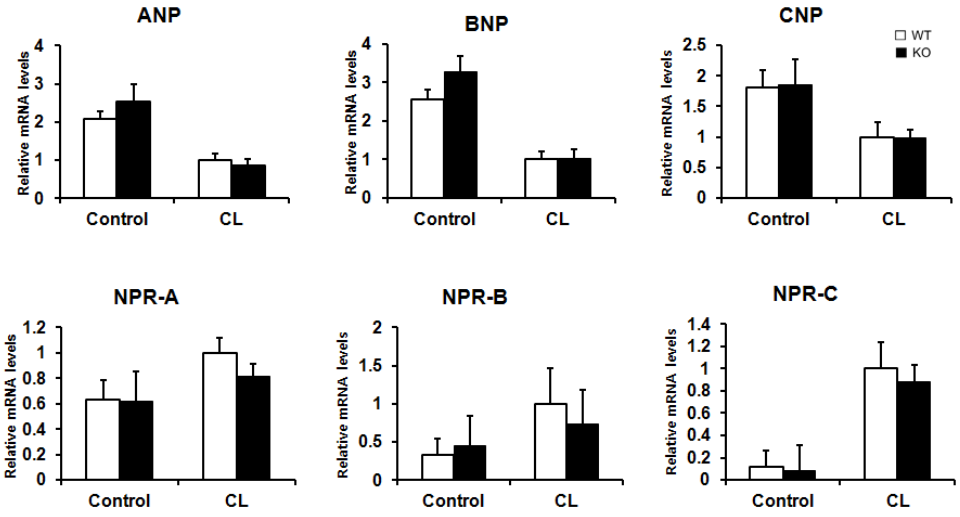

Figure 3-10. AHNAK deficiency enhanced NPs expression in BAT in response to β-adrenergic stimulation.

mRNA levels of NPs and NP receptors in BAT (n=5-7). The data are presented as the ± SEM, *P < 0.05, **P < 0.01, ***P < 0.001, wild-type (WT) versus *Ahnak*$^{-/-}$ (KO) mice.

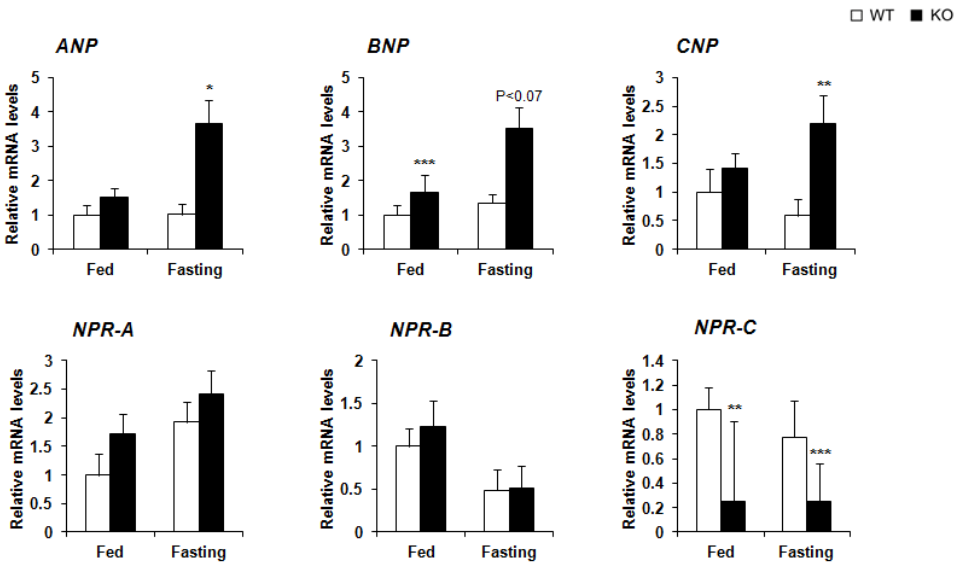

Figure 3-11. AHNAK deficiency enhanced NPs expression in eWAT during fasting condition

The data are presented as the ± SEM (n=5), *P < 0.05, **P < 0.01, ***P < 0.001, wild-type (WT) versus *Ahnak*$^{-/-}$ (KO) mice.

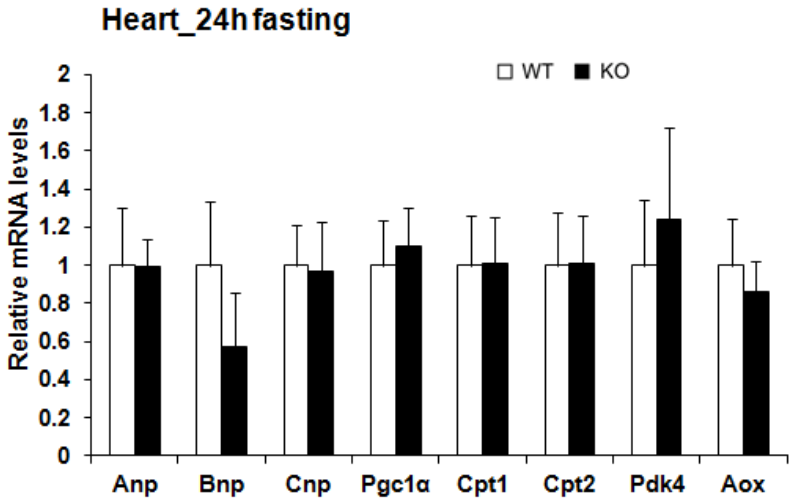

Figure 3-12. NPs expression in heart

The data are presented as the ± SEM (n=5), *P < 0.05, **P < 0.01, ***P < 0.001, wild-type (WT) versus *Ahnak*$^{-/-}$ (KO) mice.

3.4. DISCUSSION

ADRB3 activation stimulates cAMP and PKA activation, which promotes adipocyte lipolysis via HSL phosphorylation (Deiuliis et al., 2010). In this study, AHNAK-deficient CL-316243-stimulated mice demonstrated PKA activation in WAT, which was accompanied by increased phosphorylation of HSL and FFA mobilization, indicating enhanced lipolysis. Moreover, *AHNAK* genetic ablation increased expression levels of the genes involved in fat browning (*Ucp1*, *Pgc1a*, and *Cpt2*) and mitochondrial oxidative phosphorylation in response to β-adrenergic signaling. Our results suggest that AHNAK deficiency may contribute to improved catecholamine sensitivity by enhancing ADRB3 expression and signaling in WAT.

NPs, on the other hand, increases cGMP, and subsequently activates cGMP-dependent protein kinase leading to lipolysis (Potter and Hunter, 2001; Sengenès et al., 2003). Since NPs system via PKG appeared to share a common mechanism to increase lipolysis with β-agonists through PKA (Lafontan et al., 2008). The lipolytic effect of NPs may be determined by the ratio of NPR-A to the clearance receptor NPR-C in adipocytes (Moro and Lafontan, 2013; Sengenès et al., 2002).In ealier work, NPs promote browning of WAT to increase energy expenditure (Bordicchia et al., 2012). Here we show that AHNAK null mice promoted lipolysis via enhanced responsiveness to β3-adrenergic signals, accompanied by the elevated levels of NPs system and the ratio of NPRA to NPR-C expression. Although it still

remains to be determined the role of AHNAK in WAT, possible candidate sites are proposed; recruitment of eosinophil, regulation of β3-AR, NPR-A and NPR-C activity(Figure 3-13). We suggest that AHNAK could regulate thermogenesis and lipolysis through those potential mechanisms.

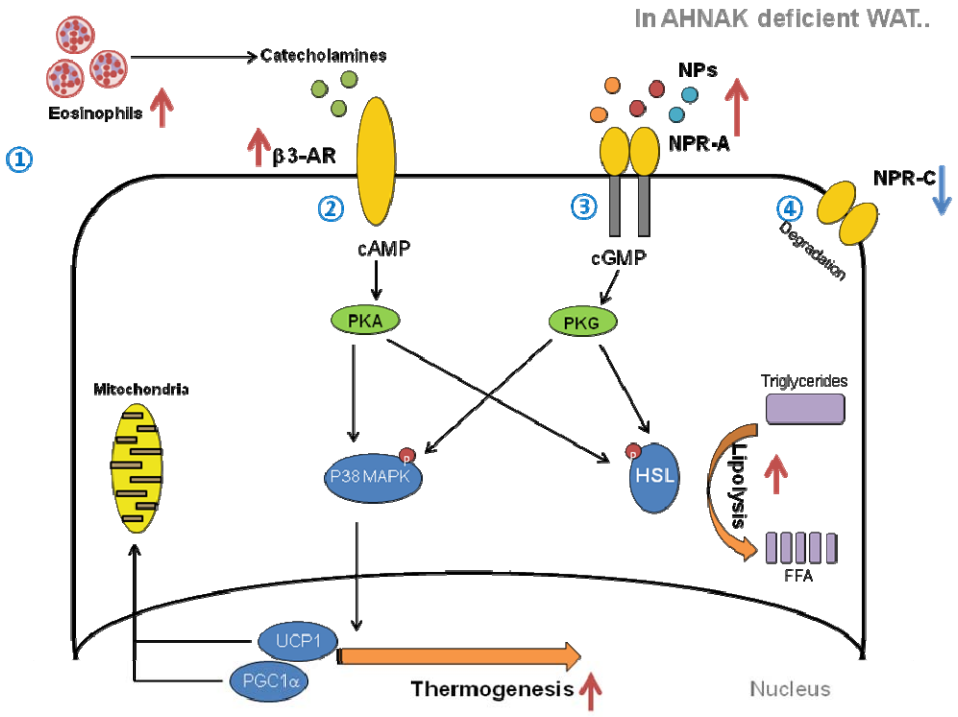

Figure 3-13. Putative model for parallel activation of β3-AR and NPs in AHNAK deficient WAT

Table 1. Sequences of primers used for real-time PCR

Gene	Sequence	Gene	Sequence
Abhd5	TGGTGTCCCACATCTACATCA CAGCGTCCATATTCTGTTTCCA	*Dgat2*	TCTCAGCCCTCCAAG ACATC GCCAGCCAGGTGAAGTAGAG
Acrp30	GGCAGGAAAGGAGAACCTGG AGCCTTGTCCTTCTTGAAGAG	*Dio2*	CAGTGTGGTGCACGTCTCCAATC TGAACCAAAGTTGACCACCAG
Adrb1	CTCATCGTGGTGGGTAACGTG ACACACAGCACATCTACCGAA	*Glut4*	AAAAGTGCCTGAAACCAGAG TCACCTCCTGCTCTAAAAGG
Adrb2	GGGAACGACAGCGACTTCTT GCCAGGACGATAACCGACAT	*HSL*	GGAGCACTACAAACGCAAC TCCCGTAGGTCATAGGAGAT
Adrb3	ATTGGCGCTGACTGGCCATT GCCGTGTTAAGGAATCTGCTG	*IL-4*	GGTCTCAACCCCCAGCTAGT GCCGATGATCTCTCTCAAGTGAT
Ahnak	TGTCACTGGCTCACCTGAAG CTTGCCTTTAGCGTCTCCAC	*IL-4R*	GTCACAGAGCAGCCTTCACA AAAACTCCGGTAGGCAGGAT
Anp	CCTGTGTACAGTGCGGTGTC CCTAGAAGCACTGCCGTCTC	*IL-13*	CCTGGCTCTTGCTTGCCTT GGTCTTGTGTGATGTTGCTCA
aP2	TTCGATGAAATCACCGCAGA AGGGCCCCGCCATCT	*LPL*	TCTGTACGGCACAGTGG CCTCTCGATGACGAAGC
Bnp	CTGAAGGTGCTGTCCCAGAT GTTCTTTTGTGAGGCCTTG	*NPR-A*	AGTACGCCAACAACCTGGAG AAGAGCTGTAAAGCCCACGA
Ccr3	TCGAGCCCGAACTGTGACT CCTCTGGATAGCGAGGACTG	*NPR-B*	TCATGACAGCCCATGGTAA GGTGACAATGCAGATGTTGG
C/EBPα	GACATCAGCGCCTACATCGA TCGGCTGTGCTGGAAGAG	*NPR-C*	TGACACCATTCGGAGAATCA TTTCACGGTCCTCAGTAGGG
C/EBPβ	ATTTCTATGAGAAAAGAGGC GTATGT AAATGTCTTCACTTTAATGCTC GAA	*Pgc1α*	CCCTGCCATTGTTAAGACC TGCTGCTGTTCCTGTTTTC
C/EBPδ	TTCCAACCCCTTCCCTGAT CTGGAGGGTTTGTGTTTTCTGT	*Ppar*	TCGGCGAACTATTCGGCTG GCACTTGTGAAAACGGCAGT
Cidea	TGCTCTTCTGTATCGCCCAGT GCCGTGTTAAGGAATCTGCTG	*Pparβ/δ*	TTGAGCCCAAGTTCGAGTTTG CGGTCTCCACACAGAATGATG
Cnp	AGCCAATCTCAAGGGAGACC TAACATCCCAGACCGCTCAT	*Prdm16*	CAGCACGGTGAAGCCATTC GCGTGCATCCGCTTGTG
Cox8b	GAACCATGAAGCCAACGACT GCGAAGTTCACAGTGGTTCC	*Rgs2*	GAGAAAATGAAGCGGACACTCT GCAGCCAGCCCATATTTACTG
Cpt1	TCTATGAGGGCTCGCG CGTCAGGGTTGTAGCA	*Siglec-F*	CTGGCTACGGACGGTTATTCG GGAATTGGGGTACTGGACTTG
Cpt2	GCCCAGCTTCCATCTTTACT CAGGATGTTGTGGTTTATCCGC	*Ucp1*	ACTGCCACACCTCCAGTCATT CTTTGGCTCACTCAGGATTGG

Gene	Sequence	Gene	Sequence
Ucp2	CAGATGTGGTAAAGGTCCGCT TTCCTCTCGTGCAATGGTCTT	*36B4*	GAGGAATCAGATGAGGATATGGGA AAGCAGGCTGACTTGGTTGC
Ucp3	GAGATGGTGACCTACGACATCA GCGTTCATGTATCGGGTGTTTA		

General Conclusion

The results of this study demonstrated that AHNAK promotes adipose tissue development and obesity by potentiating BMP4/SMAD1 signaling and that AHNAK can serve as a novel regulator of metabolic homeostasis. Our data thus expand the current knowledge regarding the early determination of adipose tissue development and highlight a potential indication for treating obesity-associated metabolic disorders. Moreover, enhanced response to β-adrenergic signaling in *AHNAK* KO mice induces to the development of beige fat, which promotes thermogenic effects with minimal alteration in BAT activity and mass. AHNAK null mice also promoted lipolysis via enhanced responsiveness to β3-adrenergic signals, accompanied by the elevated levels of NPs system and the ratio of NPRA to NPR-C expression. Enhanced β–adrenergic and NPs signaling could increase thermogenic ability and lipolytic activity in *AHNAK* KO mice. Although the precise molecular mechanism underlying AHNAK involvement in β-adrenergic signaling remains to be determined, the downregulation of AHNAK levels can be a new approach to increase energy metabolism in response to β-adrenergic stimulation and NPs signals in adipose tissue, suggesting a promising strategy to treat obesity.

REFERENCES

Alli AA and Gower WR Jr. (2009) The C type natriuretic peptide receptor tethers AHNAK1 at the plasma membrane to potentiate arachidonic acid-induced calcium mobilization. Am J Physiol Cell Physiol *297*, C1157-1167.

Alvarez J, Hamplova J, Hohaus A, Morano I, Haase H, and Vassort G (2004) Calcium Current in Rat Cardiomyocytes Is Modulated by the Carboxyl-terminal Ahnak Domain. J Biol Chem *279*, 12456-12461.

Arch J and Wilson S (1996) Prospects for β3-adrenoceptor agonists in the treatment of obesity and diabetes. Int J Obes Relat Metab Disord *20*, 191-199.

Arch JR (2002). β3-Adrenoceptor agonists: potential, pitfalls and progress. Eur J Pharmacol *440*, 99-107.

Arch JR (2011) Challenges in β(3)-Adrenoceptor Agonist Drug Development. Ther Adv Endocrinol Metab *2*, 59-64.

Atgié C, Faintrenie G, Carpéné C, Bukowiecki LJ, and Géloën A (1998) Effects of chronic treatment with noradrenaline or a specific β3-adrenergic agonist, CL 316 243, on energy expenditure and epididymal adipocyte lipolytic activity in rat. Comp Biochem Physiol A: Mol Integr Physiol *119*, 629-636.

Bachman ES, Dhillon H, Zhang C-Y, Cinti S, Bianco AC, Kobilka BK, and Lowell BB (2002) βAR signaling required for diet-induced thermogenesis and obesity resistance. Science *297*, 843-845.

Bartelt A, and Heeren J (2014) Adipose tissue browning and metabolic health. Nat Rev Endocrinol *10*, 24-36.

Blitz IL, and Cho KW (2009) Finding partners: How BMPs select their targets. Dev Dyn *238*, 1321-1331.

Bordicchia M., Liu D, Amri EZ, Ailhaud G, Dessi-Fulgheri P, Zhang, C, *et al.* (2012) Cardiac natriuretic peptides act via p38 MAPK to induce the brown fat thermogenic program in mouse and human adipocytes. J Clin Invest *122*, 1022-1036.

Borgonovo B, Cocucci E, Racchetti G, Podini P, Bachi A, and Meldolesi J (2002) Regulated exocytosis: a novel, widely expressed system. Nat Cell Biol *4*, 955-963.

Bostrom P, Wu J, Jedrychowski MP, Korde A, Ye L, Lo JC, *et al.* (2012) A PGC1-α-dependent myokine that drives brown-fat-like development of white fat and thermogenesis. Nature *481*, 463-468.

Bowers RR, Kim JW, Otto, TC, and Lane MD (2006) Stable stem cell commitment to the adipocyte lineage by inhibition of DNA methylation: role of the BMP-4 gene. Proc Natl Acad Sci USA *103*, 13022-13027.

Brestoff JR, Kim BS, Saenz SA, Stine RR, Monticelli LA, Sonnenberg, GF, *et al.* (2014) Group 2 innate lymphoid cells promote beiging of white adipose tissue and limit obesity. Nature *519*, 242-246

Cao, W, Daniel, KW, Robidoux, J, Puigserver, P, Medvedev, AV, Bai, X, *et al*. (2004) p38 Mitogen-Activated Protein Kinase Is the Central Regulator of Cyclic AMP-Dependent Transcription of the Brown Fat Uncoupling Protein 1 Gene. Mol Cell Biol *24*, 3057-3067.

Cao, W, Medvedev, AV, Daniel, KW, and Collins, S. (2001) β-adrenergic activation of p38 MAP kinase in adipocytes: cAMP induction of uncoupling protein 1 (UCP1) gene requires p38 MAP kinase J Biol Chem *276*, 27077-27082.

Chen-Tournoux, A, Khan AM, Baggish AL, Castro VM, Semigran MJ, McCabe EL, *et al.* (2010) Effect of weight loss after weight loss surgery on plasma

N-terminal pro-B-type natriuretic peptide levels. Am J Cardiol *106*, 1450-1455.

Chen D, Zhao M., and Mundy G.R. (2004) Bone morphogenetic proteins. Growth factors *22*, 233-241.

Chinkers M, Garbers DL, Chang MS, Lowe DG, Chin H, Goeddel DV, e*t al*. (1989) A membrane form of guanylate cyclase is an atrial natriuretic peptide receptor. Nature *338*, 78-83

Cinti S (2001) The adipose organ: morphological perspectives of adipose tissues. Proc Nutr Soc *60*, 319-328.

Collins S, Yehuda-Shnaidman E, and Wang H. (2010) Positive and negative control of Ucp1 gene transcription and the role of β-adrenergic signaling networks. Int J Obes *34*, S28-S33.

Cypess AM, Lehman S, Williams G, Tal I, Rodman D, Goldfine AB, *et al.* (2009) Identification and importance of brown adipose tissue in adult humans. New Eng J Med *360*, 1509-1517.

Cypess AM, Weiner LS, Roberts-Toler C, Elía EF, Kessler SH, Kahn PA, *et al.* (2015). Activation of human brown adipose tissue by a β3-adrenergic receptor agonist. Cell Metab *21*, 33-38.

Davis TA, Loos B, and Engelbrecht AM (2014) AHNAK: The giant jack of all trades. Cell Signal *26*, 2683-2693.

De Jesus LA, Carvalho SD, Ribeiro MO, Schneider M, Kim SW, Harney JW, *et al*. (2001) The type 2 iodothyronine deiodinase is essential for adaptive thermogenesis in brown adipose tissue. J Clin Invest *108*, 1379-1385.

Deiuliis JA, Liu LF, Belury MA, Rim JS, Shin S, and Lee K. (2010) β3-Adrenergic signaling acutely down regulates adipose triglyceride lipase in brown adipocytes. Lipids *45*, 479-489.

Despres JP, and Lemieux I (2006) Abdominal obesity and metabolic syndrome. Nature *444*, 881-887.

Eckel RH, Grundy SM, and Zimmet PZ (2005) The metabolic syndrome. Lancet *365*, 1415-1428.

Fajas L (2003) Adipogenesis: a cross-talk between cell proliferation and cell differentiation. Ann Med *35*, 79-85.

Fredriksson JM, Thonberg H, Ohlson KB, Ohba K, Cannon B, Nedergaard J (2001) Analysis of inhibition by H89 of UCP1 gene expression and thermogenesis indicates protein kinase A mediation of β3-adrenergic s ignalling rather than β3-adrenoceptor antagonism by H89. Biochim Biophys Acta *1538*, 206-217.

Gentil BJ, Benaud C, Delphin C, Remy C, Berezowski V, Cecchelli R, *et al.* (2005) Specific AHNAK expression in brain endothelial cells with barrier properties. J Cell Physiol *203*, 362-371.

Gesta S, Tseng YH, and Kahn CR (2007) Developmental origin of fat: tracking obesity to its source. Cell *131*, 242-256.

Granneman JG, Li P, Zhu Z, and Lu Y (2005) Metabolic and cellular plasticity in white adipose tissue I: effects of β3-adrenergic receptor activation. Am J Physiol Endocrinol Metab *289*, E608-E616.

Griffith ML, Younk LM, and Davis SN (2010) Visceral adiposity, insulin resistance, and type 2 diabetes. Am J Lifestyle Med *4*, 230-243.

Grundy, S.M. (2006). Metabolic syndrome: connecting and reconciling cardiovascular and diabetes worlds. J Am Coll Cardiol *47*, 1093-1100.

Guo CA, Kogan S, Amano SU, Wang M, Dagdeviren S, Friedline RH, *et al.* (2013) CD40 deficiency in mice exacerbates obesity-induced adipose tissue inflammation, hepatic steatosis, and insulin resistance. Am J Physiol Endocrinol Metab *304*, E951-E963.

Guo T, Marmol P, Moliner A, Björnholm M, Zhang C, Shokat KM, *et al.* (2014) Adipocyte ALK7 links nutrient overload to catecholamine

resistance in obesity. elife *3*. e03245. doi: 10.7554/eLife.03245

Harms M, and Seale P (2013) Brown and beige fat: development, function and therapeutic potential. Nat Med *19*, 1252-1263.

Hashimoto T, Gamou S, Shimizu N, Kitajima Y, and Nishikawa T (1995) Regulation of translocation of the desmoyokin/AHNAK protein to the plasma membrane in keratinocytes by protein kinase C. Exp Cell Res *217*, 258-266.

Hata K, Nishimura R, Ikeda F, Yamashita K, Matsubara T, Nokubi T, *et al.* (2003) Differential roles of Smad1 and p38 kinase in regulation of peroxisome proliferator-activating receptor γ during bone morphogenetic protein 2-induced adipogenesis. Mol Biol Cell *14*, 545-555.

Himms-Hagen J, Cui J, Danforth E, Taatjes D, Lang S, Waters B, *et al.* (1994) Effect of CL-316,243, a thermogenic β3-agonist, on energy balance and brown and white adipose tissues in rats. Am J Physiol *266*, R1371-R1382.

Himms-Hagen J, Melnyk A, Zingaretti MC, Ceresi E, Barbatelli G, and Cinti S (2000) Multilocular fat cells in WAT of CL-316243-treated rats derive directly from white adipocytes. Am J Physiol Cell Physiol *279*,C670-681.

Hohaus A, Person V, Behlke J, Schaper J, Morano I, and Haase H (2002) The carboxyl-terminal region of ahnak provides a link between cardiac L-type Ca2+ channels and the actin-based cytoskeleton. FASEB J *16*, 1205-1216.

Holm C (2003) Molecular mechanisms regulating hormone-sensitive lipase and lipolysis. Biochem Soc Trans *31*, 1120-1124.

Hondares E, Iglesias R, Giralt A, Gonzalez FJ, Giralt M, Mampel T, *et al.* (2011) Thermogenic activation induces FGF21 expression and release in brown adipose tissue. J Biol Chem *286*, 12983-12990.

Huang H, Song TJ, Li X, Hu L, He Q, Liu M, Lane MD, *et al.* (2009) BMP

signaling pathway is required for commitment of C3H10T1/2 pluripotent stem cells to the adipocyte lineage. Proc Natl Acad Sci U S A *106*, 12670-12675.

Huang Y, Laval SH, van Remoortere A, Baudier J, Benaud C, Anderson LV, *et al.* (2007) AHNAK, a novel component of the dysferlin protein complex, redistributes to the cytoplasm with dysferlin during skeletal muscle regeneration. FASEB J *21*, 732-742.

Ishibashi J, and Seale P (2010) Beige can be slimming. Science *328*, 1113-1114.

Jin W, Takagi T, Kanesashi SN, Kurahashi T, Nomura T, Harada J, *et al.* (2006) Schnurri-2 controls BMP-dependent adipogenesis via interaction with smad proteins. Dev Cell *10*, 461-471.

Jocken JW, Blaak EE, van der Kallen CJ, van Baak MA, and Saris WH (2008) Blunted β-adrenoceptor–mediated fat oxidation in overweight subjects: a role for the hormone-sensitive lipase gene. Metabolism *57*, 326-332.

Kang Q, Song WX, Luo Q, Tang N, Luo J, Luo X, *et al.* (2008) A comprehensive analysis of the dual roles of BMPs in regulating adipogenic and osteogenic differentiation of mesenchymal progenitor cells. Stem Cells Dev *18*, 545-558.

Karasawa H, Takaishi K, and Kumagae Y (2011) Obesity-induced diabetes in mouse strains treated with gold thioglucose: a novel animal model for studying β-cell dysfunction. Obesity *19*, 514-521.

Kim H, Pennisi PA, Gavrilova O, Pack S, Jou W, Setser-Portas J, *et al.* (2006) Effect of adipocyte β3-adrenergic receptor activation on the type 2 diabetic MKR mice. Am J Physiol Endocrinol Metab *290*, E1227-1236.

Kim IY, Jung J, Jang M, Ahn YG, Shin JH, Choi JW, *et al.* (2010) 1H NMR-based metabolomic study on resistance to diet-induced obesity in AHNAK knock-out mice. Biochem Biophys Res Commun *403*, 428-434.

Komuro A, Masuda Y, Kobayashi K, Babbitt R, Gunel, M., Flavell RA, *et al.*

(2004) The AHNAKs are a class of giant propeller-like proteins that associate with calcium channel proteins of cardiomyocytes and other cells. Proc Natl Acad Sci U S A *101*, 4053-4058.

Kouno M, Kondoh G, Horie K, Komazawa N, Ishii N, Takahashi Y, *et al.* (2004) Ahnak/Desmoyokin is dispensable for proliferation, differentiation, and maintenance of integrity in mouse epidermis. J Invest Dermatol *123*, 700-707.

Lafontan M, Moro C, Berlan M, Crampes F, Sengenes C, and Galitzky J (2008) Control of lipolysis by natriuretic peptides and cyclic GMP. Trends Endocrinol Metab *19*, 130-137.

Lafontan M, Moro C, Sengenes C, Galitzky J, Crampes F, and Berlan M (2005) An unsuspected metabolic role for atrial natriuretic peptides: the control of lipolysis, lipid mobilization, and systemic nonesterified fatty acids levels in humans. Arterioscler Thromb Vasc Biol *25*, 2032-2042.

Larsen TM, Toubro S, van Baak MA, Gottesdiener KM, Larson P, Saris WH, *et al.* (2002) Effect of a 28-d treatment with L-796568, a novel β3-adrenergic receptor agonist, on energy expenditure and body composition in obese men. Am J Clin Nutr *76*, 780-788.

Lee H, Kim HJ, Lee YJ, Lee MY, Choi H, Lee H, *et al.* (2012a) Krüppel-like factor KLF8 plays a critical role in adipocyte differentiation. PLoS One *7*, e52474. doi: 10.1371/journal.pone.0052474.

Lee IH, Lim HJ, Yoon S, Seong JK, Bae DS, *et al.* (2008) Ahnak protein activates protein kinase C (PKC) through dissociation of the PKC-protein phosphatase 2A complex. J Biol Chem *283*, 6312-6320.

Lee IH, Sohn M, Lim HJ, Yoon S, Oh H, Shin S, e*t al.* (2014) Ahnak functions as a tumor suppressor via modulation of TGFβ/Smad signalingpathway. Oncogene *33*, 4675-4684

Lee IH, You JO, Ha KS, Bae DS, Suh PG, Rhee SG., *et al.* (2004) AHNAK-mediated activation of phospholipase C-γ1 through protein kinase C. J

Biol Chem *279*, 26645-26653.

Lee J, Ellis JM, and Wolfgang, MJ. (2015a) Adipose fatty acid oxidation is required for thermogenesis and potentiates oxidative stress-induced inflammation. Cell Rep *10*, 266-279.

Lee MW, Odegaard JI., Mukundan L, Qiu Y., Molofsky AB, Nussbaum, JC, e*t al.* (2015b) Activated type 2 innate lymphoid cells regulate beige fat Biogenesis. Cell *160*, 74-87.

Lee YH, Petkova AP, Mottillo EP., and Granneman, JG. (2012b) In vivo identification of bipotential adipocyte progenitors recruited by β3-adrenoceptor activation and high-fat feeding. Cell Metab *15*, 480-491.

Leone TC, Lehman JJ, Finck BN, Schaeffer PJ, Wende AR, Boudina S, *et al.* (2005) PGC-1α deficiency causes multi-system energy metabolic derangements: muscle dysfunction, abnormal weight control and hepatic steatosis. PLoS Biol *3*, e101.

Li J, Yu X, Pan W, and Unger RH (2002). Gene expression profile of rat adipose tissue at the onset of high-fat-diet obesity. Am J Physiol Endocrinol Metab *282*, E1334-1341.

Lim HJ, Kang DH, Lim JM, Kang DM, Seong JK, Kang SW, *et al.* (2013) Function of Ahnak protein in aortic smooth muscle cell migration t hrough Rac activation. Cardiovasc Res *97*, 302-310.

Liu F, Hata A, Baker JC, Doody J, Carcamo J, Harland RM, *et al.* (1996) A human Mad protein acting as a BMP-regulated transcriptional activator. Nature *381*, 620-623.

Lowell BB, and Bachman ES (2003) β-adrenergic receptors, diet-induced thermogenesis, and obesity. J Biol Chem *278*, 29385-29388.

Lumeng CN, DeYoung SM, Bodzin JL, and Saltiel AR (2007) Increased inflammatory properties of adipose tissue macrophages recruited during diet-induced obesity. Diabetes *56*, 16-23.

Maffei M, Halaas J, Ravussin E, Pratley RE, Lee GH, Zhang Y, *et al.* (1995) Leptin levels in human and rodent: Measurement of plasma leptin and ob RNA in obese and weight-reduced subjects. Nat Med *1*, 1155-1161.

Margoni A, Fotis L, and Papavassiliou AG (2012) The transforming growth factor-β/bone morphogenetic protein signalling pathway in adipogenesis. Int J Biochem Cell Biol *44*, 475-479.

Matza D, Badou A, Kobayashi KS, Goldsmith-Pestana K, Masuda Y, Komuro A, *et al.* (2008) A scaffold protein, AHNAK1, is required for calcium signaling during T cell activation. Immunity *28*, 64-74.

Moro C, Crampes F, Sengenes C, De Glisezinski I, Galitzky J, Thalamas C, *et al.* (2004) Atrial natriuretic peptide contributes to physiological control of lipid mobilization in humans. FASEB J *18*, 908-910.

Moro C, and Lafontan M (2013) Natriuretic peptides and cGMP signaling control of energy homeostasis. Am J Physiol Heart Circ Physiol *304*, H358-H368.

Moro C, Polak J, Hejnov, J, Klimcakova E, Crampes F, Stich V, *et al.* (2006). Atrial natriuretic peptide stimulates lipid mobilization during repeated bouts of endurance exercise. Am J Physiol Endocrinol Metab *290*, E864-E869.

Mottillo EP, Shen XJ, and Granneman JG (2007) Role of hormone-sensitive lipase in β-adrenergic remodeling of white adipose tissue. Am J Physiol Endocrinol Metab *293*, 1188-1197.

Nahmias C, Blin N, Elalouf JM, Mattei MG, Strosberg AD, and Emorine LJ (1991) Molecular characterization of the mouse β3-adrenergic receptor: relationship with the atypical receptor of adipocytes. EMBO J *10*, 3721-3727.

Nguyen KD, Qiu Y, Cui X, Goh YP, Mwangi J, David T, *et al.* (2011) Alternatively activated macrophages produce catecholamines to

sustain adaptive thermogenesis. Nature *480*, 104-108.

Nie Z, Ning W, Amagai M, and Hashimoto T (2000) C-terminus of Desmoyokin/AHNAK protein is responsible for its translocation between the nucleus and cytoplasm. J Invest Dermatol *114*, 1044-1049.

Nunn, C., Zou, M.-X., Sobiesiak, A.J., Roy, A.A., Kirshenbaum, L.A., and Chidiac, P. (2010) RGS2 inhibits β-adrenergic receptor-induced cardiomyocyte hypertrophy. Cell Signal *22*, 1231-1239.

Pan Q, Yu Y, Chen Q, Li C, Wu H, Wan, Y., *et al.* (2008) Sox9, a key transcription factor of bone morphogenetic protein-2-induced chondrogenesis, is activated through BMP pathway and a CCAAT box in the proximal promoter. J Cell Physiol *217*, 228-241.

Parikh H, Nilsson E, Ling C, Poulsen P, Almgren P, Nittby H, *et al.* (2008) Molecular correlates for maximal oxygen uptake and type 1 fibers. Am J Physiol Endocrinol Metab*294*, E1152-E1159.

Pfeifer A, and Hoffmann LS (2015) Brown, beige, and white: the new color code of fat and its pharmacological implications. Annu Rev Pharmacol Toxicol *55*, 207-227.

Phimphilai M, Zhao Z, Boules H, Roca H, and Franceschi RT (2006) BMP signaling is required for RUNX2-dependent induction of the osteoblast p henotype. J Bone Miner Res *21*, 637-646.

Potter LR, and Hunter T (2001) Guanylyl cyclase-linked natriuretic peptide receptors: structure and regulation. J Biol Chem *276*, 6057-6060.

Qiu Y, Nguyen KD, Odegaard JI, Cui X, Tian X, Locksley RM, *et al.* (2014) Eosinophils and type 2 cytokine signaling in macrophages orchestrate development of functional beige fat. Cell *157*, 1292-1308.

Rajkumar K, Modric T, and Murphy L (1999) Impaired adipogenesis in insulin-like growth factor binding protein-1 transgenic mice. J Endocrin *162*, 457-465.

Ramdas M, Harel C, Armoni M, and Karnieli E. (2015) AHNAK KO mice are protected from diet-induced obesity but are glucose intolerant. Horm Metab Res *47*, 265-272.

Rao RR, Long JZ, White JP, Svensson KJ, Lou J, Lokurkar I, *et al.* (2014) Meteorin-like is a hormone that regulates immune-adipose interactions to increase beige fat thermogenesis. Cell *157*, 1279-1291.

Redman LM, de Jonge L, Fang X, Gamlin B, Recker D, Greenway FL, *et al.* (2007) Lack of an effect of a individuals: a double-blind, placebo-controlled randomized study. J Clin Endocrinol Metab *92*, 527-531.

Reichert M, and Eick D (1999) Analysis of cell cycle arrest in adipocyte differentiation. Oncogene *18*, 459-466.

Reshef R, Maroto M, and Lassar AB (1998) Regulation of dorsal somitic cell fates: BMPs and Noggin control the timing and pattern of myogenic regulator expression. Genes Dev *12*, 290-303.

Riordan NH, Ichim TE, Min WP, Wang H, Solano F, Lara F, *et al.*. (2009) Non-expanded adipose stromal vascular fraction cell therapy for multiple sclerosis. J Transl Med *7*, 29-29.

Robidoux J, Martin, TL, and Collins S (2004) Beta-adrenergic receptors and regulation of energy expenditure: a family affair. Annu Rev Pharmacol Toxicol *44*, 297-323.

Rodeheffer MS, Birsoy K, and Friedman JM (2008) Identification of white adipocyte progenitor cellls in vivo. Cell *135*, 240-249.

Rosen ED, and MacDougald OA (2006) Adipocyte differentiation from the inside out. Nat Rev Mol Cell Biol *7*, 885-896.

Rosen ED, and Spiegelman BM (2006) Adipocytes as regulators of energy balance and glucose homeostasis. Nature *444*, 847-853.

Rosen ED, and Spiegelman BM (2014) What we talk about when we talk

about fat. Cell *156*, 20-44.

Sarzani R, Paci VM, Zingaretti CM, Pierleoni C, Cinti S, Cola G., *et al.* (1995) Fasting inhibits natriuretic peptides clearance receptor expression in rat adipose tissue. J of hypertens *13*, 1241-1246.

Schulz TJ, Huang P, Huang TL, Xue R, McDougall LE, Townsend KL, *et al.* (2013) Brown-fat paucity due to impaired BMP signalling induces compensatory browning of white fat. Nature *495*, 379-383.

Schulz TJ, and Tseng YH (2009) Emerging role of bone morphogenetic proteins in adipogenesis and energy metabolism. Cytokine Growth Factor Rev *20*, 523-531.

Sengenès C, Bouloumié A, Hauner, H., Berlan, M., Busse, R., Lafontan, M., and Galitzky, J. (2003) Involvement of a cGMP-dependent pathway in the natriuretic peptide-mediated hormone-sensitive lipase phosphorylation in human adipocytes. J Biol Chem *278*, 48617-48626.

Sengenès C, Zakaroff-Girard A, Moulin A, Berlan M, Bouloumie A, Lafontan, M., *et al.* (2002) Natriuretic peptide-dependent lipolysis in fat cells is a primate specificity. Am J Physiol Regul Integr Comp Physiol *283*, R257-R265.

Sengenès C, Berlan M, De Glisezinski I, Lafontan M, Galitzky J (2000) Natriuretic peptides: a new lipolytic pathway in human adipocytes. FASEB J *14*, 1345-1351.

Shin JH, Kim IY, Kim YN, Shin SM, Roh KJ, Lee SH, *et al.* (2015) Obesity resistance and enhanced insulin sensitivity in *Ahnak*$^{-/-}$ mice fed a high fat diet are related to impaired adipogenesis and increased energy expenditure. PLoS ONE *10*, e0139720.

Shtivelman E, and Bishop JM (1993) The human gene AHNAK encodes a large phosphoprotein located primarily in the nucleus. J Cell Biol *120*, 625-630.

Shtivelman E, Cohen FE, and Bishop JM (1992) A human gene (AHNAK) encoding an unusually large protein with a 1.2-microns polyionic rod structure. Proc Natl Acad Sci U S A *89*, 5472-5476.

Sugisawa T, Kishimoto I, Kokubo Y, Makino H, Miyamoto Y, and Yoshimasa Y (2010) Association of plasma B-type natriuretic peptide levels with obesity in a general urban Japanese population: the Suita Study. Endocr J *57*, 727-733.

Takahashi A, Morita M, Yokoyama K, Suzuki T, and Yamamoto T (2012) Tob2 inhibits peroxisome proliferator-activated receptor γ2 expression by sequestering Smads and C/EBPα during adipocyte differentiation. Mol Cell Biol *32*, 5067-5077.

Tang QQ, Otto TC, and Lane MD (2004) Commitment of C3H10T1/2 pluripotent stem cells to the adipocyte lineage. Proc Natl Acad Sci U S A *101*, 9607-9611.

Vaillant F, Lauzier B, Poirier I, Gélinas R, Rivard ME, Robillard Frayne I, *et al.* (2014) Mouse strain differences in metabolic fluxes and function of ex vivo working. Am J Physiol Heart Circ Physiol *306*, H78-87 doi: 10.1152/ajpheart.00465.2013.

Wang E, Israel D, Kelly S, and Luxenberg D (1993) Bone morphogenetic protein-2 causes commitment and differentiation in C3Hl0T1/2 and 3T3 cells. Growth Factors *9*, 57-71.

Whittle AJ, Carobbio S, Martins L, Slawik M, Hondares E, Vázquez MJ, *et al.* (2012) BMP8B increases brown adipose tissue thermogenesis through both central and peripheral actions. Cell *149*, 871-885.

Wong KE, Kong J, Zhang W, Szeto FL, Ye H, Deb DK, *et al.* (2011) Targeted expression of human vitamin D receptor in adipocytes decreases energy expenditure and induces obesity in mice. J Biol Chem *286*, 33804-33810.

Wu J, Boström P, Sparks LM, Ye L, Choi JH, Giang AH, *et al.* (2012) Beige adipocytes are a distinct type of thermogenic fat cell in mouse and human. Cell *150*, 366-376.

Yadav H, Quijano C, Kamaraju AK, Gavrilova O, Malek R, Chen W, Zerfas P, Zhigang D, Wright EC, and Stuelten C. (2011) Protection from obesity and diabetes by blockade of TGF-β/Smad3 signaling. Cell Metab *14*, 67-79.

Yamamoto N, Akamatsu H, Hasegawa S, Yamada T, Nakata S, Ohkuma M, *et al.* (2007) Isolation of multipotent stem cells from mouse adipose tissue. J Dermatol Sci *48*, 43-52.

Yoneshiro T, Aita S, Matsushita M, Kayahara T, Kameya T, Kawai Y, *et al.* (2013) Recruited brown adipose tissue as an antiobesity agent in humans. J Clin Invest *123*, 3404-3408.

Zamani N, and Brown CW (2011) Emerging roles for the transforming growth factor-β superfamily in regulating adiposity and energy expenditure. Endocr Rev *32*, 387-403.

Zehentner BK, Dony C, and Burtscher H (1999) The transcription factor Sox9 is involved in BMP-2 signaling. J Bone Miner Res *14*, 1734-1741.

Zhao GQ (2003) Consequences of knocking out BMP signaling in the mouse. Genesis *35*, 43-56.

국문 초록

AHNAK 단백질은 약 700kDa에 이르는 거대한 크기의 인산화단백질(phosphoprotein)로서, 세포부착(cell adhesion), 세포증식(Proliferation), 칼슘신호전달 등에서 중요한 역할을 한다. 최근에 AHNAK 발현이 비만상태에서 변화한다는 새로운 증거들이 밝혀지고 있다. 그럼에도 불구하고, 지방조직 발생과정에서 AHNAK의 역할은 잘 알려져 있지 않다. 이번 연구에서 지방세포분화와 포도당 항상성 (glucose homeostasis) 에 있어서 AHNAK의 분자적 기전을 밝여내고자 한다. AHNAK 유전자 결손 마우스는 고지방식이에 의한 비만발생에 저항성을 갖고 이는 지방축적의 감소에 기인한다. 지방세포분화는 체내의 지방 축적에 영향을 미치는데, AHNAK 유전자 결손 마우스의 지방유래중간엽줄기세포 (adipose derived mesenchymal stem cells)을 이용한 지방세포로의 분화능이 감소해 있었다. 또한 AHNAK의 결핍은 BMP4/SMAD1 신호전달의 감소로 이어졌고, 그 결과 지방세포분화와 관련한 주요조절인자들의 발현이 감소하였다. AHNAK은 SMAD1과 상호작용하여 PPARγ2의 전사활성에 영향을 미친다. 동시에, 고지방식이를 먹인 AHNAK 결손 마우스는 대조군에 비해 에너지 섭취나 활동량에는 변화가 없이 포도당 내성(glucose tolerace), 인슐린 민감도(insulin sensitivity)가 개선되고 그리고 에너지 소비가 증가하는 등 대사지표가 향상되었다. 따라서 본 연

구 결과로 미루어 볼 때 AHNAK은 SMAD1 단백질과의 상호작용을 통해 지방조직발달을 조절하여 체내 지방축적에 중요한 역할을 하며 대사항상성에도 관여되어 있다고 생각한다.

이와 더불어 열생성을 통한 갈색지방의 활성과 에너지 소비의 변화는 는 비만에 대한 치료타겟으로 전도유망하다고 생각된다. 지방조직에서 베타3 특이적인 아드레너직 수용체 작용물질(β_3 specific adrenergic receptor agonist)은 지방분해와 지방 산화뿐만 아니라, 열생성에도 관련되어 있다. 고지방 식이를 먹인 마우스의 백색 지방 조직에서 AHNAK 유전자 결핍시에 열발생이 증가하였고, 이 결과는 베이지 지방이 발달하여 에너지 소비가 향상된 것을 예상할 수 있다. 본 연구에서 AHNAK 결손 마우스에 CL-316243을 주사하였을 때 백색지방에서는 갈색지방화와 열발생 관련 유전자의 발현을 증가시켰지만 갈색지방에서는 변화가 없었다. 동시에 AHNAK 결손 마우스에서는 CL-316243에 반응한 백색지방에서 미토콘드리아 생합성 증가를 수반하는 에너지 소비가 증가하였다. CL-316243은 AHNAK 결손 마우스에서 대조군과 비교하여 PKA 신호전달을 활성화시켜 HSL의 인산화를 증가시켰고, 지방분해를 증가시켜 글리세롤이 분비가 증가하였다. AHNAK 유전자가 결손된 지방조직은 대조군에 비해 호산구(eosinophil)과 2형 사이토카인 (type2 cytokine)인 IL-4/IL-13의 양이 증가해있었고, 이는 CL-316243에 반응하여 백색지방의 갈색지방화와 미토콘드리아의 생합성을 향상시킨 것으로 생각된다. 이것은 AHNAK 결손 마우스의 백색지방에서 Adrb3유전자와 tyrosine hydroxylase 유전자의 발현증가로 인한 교감신경 활성도가 증가한 것과 관련이 있다. 따라서 본 연구 결과는

AHNAK 유전자가 베타 아드레너직 신호를 통해 백색지방에서의 열발생과 지방분해를 조절하는데 중요한 역할을 한다는 것을 보여준다.

Keywords: Ahnak, adipogenesis, BMP4/SMAD1, obesity, browning, lipolysis, thermogenesis, β-adrenergic signaling

Student Number: 2009-21627